UNIVERSITÄT OSNABRÜCK

A role of actin-regulatory proteins in the formation of needle-shaped spores in the filamentous fungus *Ashbya gossypii*

Dissertation

zur Erlangung des akademischen Grades
Doctor rerum naturalium
(Dr. rer. nat.)

Fachbereich Biologie/Chemie der Universität Osnabrück

vorgelegt von
Manuela Lickfeld

Osnabrück, im März 2012

Table of contents

1 Summary

Spore formation is an essential step in the fungal life cycle that contributes to the dispersal of the organism and also to survival under harsh environmental conditions. The morphology of spores shows an astonishing diversity in the fungal kingdom and varies from very simple round and small spores to very complex multi-armed or sigmoid structures. With exception of the regulation of ascospore formation in *Saccharomyces cerevisiae* and *Schizosaccharomyces pombe,* which are well-characterized model organisms for spore development in fungi, little is currently known about the regulation of more complex spore morphologies.

In this study, the filamentous ascomycete *Ashbya gossypii* is used as a model system for the investigation of a complex and composite spore morphology. *A. gossypii* produces linear, needle-shaped spores possessing a length of 30 µm, which can be divided into three major segments: a rigid tip segment, a more fragile membrane compartment and a stable tail-cap. Furthermore, the different compartments were shown to correlate with distinct materials. While the tip segment and the tail-cap of the spores consist of stabilizing materials like chitin and chitosan, these materials are absent from the compartment in the middle.

The actin cytoskeleton plays an essential role in several steps of spore formation in *A. gossypii*. Different regions of actin accumulation were identified that directly correlate with the developing spores. Especially the developing tip segment is characterized by heavy-bundled linear actin structures. Furthermore, proteins of the formin family, a class of actin organizing proteins, were identified to be directly involved in spore formation in *A. gossypii.* The formin *Ag*Bnr2 fulfills an actin-related key function during spore development by linking actin to the spindle pole body during sporulation. Downregulation of *AgBNR2* leads to severe sporulation defects, indicating a central function in spore development. Moreover, *Ag*Bni1, another representative of the formin family, also has a regulatory function in size determination of the typical needle-shaped spores of *A. gossypii.* Using a modified yeast two-hybrid approach, four potential activators of the formin *Ag*Bni1 were identified: the Rho-type GTPases *Ag*Rho1a, *Ag*Rho1b, *Ag*Rho3 and *Ag*Rho4. The interaction of *Ag*Bni1 with the

two Rho1 GTPases plays an important role during spore development. In this study, the Rho binding domain of *Ag*Bni1 was further examined to identify amino acids that are essential for the interaction with the Rho-type GTPases. Using random mutagenesis combined with a two-hybrid screen, the point mutation S250P in the Rho binding domain of *Ag*Bni1 was identified to reduce the interaction of the formin with the Rho1 GTPases. Integration of *Ag*Bni1$_{S250P}$ causes an increase in spore length, suggesting a direct effect of this signaling pathway in spore length determination. An actin-regulating protein network that includes the formin *Ag*Bni1, the Rho-type GTPases *Ag*Rho1a and *Ag*Rho1b and the paxillin-like protein *Ag*Pxl1 was identified to be mainly involved in the regulation of the spore length. Thereby, this network seems to be involved in the arrangement of the different spore compartments via the actin cytoskeleton.

2 Introduction

2.1 *Ashbya gossypii* - a model for the investigation of cell biological processes

Fungi are organisms with a unique cellular structure and growth behavior. One special hallmark of fungi is the complex spectrum of biological activities: By degrading organic materials, fungi fulfill important roles as decomposers and recyclers and they produce many important secondary metabolites, which are of industrial importance. Another important role of fungi is their application as model organisms for research. This is also due to the fact that many fungi are pathogenic organisms causing diseases in humans, animals and plants (Deacon, 2006).

This study bases on the plant-pathogenic fungus *Ashbya gossypii,* which is known to cause stigmatomycosis in diverse economic important crop plants, especially in cotton and citrus fruits (Ashby and Nowell, 1926). *A. gossypii,* which is also known as *Eremothecium gossypii* or *Nematospora gossypii* (Kurtzman, 1995), is a filamentous fungus and was first isolated from cotton balls where it infects the lint fibers. The infection causes a color change to dirty-yellowish, which gives the disease its alternative name "Cotton staining" (Pridham and Raper, 1950). Dissemination by insects contributes to the dispersal of this pathogen and led to great problems in the cultivation of cotton in many parts of the subtropics (Batra, 1973). The insects transmit the fungus from plant to plant. Therefore, mycelia or spores of *A. gossypii* stick to the mouth part of the insect or they are carried in the deep stylet pouches (Pridham and Raper, 1950). For dispersal, vegetative cells or spores can be deposited on the plant, which again favors an infection. Another possibility of infection bases on the characteristic morphology of the spores produced by *A. gossypii.* The spores, which possess a needle-shaped, linear structure, can be injected by the insect into the tissue of the plant (Pridham and Raper, 1950).

Because of several morphological and biochemical hallmarks, *A. gossypii* became an attractive model organism for the investigation of cell biological questions and for industry. *A. gossypii* is a natural overproducer of riboflavin (vitamin B_2), which is commercially used as a yellow colorant and food additive

(Wickerham *et al.*, 1946, Stahmann *et al.*, 2000). Mycelia of *A. gossypii* possess an intense yellow color, which is due to the production of high amounts of riboflavin. The accumulation of vitamin B_2 fulfills an important function: It offers protection from UV-light (Stahmann *et al.*, 2001), which is supposed to be of great importance for a plant-pathogenic organism that grows in the subtropics. The production of riboflavin dramatically increases during sporulation. Approximately 70% of the total riboflavin is produced simultaneously with spore production, suggesting a key role for this secondary metabolite during this developmental stage. In fact, riboflavin was shown to act as a photoprotectant for the hyaline spores of *A. gossypii* from UV-light (Stahmann *et al.*, 2001).

In addition to its industrial importance, *A. gossypii* is a well-established model system for the investigation of polar growth. As a filamentous growing fungus, it produces hyphae that permanently elongate at their tips (Philippsen *et al.*, 2005). In contrast to other filamentous organisms (e.g. algae), which grow by repeated cell divisions to produce a chain of cells, filamentous fungi produce hyphae that only extend at their hyphal tips (Deacon, 2006). Thus, the growth mode of filamentous fungi shows a unique cellular organization. The formation of a mycelium consisting of several branched hyphae is an extreme form of polar growth and makes *A. gossypii* interesting for research.

In addition to its cellular organization, *A. gossypii* offers many advantages for its use in research. First, *A. gossypii* has a small genome of 9 million base pairs and 4700 protein-coding genes organized in haploid nuclei (Philippsen *et al.*, 2005). Furthermore, the genome sequence of *A. gossypii* revealed that, despite of the completely different growth modes, this ascomycete is closely related to the budding yeast *S. cerevisiae.* In fact, 95% of the genes, which can be found in *A. gossypii* have orthologues in *S. cerevisiae* (Philippsen *et al*., 2005). Such a high level of gene order conservation allows comparative investigations on *A. gossypii* as a representative of filamentous fungi and *S. cerevisiae*, an organism that grows by budding. Important molecular tools for genetic manipulation of *A. gossypii* have been successfully established. *A. gossypii* integrates linear DNA by homologous recombination very efficiently (Wendland *et al.*, 2000, Wendland, 2003) and can be transformed with plasmids that harbor autonomously replicating sequences of *S. cerevisiae* (Wright & Philippsen, 1991). Moreover, selection markers that base on auxotrophy for leucine or

mediate resistance to antibiotics like geneticin and clonNat have been developed.

Furthermore, *A. gossypii* is one of the filamentous fungi possessing a relatively simple life cycle (Figure 1), which is advantageous for cultivation and genetic manipulation. The development of an *A. gossypii* mycelium starts with germination of a needle-shaped spore and the production of a germ bubble, which displays a short period of isotropic growth. Afterwards, isotropic growth switches to polar growth, which leads to the production of the first hyphal tube. A second germ tube is established at the opposite side of the first germ tube. Once switched to polar growth, hyphae permanently elongate at their tips and produce lateral branches to generate a young mycelium. The increase in the growth speed of the hyphal tips is accompanied by a second type of tip differentiation that is called apical branching or tip-splitting and leads to the production of Y-shaped filaments. After approximately 24 hours, *A. gossypii* has produced a mature mycelium (Wendland & Walther, 2005). In older parts of the mycelium, new spores are developed. Sporulation in *A. gossypii* seems to be affected by the pheromone response pathway (Wendland *et al.*, 2011). In fact, the deletion of the transcription factor *Ag*Ste12, which is a key component of the pheromone response pathway, led to a hypersporulation phenotype. *Ag*Ste12 binds to specific DNA sequences in the promoter region of the regulated genes, the so-called pheromone-response elements. In *S. cerevisiae,* the components of this MAP kinase cascade regulates cellular processes like mating, the formation of shmoos, but also pseudohyphal growth under nutritional limitations (Gimeno *et al.*, 1992, Herskowitz, 1995). The genome of *A. gossypii* encodes homologs of most of the genes that are involved in the pheromone response pathway. The role of this MAP kinase cascade in *A. gossypii* remained unknown so far. The hyperphosphorylation phenotype of *Agste12* suggests a role of this signaling pathway for sporulation (Wendland *et al.*, 2011). For the activation of genes that are required for filamentation, *Sc*Ste12 interacts with the transcription factor *Sc*Tec1 in *S. cerevisiae.* Strikingly, the deletion of *Ag*Tec1 also causes hypersporulation in *A. gossypii,* suggesting that *Ag*Ste12 and *Ag*Tec1 might cooperate in the regulation of spore formation (Wendland *et al.*, 2011). Moreover, sporulation is negatively affected by the stress signal cAMP (Stahmann *et al.*, 2001). Treatment of cells with the second messenger cAMP

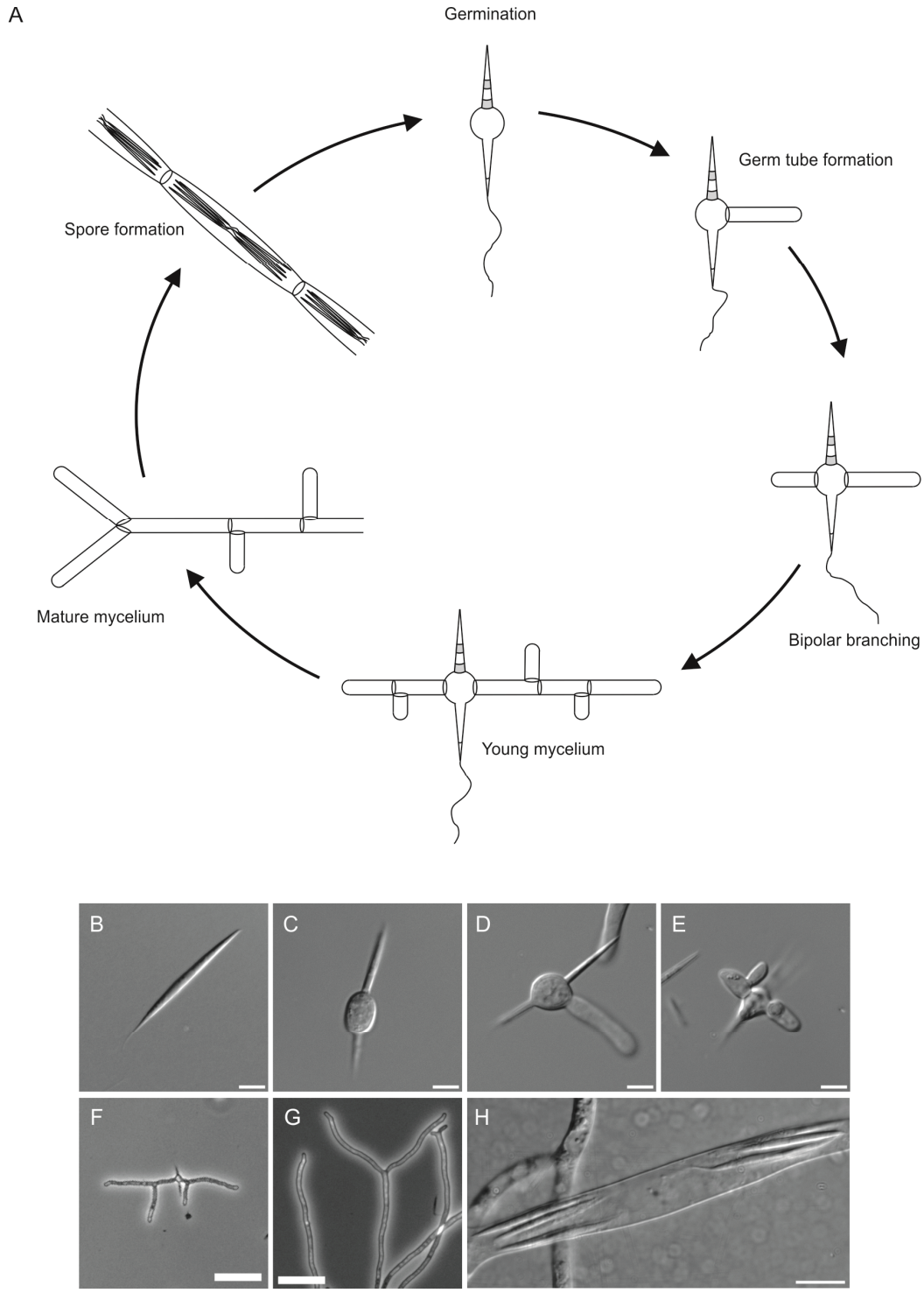

Figure 1: The life cycle of *A. gossypii.* A) The most important growth stages in the life cycle of *A. gossypii* (see text for details). Modified by Wendland and Walther, 2005. B) A needle-shaped spore of *A. gossypii.* C) Formation of a germ bubble. D) Germ tube formation. E) Bipolar branching. F) Young mycelium. G) Mature mycelium. H) Sporangium. The scale bars represent either 5 µm (B,C,D and E), 40 µm (F and G) or 10 µm (H).

leads to a complete loss of spore formation and simultaneously to a decrease in riboflavin production.

A. gossypii produces vegetative spores that are organized in bundles within a sporangium and possess single haploid nuclei. The spores show a characteristic and complex morphology, which appears closely adapted to the way of dispersal. Spores are highly polar and needle-shaped possessing an average length of about 30 µm and a width of one to two µm (Batra, 1973). To date, sporulation has been studied in the well-established model organisms *S. cerevisiae* and *S. pombe*, fungi that produce simple, round spores. Little is currently known about the molecular mechanisms that are involved in the regulation of more complex spore morphologies. Spore size and morphology is directly adapted to the way of spore dispersal and the kind of infection (Deacon, 2006). Investigations on *A. gossypii* as an organism that produces highly polar, linear spores will offer new insights into the regulation of sporulation in ascomycetes. The investigation of molecular regulation mechanisms of spore formation in *A. gossypii* is one important focus of this study.

2.2 Sporulation in ascomycetes

Sporulation is a special morphogenetic program that has been best-studied in the model organisms *S. cerevisiae* and *S. pombe* (see Neiman, 2005 and Shimoda, 2004 for review). In contrast to *A. gossypii,* which builds asexual vegetative spores*, S. cerevisiae and S. pombe* produce meiotic ascospores. Sporulation in *S. cerevisiae* is performed in the absence of a nitrogen source and in the presence of a non-fermentable carbon source (e.g. acetate) (Esposito and Klapholz, 1981). Under these growth conditions, vegetative yeast cells exit the mitotic cycle in the G_1 phase, undergo meiosis and sporulate (Esposito and Klapholz, 1981). In general, ascospore formation includes three major developmental steps: meiosis, the formation of a prospore membrane and the assembly of the spore wall (Figure 2). One structure that plays an important role for spore formation is the spindle pole body (SPB), the sole microtubule organizing center in *S. cerevisiae.* In the G_1 phase, there is only one SPB present in each cell. For sporulation, the SPB is duplicated prior to meiosis I. Therefore, the new SPB is assembled adjacent to the mother SPB and then moves to the opposite side of the nucleus to form a spindle (Adams &

Kilmartin, 2000). Prior to meiosis II, the SPBs duplicate again to generate the two meiosis II spindles that enable the separation of the sister chromatids. The spindle pole body is a complex consisting of several proteins that either permanently or temporarily localize to this structure. As a multi-component structure, the SPB can be divided into three major parts: The inner plaque, which is the basis for the nucleation of the spindle microtubules, the central plaque, which spans the nuclear envelope and the outer plaque, which is involved in the organization of the cytoplasmic microtubules. During sporulation, the composition of specifically the outer plaque changes. In vegetative growing cells, the outer layer of the SPB consists of the three proteins *Sc*Cnm67, *Sc*Nud1 and *Sc*Spc72 (Wigge *et al.*, 1998), in which *Sc*Spc72 anchors the cytoplasmic microtubules to the SPB (Knop & Schiebel, 1998). In meiosis II, *Sc*Spc72 is removed from the SPB and replaced by meiosis-specific proteins (Knop & Strasser, 2000). This modification of the outer plaque is correlated with a change in function from microtubule nucleation to membrane production and can be seen as a condition for prospore formation in *S. cerevisiae.* The structure of the meiosis II outer plaque includes *Sc*Mpc54, *Sc*Spo21, *Sc*Spo74 and *Sc*Ady4 (Bajgier *et al.*, 2001, Knop & Strasser, 2000, Nickas *et al.*, 2003), a composition that is essential for prospore membrane formation. This special composition is important for the coalescence of post-Golgi vesicles to form the prospore membrane on the one hand and to couple this new developing membrane to the nucleus on the other hand. The mechanism of vesicle transport to the developing prospore membrane is unknown so far. However, the growth of the prospore membrane by the fusion of vesicles is realized by v-SNAREs, t-Snares and SNAP-25 proteins (Neiman, 1998, Neiman *et al.*, 2000). The development of the prospore membrane is a controlled process to ensure that the nucleus is enclosed. One component that is mainly involved in an organized assembly of the prospore membrane is the leading-edge complex including the proteins *Sc*Ssp1, *Sc*Ady3 and *Sc*Don1 (Moreno-Borchart *et al.*, 2001, Nickas & Neiman, 2002). The three proteins build a ring-like structure at the mouth of the prospore membrane during growth (Knop & Strasser, 2000). The deletion of the leading-edge protein *Sc*Ssp1 leads to a complete block of sporulation in *S. cerevisiae.* The deletion cells still produce prospore membranes but they are completely abnormal in structure. The prospore

membranes of the *Scssp1* deletion strain are not round, grow into the wrong direction and do not enclose the nucleus, indicating a central function of the leading edge complex in the organized assembly of this sporulation specific structure (Moreno-Borchart *et al.*, 2001). Prospore membrane closure terminates this step in spore development.

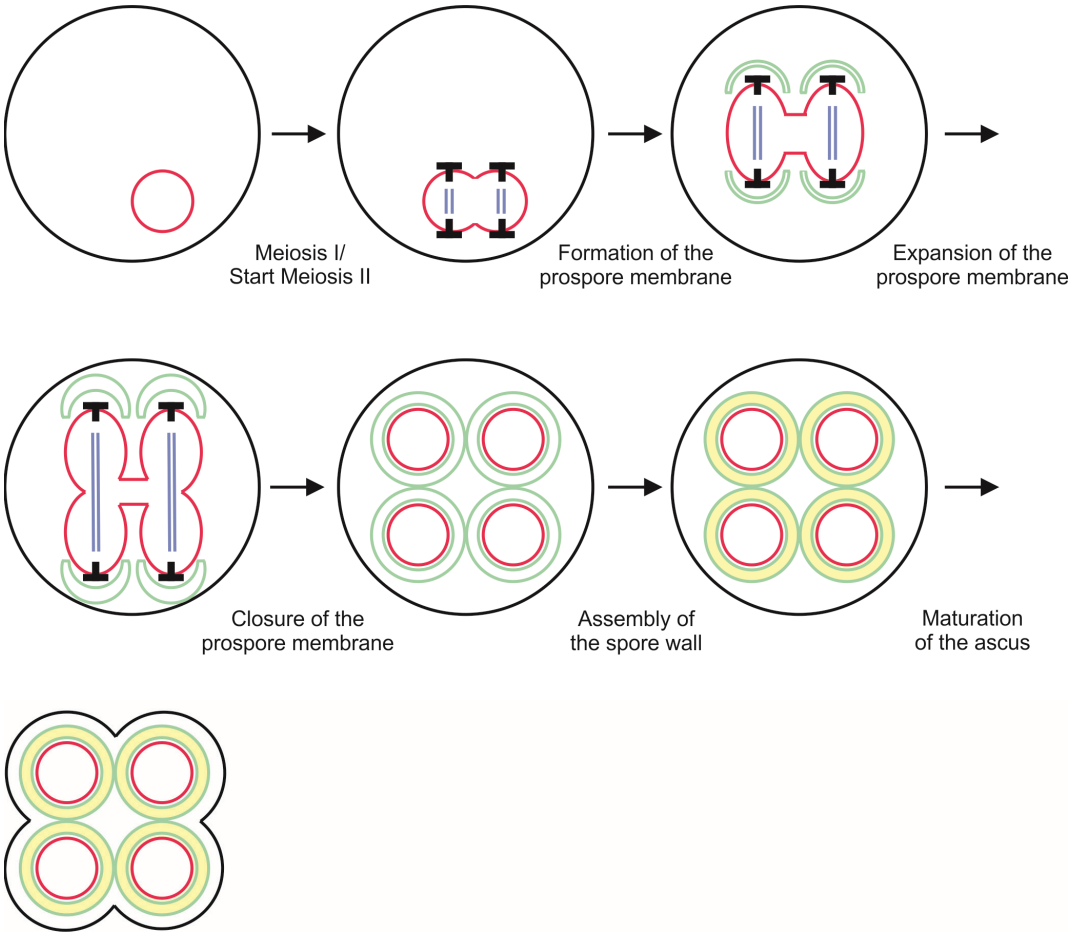

Figure 2: Ascospore formation in *S. cerevisiae.* During meiosis II, the prospore membranes (shown in green) starts to develop at the spindle pole bodies (SPBs, indicated as **T**), which are embedded in the nuclear envelope (shown in red). The prospore membranes grow and enclose the haploid nuclei to produce four prospores. The assembly of the spore wall (shown in yellow) is performed in the lumen between the two membranes of the prospore (shown in green). After spore wall production, the mother cell is modified to form the ascus. See text for details. Modified by Neiman, 2005.

Nevertheless, the production of mature spores requires the assembly of a stable spore wall, which is realized in the lumen between the two membranes of the prospore membrane (Figure 2). In contrast to the cell wall of vegetative *S. cerevisiae* cells that consist of two layers (Klis *et al.*, 2002), the spore wall consists of four layers (Smits *et al.*, 2001). The first, innermost layer that is located to the plasma membrane consists of mannan while the second is composed of β-glucan (Kreger-Van Rij, 1978). These are the same components, which can be also found in the cell wall of vegetative cells but their order is reversed with respect to the plasma membrane. In addition, the spore wall exposes two additional layers consisting of chitosan (Briza *et al.*, 1988), the deacetylated form of chitin, and dityrosine which builds the thin outermost layer (Briza *et al.*, 1986). The formation of the first layer of the spore wall is realized by the deposition of mannoproteins into the lumen of the prospore membrane (Coluccio *et al.*, 2004). In contrast, β-glucan, which is required for the assembly of the second layer, is directly produced by a β-glucan synthase located at the spore plasma membrane. There are three alternative subunits of the glucan synthase complex of *S. cerevisiae,* which are used in different cellular contexts. While *Sc*Fks1 is the catalytic subunit that plays a role for vegetative growth (Mazur *et al.*, 1995), *Sc*Fks2 was shown to be the major subunit during spore wall assembly (Mazur et al., 1995, Ishihara *et al.*, 2007). There is also a third homologous subunit encoded by *ScFKS3,* which also plays a role for spore formation (Ishihara *et al.*, 2007). The assembly of the β-glucan containing layer of the spore wall is also the time-point when the outer membrane, originally provided by the prospore membrane, disappears. Afterwards, the third spore wall layer consisting of chitosan is established. Therefore, the spore plasma membrane-associated chitin synthase *Sc*Chs3 produces chitin polymers and extrude them through the spore plasma membrane (Henar Valdivieso *et al.*, 1999). Assembly of the chitosan layer requires the two chitin deacetylases *Sc*Cda1 and *Sc*Cda2, which convert chitin to chitosan by deacetylation (Christodoulidou *et al.*, 1996). The chitin synthase *Sc*Chs3 that is not only required for spore formation but also for vegetative growth is regulated by a directed transport to the place of action, which is realized by a signaling pathway involving the protein kinase *Sc*Pkc1 and *Sc*Rho1 (Valdivia &

Schekman, 2003). Chitosan is also the material that forms inter spore bridges between the spores of an ascus (Coluccio & Neiman, 2004). After completion of the chitosan layer, the outermost dityrosine layer is assembled, which is mainly composed of N,N-bisformyldityrosine (Briza *et al.*, 1990). Therefore, dityrosine is first synthesized in the cytoplasm by the formyltransferase *Sc*Dit1 that modifies the amino group of L-tyrosine and *Sc*Dit2, a cytochrome P450 family protein that couples the benzyl rings of two N-formyl-tyrosine molecules (Briza *et al.*, 1994). The transport of dityrosine, which is produced in the cytoplasm, is performed by the transporter *Sc*Dtr1 that is located to the prospore membrane (Felder *et al.*, 2002). After completion, the spore wall confers the spore resistance to distinct external influences. After the establishment of the four *S. cerevisiae* ascospores, the mother cell is remodeled and encloses the four spores to an ascus.

In contrast to *S. cerevisiae,* little is currently known about the molecular mechanisms and the course of events during spore development in the closely related organism *A. gossypii.* A striking fact is that most of the components that are involved in spore formation in *S. cerevisiae* have homologs in *A. gossypii* (Dietrich *et al*., 2004). In fact, all components of the *S. cerevisiae* meiotic outer plaque are conserved in *A. gossypii,* suggesting similar regulatory mechanisms in both organisms.

2.3 The role of actin in spore development

Previous investigations performed on sporulation in *S. cerevisiae* revealed that actin plays an essential role for spore formation (Taxis *et al.*, 2006). A central question in the study was whether actin filaments are required for the development of the ascospores. During vegetative growth, a polarized actin cytoskeleton was shown to be essential while the role of actin in meiotic cells was unclear so far. Strikingly, depolymerization of actin structures by a treatment of sporulating cells with Latrunculin A completely abolishes sporulation (Taxis *et al.*, 2006). Treatment with this drug is also capable to block spore development in a very late stage of this process. Although the precursors of the prospore membrane are transported actively along actin filaments, the assembly of the prospore membrane does not depend on actin cables. In general, actin cables form a highly dynamic network of interacting filaments that

is located directly underneath the plasma membrane of sporulating cells. In contrast, actin patches can be found at the interior part of the cell near the growing prospore membranes during meiosis II (Taxis *et al.*, 2006). To further characterize the specific roles of actin cables and actin patches during spore formation, mutant strains showing defects in either actin cable or patch formation were used. The temperature-sensitive mutant that shows defects in the assembly of actin patches possess a mutant allele of *ScARP*2 (*arp2-1*), an essential component of the Arp2/3 complex that is mainly involved in actin patch formation (Moreau *et al.*, 1996). At the restrictive temperature, *arp2-1* cells produced almost no spores, indicating a key role of actin patches in sporulation. In contrast, the temperature-sensitive strain *Δtpm2, tpm1-2* that is impaired in the stability of actin cables (Pruyne *et al.*, 1998) shows no decrease in sporulation efficiency (Taxis *et al.*, 2006). That hints that actin cables are not essential for spore development in *S. cerevisiae.* Furthermore, the essential role of actin patches seems to affect the maturation of the spore wall. Electron microscopy and calcofluor white staining of *arp2-1* cells at the restrictive temperature revealed that the few spores that are produced under these conditions possess no chitosan and in consequence no dityrosine layer. All in all, the essential function of *Sc*Arp2 as a component of the actin polymerizing Arp2/3 complex for the development of the spore wall seems to affect the accumulation of the chitosan layer. Thereby, *Sc*Arp2 might fulfill a key role for the transport of precursor material for the chitosan layer of the spore wall (Taxis *et al.*, 2006).

Summarizing, the investigations of spore formation in *S. cerevisiae* revealed that filamentous actin structures are not required to produce small and round ascospores. But how is the situation in an organism that produces more complex linear spores? Polarity establishment in *A. gossypii* leads primarily to the production of hyphae. However, the needle-shaped structure of the spores produced by *A. gossypii* suggests that polarity is also an essential factor for the production of these linear structures. Therefore, the investigation of proteins that regulate cell polarity and the dynamic organization of the actin cytoskeleton might offer deeper insight into the regulation of spore development. Proteins of the formin family and small GTPases of the Rho family are actin-regulating proteins and act as key factors for the establishment of cell polarity. Formin

proteins polymerize linear actin cables and are conserved in all eukaryotic organisms. They are required for the dynamic remodeling of the actin cytoskeleton and for polarized cell growth (Wallar & Alberts, 2003). Formins of the DRF (Diaphanous related formin) family directly interact with the actin monomer binding protein profilin at the FH1 (formin homology 1) domain (Sagot *et al.*, 2002) and nucleate the free actin monomers to filaments at the FH2 (formin homology 2) domain (Pruyne *et al.*, 2002). Furthermore, they remain attached to the growing barbed end of the actin cable and protect it from capping proteins that would abolish elongation of the filament. This function is also described as "processive capping" (Xu *et al.*, 2004). Moreover, some proteins of the formin family also bind to the sides of actin filaments and bundle these structures (Moseley & Goode, 2005, Harris *et al.*, 2004).

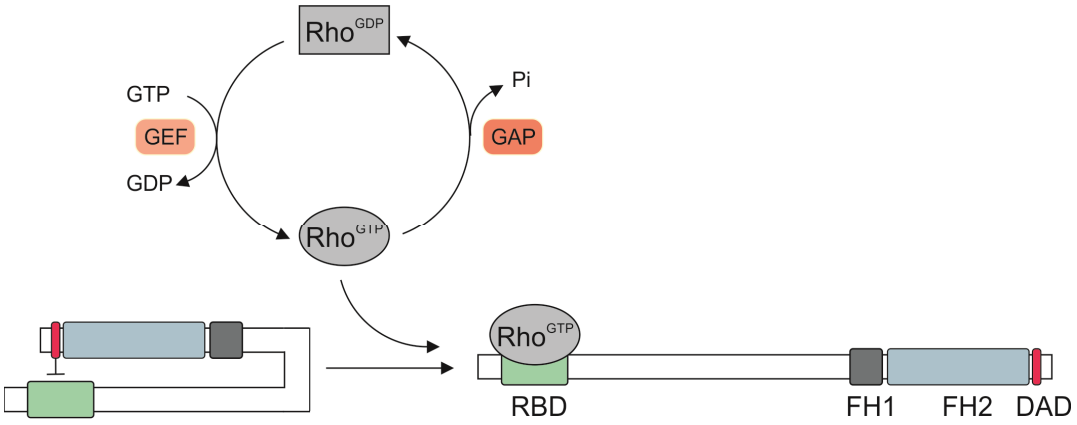

Figure 3: Regulation of Diaphanous related formins (DRFs). DRFs are activated by small GTPases of the Rho family. Therefore, Rho^{GTP} binds to the Rho binding domain (RBD, shown in green) of the formin. Binding of Rho^{GTP} disturbs the intramolecular interaction of the Diaphanous autoregulatory domain (DAD, shown in red) and the RBD, which activates the formin. The formin homology domains 1 (FH1, shown in grey) and 2 (FH2, shown in blue) are involved in actin polymerization. Rho GTPases are regulated by guanine nucleotide exchange factors (GEFs, show in light orange), which promote the GTP bound state and GTPase activating proteins (GAPs, shown in dark orange), which promote the formation of the GDP bound form.

Proteins of the formin family are regulated by Rho-type GTPases (Figure 3). Rho proteins display a subfamily of the Ras superfamily. A special hallmark that distinguishes Rho proteins from other small GTPases is the so-called Rho insert domain (Valencia *et al.*, 1991). This unique domain is involved in the interaction with special effectors, such as guanine nucleotide dissociation inhibitors (GDIs) (Wu *et al.*, 1997). In addition, they possess two switch domains, called "switch I" (also called Ras like effector region) and "switch II" that also mediate the interaction with specific effector proteins. Rho-type GTPases are modified by isoprenylation. This post-translational modification is performed at the C-terminal located CAAX motif and is important for membrane attachment and proper function (Adamson *et al.*, 1992). Rho proteins bind GDP and GTP with high affinities and cycle between the active, GTP-bound state and the inactive, GDP-bound state. Cycling is realized by guanine nucleotide exchange factors (GEFs), which promote the formation of the GTP-bound state and GTPase-activating proteins (GAPs), which promote the formation of the GDP-bound state by catalyzing the intrinsic GTPase activity (for review see Etienne-Manneville & Hall, 2002).

The active, GTP-bound form of specific Rho-type GTPases directly binds to the N-terminal located Rho binding domain of a formin protein and activates it (Evangelista *et al.*, 1997). Thereby, binding of the Rho protein at the N-terminal located Rho binding domain of the formin disrupts the auto-inhibitory interaction of the N-terminal located Diaphanous inhibitory domain and the C-terminal located Diaphanous autoregulatory domain (Alberts, 2001).

2.4 Aims of this study

The current knowledge of spore formation in ascomycetes is limited to ascospore producing fungi like *S. cerevisiae* and *S. pombe* that produce relatively simple spore morphologies. In contrast, little is currently known about the formation of more complex spore morphologies in the fungal kingdom.

A special aim of this study was to further characterize the composition and the materials of the highly polar, needle-shaped spores of the filamentous ascomycete *A. gossypii* and to get further insight into the molecular regulation of spore-specific properties like size and morphology. A special emphasis was placed on the importance of the actin cytoskeleton during this morphogenetic

program. Therefore, formin proteins as actin regulators and Rho-type GTPases and paxillin-like proteins that are involved in formin regulation, were investigated in detail. The formin *Ag*Bni1, its regulation and role during spore development displays a special focus in this study.

References

Adams, I. R. & J. V. Kilmartin, (2000) Spindle pole body duplication: a model for centrosome duplication? *Trends Cell Biol* **10**: 329-335.

Adamson, P., C. J. Marshall, A. Hall & P. A. Tilbrook, (1992) Post-translational modifications of p21rho proteins. *J Biol Chem* **267**: 20033-20038.

Alberts, A. S., (2001) Identification of a carboxyl-terminal diaphanous-related formin homology protein autoregulatory domain. *J Biol Chem* **276**: 2824-2830.

Ashby SF, Nowell W, (1926) The Fungi of Stigmatomycosis. Ann Bot (Lond), ***40***: 69-86.

Bajgier, B. K., M. Malzone, M. Nickas & A. M. Neiman, (2001) *SPO21* is required for meiosis-specific modification of the spindle pole body in yeast. *Mol Biol Cell* **12**: 1611-1621.

Batra, L. R., (1973) Nematosporaceae (Hemiascomycetidae): Taxonomy, Pathogenicity, Distribution and Vector Relations, U.S. Department of Agriculture

Briza, P., M. Eckerstorfer & M. Breitenbach, (1994) The sporulation-specific enzymes encoded by the *DIT1* and *DIT2* genes catalyze a two-step reaction leading to a soluble LL-dityrosine-containing precursor of the yeast spore wall. *Proc Natl Acad Sci U S A* **91**: 4524-4528.

Briza, P., A. Ellinger, G. Winkler & M. Breitenbach, (1988) Chemical composition of the yeast ascospore wall. The second outer layer consists of chitosan. *J Biol Chem* **263**: 11569-11574.

Briza, P., A. Ellinger, G. Winkler & M. Breitenbach, (1990) Characterization of a DL-dityrosine-containing macromolecule from yeast ascospore walls. *J Biol Chem* **265**: 15118-15123.

Briza, P., G. Winkler, H. Kalchhauser & M. Breitenbach, (1986) Dityrosine is a prominent component of the yeast ascospore wall. A proof of its structure. *J Biol Chem* **261**: 4288-4294.

Christodoulidou, A., V. Bouriotis & G. Thireos, (1996) Two sporulation-specific chitin deacetylase-encoding genes are required for the ascospore wall rigidity of *Saccharomyces cerevisiae*. *J Biol Chem* **271**: 31420-31425.

Coluccio, A., E. Bogengruber, M. N. Conrad, M. E. Dresser, P. Briza & A. M. Neiman, (2004) Morphogenetic pathway of spore wall assembly in *Saccharomyces cerevisiae. Eukaryot Cell* **3**: 1464-1475.

Coluccio, A. & A. M. Neiman, (2004) Interspore bridges: a new feature of the *Saccharomyces cerevisiae* spore wall. *Microbiology* **150**: 3189-3196.

Deacon, J. W., (2006) Fungal Biology. Malden, MA: Blackwell Pub.

Dietrich, F. S., S. Voegeli, S. Brachat, A. Lerch, K. Gates, S. Steiner, C. Mohr, R. Pohlmann, P. Luedi, S. Choi, R. A. Wing, A. Flavier, T. D. Gaffney & P. Philippsen, (2004) The *Ashbya gossypii* genome as a tool for mapping the ancient *Saccharomyces cerevisiae* genome. *Science* **304**: 304-307.

Esposito, R. E., and S. Klapholz, (1981) Meiosis and ascospore development, p.211-287. In J. N. Strathern, E. W. Jones and J. R. Broach (ed.), The molecular biology of the yeast *Saccharomyces*: life cycle and inheritance, Cold Spring Harbor Laboratory Press, Cold Spring Harbor, N. Y.

Etienne-Manneville, S. & A. Hall, (2002) Rho GTPases in cell biology. *Nature* **420**: 629-635.

Evangelista, M., K. Blundell, M. S. Longtine, C. J. Chow, N. Adames, J. R. Pringle, M. Peter & C. Boone, (1997) Bni1p, a yeast formin linking cdc42p and the actin cytoskeleton during polarized morphogenesis. *Science* **276**: 118-122.

Felder, T., E. Bogengruber, S. Tenreiro, A. Ellinger, I. Sa-Correia & P. Briza, (2002) Dtrlp, a multidrug resistance transporter of the major facilitator superfamily, plays an essential role in spore wall maturation in *Saccharomyces cerevisiae*. *Eukaryot Cell* **1**: 799-810.

Gimeno, C. J., P. O. Ljungdahl, C. A. Styles & G. R. Fink, (1992) Unipolar cell divisions in the yeast *S. cerevisiae* lead to filamentous growth: regulation by starvation and RAS. *Cell* **68**: 1077-1090.

Harris, E. S., F. Li & H. N. Higgs, (2004) The mouse formin, FRLalpha, slows actin filament barbed end elongation, competes with capping protein, accelerates polymerization from monomers, and severs filaments. *J Biol Chem* **279**: 20076-20087.

Henar Valdivieso, M., A. Duran & C. Roncero, (1999) Chitin synthases in yeast and fungi. *EXS* **87**: 55-69.

Herskowitz, I., (1995) MAP kinase pathways in yeast: for mating and more. *Cell* **80**: 187-197.

Ishihara, S., A. Hirata, S. Nogami, A. Beauvais, J. P. Latge & Y. Ohya, (2007) Homologous subunits of 1,3-beta-glucan synthase are important for spore wall assembly in *Saccharomyces cerevisiae*. *Eukaryot Cell* **6**: 143-156.

Klis, F. M., P. Mol, K. Hellingwerf & S. Brul, (2002) Dynamics of cell wall structure in *Saccharomyces cerevisiae*. *FEMS Microbiol Rev* **26**: 239-256.

Knop, M. & E. Schiebel, (1998) Receptors determine the cellular localization of a gamma-tubulin complex and thereby the site of microtubule formation. *EMBO J* **17**: 3952-3967.

Knop, M. & K. Strasser, (2000) Role of the spindle pole body of yeast in mediating assembly of the prospore membrane during meiosis. *EMBO J* **19**: 3657-3667.

Kreger-Van Rij, N. J., (1978) Electron microscopy of germinating ascospores of *Saccharomyces cerevisiae*. *Arch Microbiol* **117**: 73-77.

Kurtzman, C. P., (1995) Relationships among the genera *Ashbya*, *Eremothecium*, *Holleya* and *Nematospora* determined from rDNA sequence divergence. *J Ind Microbiol* **14**: 523-530.

Mazur, P., N. Morin, W. Baginsky, M. el-Sherbeini, J. A. Clemas, J. B. Nielsen & F. Foor, (1995) Differential expression and function of two homologous subunits of yeast 1,3-beta-D-glucan synthase. *Mol Cell Biol* **15**: 5671-5681.

Moreau, V., A. Madania, R. P. Martin & B. Winson, (1996) The *Saccharomyces cerevisiae* actin-related protein Arp2 is involved in the actin cytoskeleton. *J Cell Biol* **134**: 117-132.

Moreno-Borchart, A. C., K. Strasser, M. G. Finkbeiner, A. Shevchenko & M. Knop, (2001) Prospore membrane formation linked to the leading edge protein (LEP) coat assembly. *EMBO J* **20**: 6946-6957.

Moseley, J. B. & B. L. Goode, (2005) Differential activities and regulation of *Saccharomyces cerevisiae* formin proteins Bni1 and Bnr1 by Bud6. *J Biol Chem* **280**: 28023-28033.

Neiman, A. M., (1998) Prospore membrane formation defines a developmentally regulated branch of the secretory pathway in yeast. *J Cell Biol* **140**: 29-37.

Neiman, A. M., (2005) Ascospore formation in the yeast *Saccharomyces cerevisiae*. *Microbiol Mol Biol Rev* **69**: 565-584.

Neiman, A. M., L. Katz & P. J. Brennwald, (2000) Identification of domains required for developmentally regulated SNARE function in *Saccharomyces cerevisiae*. *Genetics* **155**: 1643-1655.

Nickas, M. E. & A. M. Neiman, (2002) Ady3p links spindle pole body function to spore wall synthesis in *Saccharomyces cerevisiae*. *Genetics* **160**: 1439-1450.

Nickas, M. E., C. Schwartz & A. M. Neiman, (2003) Ady4p and Spo74p are components of the meiotic spindle pole body that promote growth of the prospore membrane in *Saccharomyces cerevisiae*. *Eukaryot Cell* **2**: 431-445.

Philippsen, P., A. Kaufmann & H. P. Schmitz, (2005) Homologues of yeast polarity genes control the development of multinucleated hyphae in *Ashbya gossypii*. *Curr Opin Microbiol* **8**: 370-377.

Pridham, T.G. and Raper, K.B., (1950) *Ashbya gossypii*: Its significance in nature and in the laboratory. Mycologia ***42***, 603-623.

Pruyne, D., M. Evangelista, C. Yang, E. Bi, S. Zigmond, A. Bretscher & C. Boone, (2002) Role of formins in actin assembly: nucleation and barbed-end association. *Science* **297**: 612-615.

Pruyne, D. W., D. H. Schott & A. Bretscher, (1998) Tropomyosin-containing actin cables direct the Myo2p-dependent polarized delivery of secretory vesicles in budding yeast. *J Cell Biol* **143**: 1931-1945.

Sagot, I., A. A. Rodal, J. Moseley, B. L. Goode & D. Pellman, (2002) An actin nucleation mechanism mediated by Bni1 and profilin. *Nat Cell Biol* **4**: 626-631.

Shimoda, C., (2004) Forespore membrane assembly in yeast: coordinating SPBs and membrane trafficking. *J Cell Sci* **117**: 389-396.

Smits, G. J., H. van den Ende & F. M. Klis, (2001) Differential regulation of cell wall biogenesis during growth and development in yeast. *Microbiology* **147**: 781-794.

Stahmann, K. P., H. N. Arst, Jr., H. Althofer, J. L. Revuelta, N. Monschau, C. Schlupen, C. Gatgens, A. Wiesenburg & T. Schlosser, (2001) Riboflavin, overproduced during sporulation of *Ashbya gossypii*, protects its hyaline spores against ultraviolet light. *Environ Microbiol* **3**: 545-550.

Stahmann, K. P., J. L. Revuelta & H. Seulberger, (2000) Three biotechnical processes using *Ashbya gossypii*, *Candida famata*, or *Bacillus subtilis* compete with chemical riboflavin production. *Appl Microbiol Biotechnol* **53**: 509-516.

Taxis, C., C. Maeder, S. Reber, N. Rathfelder, K. Miura, K. Greger, E. H. Stelzer & M. Knop, (2006) Dynamic organization of the actin cytoskeleton during meiosis and spore formation in budding yeast. *Traffic* **7**: 1628-1642.

Valdivia, R. H. & R. Schekman, (2003) The yeasts Rho1p and Pkc1p regulate the transport of chitin synthase III (Chs3p) from internal stores to the plasma membrane. *Proc Natl Acad Sci U S A* **100**: 10287-10292.

Valencia, A., P. Chardin, A. Wittinghofer & C. Sander, (1991) The ras protein family: evolutionary tree and role of conserved amino acids. *Biochemistry* **30**: 4637-4648.

Wallar, B. J. & A. S. Alberts, (2003) The formins: active scaffolds that remodel the cytoskeleton. *Trends Cell Biol* **13**: 435-446.

Wendland, J., (2003) PCR-based methods facilitate targeted gene manipulations and cloning procedures. *Curr Genet* **44**: 115-123.

Wendland, J., Y. Ayad-Durieux, P. Knechtle, C. Rebischung & P. Philippsen, (2000) PCR-based gene targeting in the filamentous fungus *Ashbya gossypii*. *Gene* **242**: 381-391.

Wendland, J., A. Dunkler & A. Walther, (2011) Characterization of alpha-factor pheromone and pheromone receptor genes of *Ashbya gossypii*. *FEMS Yeast Res* **11**: 418-429.

Wendland, J. & A. Walther, (2005) *Ashbya gossypii*: a model for fungal developmental biology. *Nat Rev Microbiol* **3**: 421-429.

Wickerham, L. J., M. H. Flickinger & R. M. Johnston, (1946) The production of riboflavin by *Ashbya gossypii*. *Arch Biochem* **9**: 95-98.

Wigge, P. A., O. N. Jensen, S. Holmes, S. Soues, M. Mann & J. V. Kilmartin, (1998) Analysis of the *Saccharomyces* spindle pole by matrix-assisted laser desorption/ionization (MALDI) mass spectrometry. *J Cell Biol* **141**: 967-977.

Wright, M. C. & P. Philippsen, (1991) Replicative transformation of the filamentous fungus *Ashbya gossypii* with plasmids containing *Saccharomyces cerevisiae* ARS elements. *Gene* **109**: 99-105.

Wu, W. J., D. A. Leonard, A. C. R & D. Manor, (1997) Interaction between Cdc42Hs and RhoGDI is mediated through the Rho insert region. *J Biol Chem* **272**: 26153-26158.

Xu, Y., J. B. Moseley, I. Sagot, F. Poy, D. Pellman, B. L. Goode & M. J. Eck, (2004) Crystal structures of a Formin Homology-2 domain reveal a tethered dimer architecture. *Cell* **116**: 711-723.

3 Results

3.1 A Bnr-like formin links actin to the spindle pole body during sporulation in the filamentous fungus *Ashbya gossypii*

M. Kemper, L. Mohlzahn, M. Lickfeld, C. Lang, S. Wählisch & H.P. Schmitz, (2011) *Molecular Microbiology* **80**: 1276-1295.

3.2 Selection of STOP-free sequences from random mutagenesis for 'loss of interaction' two-hybrid studies

Lickfeld, M. & H.P. Schmitz, (2011) *Yeast* **28**: 535-545.

3.3 A network involving Rho-type GTPases, a Paxillin and a Formin homolog regulates spore length and spore wall integrity in the filamentous fungus *Ashbya gossypii*

Lickfeld, M. & H.P. Schmitz, (2012) *manuscript submitted*

3.4 Dissection of Rho-GTPase function in polar growth and sporulation of *Ashbya gossypii*

Lickfeld, M. & H.P. Schmitz, (2012) *manuscript in preparation*

3.1 A Bnr-like formin links actin to the spindle pole body during sporulation in the filamentous fungus *Ashbya gossypii*

M. Kemper, L. Mohlzahn, M. Lickfeld, C. Lang, S. Wählisch & H.P. Schmitz, (2011)

Molecular Microbiology **80**: 1276-1295

A Bnr-like formin links actin to the spindle pole body during sporulation in the filamentous fungus *Ashbya gossypii*

M. Kemper, L. Mohlzahn, M. Lickfeld, C. Lang, S. Wählisch and H.P. Schmitz, (2011)

Molecular Microbiology **80**: 1276-1295

Summary

Formin proteins are nucleators of actin filaments and regulators of the microtubule cytoskeleton. As such, they play important roles in the development of yeast and other fungi. We show here that *Ag*Bnr2, a homologue of the *Sc*Bnr1 formin from the filamentous fungus *Ashbya gossypii*, localizes to the spindle pole body (SPB), the fungal analogue of the centrosome of metazoans. This protein plays an important role in the development of the typical needle-shaped spores of *A. gossypii*, as suggested by several findings. First, downregulation of *AgBNR2* causes defects in sporangium formation and a decrease in the total spore number. Second, a fusion of *AgBNR2* to *GFP* that is driven by the native *AgBNR2* promoter is only visible in sporangia. Third, *Ag*Bnr2 interacts with a *Ag*Spo21, a sporulation-specific component of the SPB. Furthermore, we provide evidence that *Ag*Bnr2 might nucleate actin cables, which are connected to SPBs during sporulation. Our findings add to our understanding of fungal sporulation, particularly the formation of spores with a complex, elongated morphology, and provide novel insights into formin function.

3.2 Selection of STOP-free sequences from random mutagenesis for ‘loss of interaction’ two-hybrid studies

M. Lickfeld & H.P. Schmitz, (2011)

Yeast **28**: 535-545

Selection of STOP-free sequences from random mutagenesis for ‘loss of interaction’ two-hybrid studies

M. Lickfeld & H.P. Schmitz, (2011)

Yeast **28**: 535-545

Abstract

The investigation of protein–protein interactions is an essential part of biological research. To obtain a deeper insight into regulatory protein networks, the identification of the components, domains and especially single residues that are involved in these interactions is helpful. A widespread and attractive genetic tool for investigation of protein–protein interactions is the yeast two-hybrid system. This method enables large-scale screens and its application is cheap and relatively simple. For identification of the amino acids in a protein sequence that are essential for interaction with a specific partner, yeast two-hybrid assays can be combined with random mutagenesis of the sequence of interest. A common problem with such an experiment is the generation of stop codons within the mutagenized fragments, leading to the isolation of many false positives when screening for loss of interaction using the two-hybrid method. To overcome this problem, we modified the yeast two-hybrid system to allow selection for sequences without stop codons. To achieve this, we fused the *ScURA3* marker-gene in frame to the mutagenized fragments. We show here that this marker is fully functional when fused to a two-hybrid construct with a nuclear localization signal, such as a Gal4 activation domain and a prey protein, thus allowing selection of stop-free sequences on media without uracil. Using the Rho-binding domain from a Bni1-like formin and different Rho-type GTPases from *Ashbya gossypii* as examples, we further show that our system can be used to screen large numbers of transformants for loss of protein–protein interactions in combination with random mutagenesis.

3.3 A network involving Rho-type GTPases, a Paxillin and a Formin homolog regulates spore length and spore wall integrity in the filamentous fungus *Ashbya gossypii*

Running title: A regulatory network for spore length

M. Lickfeld & H.P. Schmitz

Department of Genetics, University of Osnabrück, Barbarastr. 11, 49076 Osnabrück, Germany

manuscript submitted

Summary

Fungi produce spores that allow for their dispersal and survival under harsh environmental conditions. These spores can have an astonishing variety of shapes and sizes. Using the highly polar, needle-shaped spores of the ascomycete *Ashbya gossypii* as a model, we demonstrated that spores produced by this organism are not simple continuous structures but rather consist of three different segments that correlate with the accumulation of different materials: a rigid tip segment, a more fragile membrane compartment and a solid tail segment. Little is currently known about the regulatory mechanisms that control the formation of the characteristic spore morphologies. We tested a variety of mutant strains for their spore phenotypes, including spore size, shape and wall defects. The mutants that we identified as displaying such phenotypes are all known for their roles in the regulation of hyphal tip growth, including the formin protein *Ag*Bni1, the homologous Rho-type GTPases *Ag*Rho1a and *Ag*Rho1b and the scaffold protein *Ag*Pxl1. Our observations suggest that spore length is controlled by a Rho1 signaling network, which is balanced by *Ag*Pxl1 between *Ag*Bni1-dependent regulation of actin structures and additional Rho1 effectors.

Introduction

The formation of spores is a central developmental process in the fungal life cycle. Spores, as rigid and robust structures, enable the survival of the fungus in harsh environments over long periods of time and also contribute to dispersal. In the fungal kingdom, a fascinating variety of spore shapes and sizes exists. This diversity ranges from the simple, round and small spores, which are produced by the well-known model organism *Saccharomyces cerevisiae*, to very complex structures, which can be found in some freshwater fungi (reviewed by Deacon, 2006).

Major characteristics, such as spore shape and size, are precisely matched to the requirements of the fungus for its dispersal and persistence in a unique environment. The majority of spores produced by terrestrial fungi is dispersed by environmental factors such as rain splash or wind (Deacon, 2006). Spores that use rain splash as a preferred route for dispersal are often linear or curved. This elongated morphology reduces surface mobility when the spores land on a target host. Airborne spores that are dispersed by the wind are key factors in the allergic response in humans and in various fungal diseases that occur in plants and animals (reviewed by Deacon, 2006; Simon-Nobbe *et al.*, 2008). The fungi that grow on leaf surfaces, for example, produce spores with large diameters (up to 40 µm) that favor their impact at normal wind speeds. In contrast, many soil fungi produce small spores to avoid such an impact. These spores possess an average diameter of 4 to 5 µm and therefore sediment out of the air during calm atmospheric conditions (Deacon, 2006). Another class of spores is transmitted by insect vectors. This class of spores is often linear in shape, and the spores are bundled to facilitate attachment to the insect vector. How the formation of all these different spore sizes and shapes is controlled at a molecular level remains unclear because *Saccharomyces cerevisiae* and *Schizosaccharomyces pombe*, which are the two model organisms that are commonly used to study the molecular mechanisms of fungal sporulation (Neiman, 2005), only produce simple, round spores. Therefore, we recently established *Ashbya gossypii* as a model system for the investigation of complex spore morphologies (Kemper *et al.*, 2011). *A. gossypii* is a filamentous plant pathogen causing stigmatomycosis in various crop plants, particularly cotton.

The fungus infects the developing lint fibers and is associated with a dirty-yellowish color change, giving the infection its alternative name, “Cotton Staining” (Pridham and Raper, 1950). The spores of *A. gossypii* are disseminated by sucking insects and bugs. Either they stick to the mouth part of the insect as a type of appendage, or they are carried in the deep stylet pouches where they can also germinate (Pridham and Raper, 1950). Spores of *A. gossypii* are highly polar, needle-shaped structures possessing an average length of approximately 30 µm and a width of one to two µm (Batra, 1973). The polar appearance of the spores is also supported by an appendage called a ligament, which is fused to the posterior side and is responsible for bundling of the spores.

Actin is a key factor in the development of the needle-shaped spores of *A. gossypii* (Kemper *et al.*, 2011). Sporulation-specific linear actin filaments are directly connected to the nuclei and are only found in this unique developmental stage. These specific actin structures are polymerized by the formin protein *Ag*Bnr2, which is one of two Bnr homologs encoded in the genome of *A. gossypii* (Kemper *et al.*, 2011). Furthermore, *Ag*Bnr2 links actin to the spindle pole body during sporulation, which is a function essential for spore formation. Downregulation of *Ag*Bnr2 leads to defects in the formation of sporangia and a decrease in the total spore number (Kemper *et al.*, 2011).

Because of the important role of actin in the sporulation process, in the present study, we analyzed a variety of mutants with alterations in genes that are known for their role in actin regulation and sporulation defects. Using this strategy, we identified several components of a network that regulates spore length and spore-wall integrity, providing the first insight into the mechanisms that control the spore morphologies of fungi.

Results

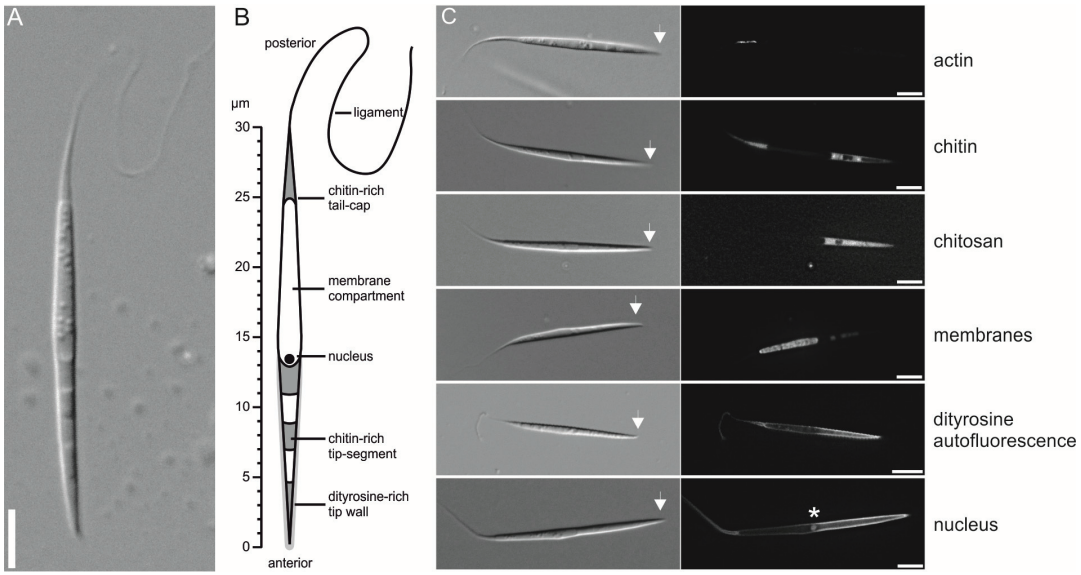

Figure 1: Spore morphology of *Ashbya gossypii.* A) A single needle-shaped spore produced by *A. gossypii.* The scale bar represents 5 µm. B) Schematic drawing of an *A. gossypii* spore, which represents the results from fluorescence microscopy shown on the right side. C) Various fluorescent-staining procedures revealed a composite spore structure. Actin staining was performed using rhodamine-phalloidin; chitin was stained with calcofluor white; chitosan was visualized using eosin Y; membranes were stained using $DiOC_6(3)$; dityrosine-autofluorescence was observed using a CFP filter; and the position of the nucleus was detected using a strain possessing a CFP-tagged version of the histone *Ag*Hhf1. Note that, in the latter case, dityrosine-autofluorescence is also visible. The asterisk indicates the position of the nucleus. The arrows indicate the anterior side of the spore. The scale bars represent 5 µm.

The needle-shaped spores of *Ashbya gossypii* are composite structures.

To allow a better characterization of spore phenotypes, we first conducted a closer examination of the architecture of the needle-shaped spores. Spores produced by *A. gossypii* display an average length of approximately 30 µm, with a narrow standard deviation of 2.5 µm and a width of one to two micrometers. Analyzing spores by light microscopy, Batra (1973) described the existence of a septum-like structure. To further characterize the spore architecture, we used epifluorescence and selective staining methods to visualize substances that were previously identified in the spores of several ascomycetes. We used rhodamine-phalloidin to stain actin structures in the spores. We found that actin was a key component of the tail segment, suggesting that actin is involved in formation of a junction between the spore and the ligament (Figure 1C),

possessing a length of approximately four to five micrometers. Calcofluor white is a dye that stains chitin and cellulose. Because cellulose is not found in *A. gossypii* spores, the dye specifically stains chitin in this organism. Staining of the spores revealed that chitin could be found in the tip and the rigid section of the tail segment. We did not observe an equal distribution of chitin in the tip segment. Instead, we found rings where chitin appeared to be concentrated within this segment. In contrast, chitin in the tail segment appeared to be evenly distributed (Figure 1C). In the close relative *S. cerevisiae*, the outer layer of the spore wall has been described as predominantly consisting of chitosan, the deacetylated form of chitin (Briza *et al.*, 1988), which is believed to strengthen the spore wall. To distinguish between chitin and chitosan, we performed staining of the spores with eosin Y, a dye that specifically stains chitosan but not chitin (Baker *et al.*, 2007). Surprisingly, we found chitosan in the tip segment but not the tail segment (Figure 1C). Within the tip segment, we observed the three regions that correlate with an accumulation of chitin. Instead, we found a more even distribution of chitosan in the tip segment. Our results demonstrate that chitin is specific to the rigid section of the tail cap and to the three ring-like structures within the tip compartment, whereas chitosan is evenly distributed in this part of the spore. Our finding that chitosan is a component of the spore wall raised the question of whether this material is essential for spore formation. Furthermore, we speculated that chitosan, which can be found particularly in the rigid tip segment, contributes to the stability of the needle-shaped spores. To investigate the importance of chitosan for sporulation, we deleted *Ag*Cda1, the sole chitin deacetylase encoded by the genome of *A. gossypii.* Interestingly, we found that deletion of this enzyme, which catalyzes the deacetylation of chitin, leads to severe sporulation defects. *Agcda1* hyphae grow as in the wild type but produce almost no spores (Supplemental Figure S1), indicating that production of chitosan is essential for spore development in *A. gossypii*. $DiOC_6(3)$, a dye that we used to localize the membrane structures within the spore, revealed that lipids are the key component of the middle compartment of the spore. It remains unclear if the membrane that was identified in this part of the spore is the sole spore membrane or if other segments also possess membranous structures that are not accessible for staining.

Identification of the various spore segments raised the question of where the nucleus is located within this structure. To answer this question, we prepared spores of a strain containing an allele of histone 4 (*Ag*Hhf1) tagged with the Cyan Fluorescent Protein (CFP). Using fluorescence microscopy, we identified a clear localization pattern of the nucleus in the spores. In all cases, the nucleus was located in the membrane compartment and was found to be near the middle section of the spore (Figure 1B and C). The position of the nucleus correlated with the widest part of the spore. Using the CFP filter, we observed strong fluorescence in the outer layer of the tip segment and, to a lesser extent, in the tail cap. An autofluorescent signal with the same localization pattern was revealed with the CFP filter in our control experiment, which involved wild-type spores possessing no CFP-tagged proteins (Figure 1C). Previous studies of *A. gossypii* have used HPLC to identify dityrosine as a central component of the needle-shaped spores (Prillinger *et al.*, 1997). Considering the excitation and emission values of dityrosine (Suda *et al.*, 2009), we concluded that the autofluorescence of the spores indicates the accumulation of this compound in the spore wall of *A. gossypii* spores.

All these microscopic observations suggest that the spores from *A. gossypii*, which at first glance appear to be simple linear structures, can each be divided into three major segments (Figure 1A and B). They possess a rigid tip segment (indicated by the presence of chitosan) followed by a more fragile membrane compartment in the middle of the spore, which lacks both chitin and chitosan, and a third segment at the posterior side, which also includes the ligament and which we named the tail segment. This segment contains chitin, but no chitosan, and thus it is probably more stable than is the membrane compartment. The dimensions of the different segments follow a clear pattern: almost one-half of the spore comprises the tip segment, whereas the other half comprises the membrane compartment and the rigid section of the tail segment (Figure 1B). The widest part of the spore is located at the border between the tip and the membrane segment.

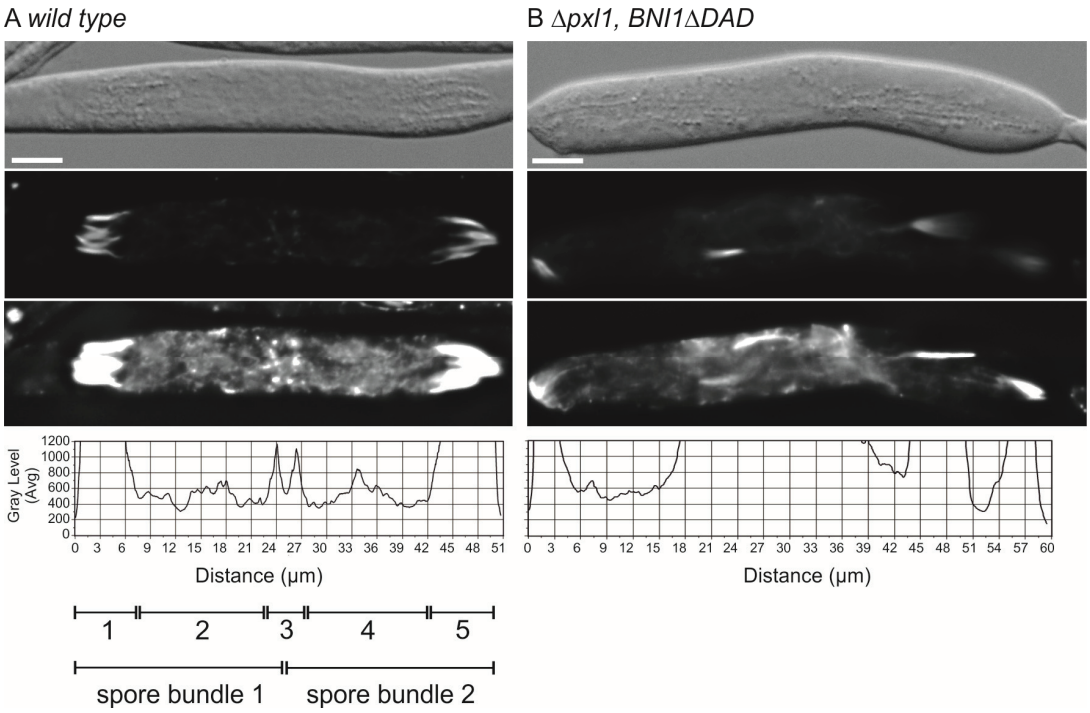

Figure 2: Actin staining of sporangia identifies five regions of actin accumulation.
A) Actin staining of wild-type sporangia with rhodamine-phalloidin. First row: brightfield image; second row: fluorescence image scaled to normal levels without overexposure; third row: same image overexposed to visualize regions of weaker staining; and fourth row: line-scan diagram displaying average grey intensities along the length and width of the entire sporangium. The diagram is scaled to visualize intensities in the weaker regions. Bars represent the different areas of actin accumulation and the corresponding actin bundles.
B) Actin staining of the sporangia of *ΔpxI1, BNI1ΔDAD* with rhodamine-phalloidin. The image types in each row are identical to the types above. The scaling of the abscissa is identical to the left graph. No clear pattern of actin accumulation was observed. The scale bars represent 10 µm.

Five regions composed of actin structures correlate with the formation of spores in a sporangium.

We have previously shown that filamentous actin structures are essential for spore formation (Kemper *et al.*, 2011). To gain a deeper insight into the role of actin in spore morphology, we stained sporangia from a two-day-old mycelium that was cultured in minimal media with rhodamine-phalloidin for observation of actin structures during spore formation. Fluorescence microscopy revealed five different regions that were characterized by an accumulation of actin (Figure 2A). The first region consisted of linear actin bundles with a length of approximately 6 µm (n=63) and a width of approximately 1 µm at the widest part (Figure 2A, regions 1 and 5). Comparison with brightfield images revealed that these structures correlated with the developing tip structures of the spores. This

finding is supported by the observation that these structures were organized in bundles of mostly four to six elements, a pattern that resembled the arrangement of the mature spores in the sporangium. Moreover, we found that the spore bundles, which are commonly found in a sporangium, were always oriented with the tips of the spores toward both ends and the ligaments toward the middle of the sporangium. The actin structures of the spore tips stained much brighter than did all the other filamentous actin structures that we have so far observed in *A. gossypii*. Therefore, the images had to be overexposed to visualize the other actin structures that were present in the sporangia. The second actin-rich region was located toward the middle of the developing spore and correlated with the membrane compartment (Figure 2A, regions 2 and 4). This part was characterized by lower amounts of actin that accumulated in patches rather than filaments, which led to a diffuse staining of this region. We also identified an additional region in which actin was concentrated within the sporangium. This part of the sporangium might correlate with the production of the tail segment, including the connection between the spore and the ligament, which we discovered to be a region in which actin was retained in mature spores (Figure 2A, region 5).

Synthetic sporulation defects in the mutant strain *ΔAgpxl1, AgBNI1ΔDAD*

Because we recently identified the formin *Ag*Bnr2 as an important factor in spore formation, we screened mutants of other formin family members, Rho-type GTPase family members, as potential formin activators, and regulators of Rho-type GTPases for sporulation defects. We observed a specific sporulation phenotype for the strain *ΔAgpxl1, AgBNI1ΔDAD*. This double-mutant strain possesses, on the one hand, a deletion of the fungal paxillin homolog *Ag*Pxl1 (Knechtle *et al.*, 2008) and, on the other hand, a constitutively active form of the formin protein *Ag*Bni1 (Schmitz *et al.*, 2006). Our investigations of the structure of the actin cytoskeleton in the developing sporangia of this double mutant revealed defects in the arrangement of the five characteristic actin-rich regions that we identified for the wild type (Figure 2B). Instead, we found a disordered accumulation of actin within the sporangia and failed to detect the typical structures, indicating that the spore development was disturbed. When we more closely observed the spores produced by this double mutant, we discovered

that all the linear spores produced by this strain displayed a significant increase in spore size (Figure 3A and B). The average spore size of the double mutant *ΔAgpxl1, AgBNI1ΔDAD* was approximately 43 µm (Figure 3B). A striking finding was that, despite the general increase in spore size, the proportions of the different segments were constant. Similar to the wild type, approximately one-half of the spore consisted of the tip segment, whereas the other half consisted of the membrane compartment and the rigid section of the tail segment. The dramatic increase in spore length was not observed in either of the single-mutant strains (Figure 3A and B). The *Agpxl1* deletion strain had an average spore length of approximately 28 µm, suggesting that its size was slightly but significantly decreased. The single mutation *AgBNI1ΔDAD* did not affect spore size. With an average spore length of approximately 30 µm, this mutant was comparable to the wild type (Figure 3A and B). In addition to the size phenotype, approximately 1% of the spores showed additional defects; the spores were Y-shaped or branched at different angles (Figure 3C). We did not find any branched spores in either single mutant strain, suggesting that the dramatic increase in spore size and the formation of branched spores is a synthetic phenotype in *A. gossypii*.

In metazoans, paxillins act as scaffold proteins that are involved in the recruitment of diverse regulatory and structural proteins. Because of this function, paxillins can be considered a central component in the dynamic organization of the cytoskeleton and in the coordination of Rho-type GTPases (Deakin & Turner, 2008). In fungi, related functions have been described. For example, the paxillin-like protein of *S. cerevisiae* coordinates *Sc*Cdc42 and *Sc*Rho1 functions during polarized growth (Gao *et al.*, 2004). Both GTPases are described as participating in related processes in yeast, and the coordination of these regulators by *Sc*Pxl1 ensures successful budding. In summary, both types of proteins (the formins and the paxillins) are involved in Rho signaling, a similarity that requires further investigations of Rho-mediated signal transduction in *A. gossypii.*

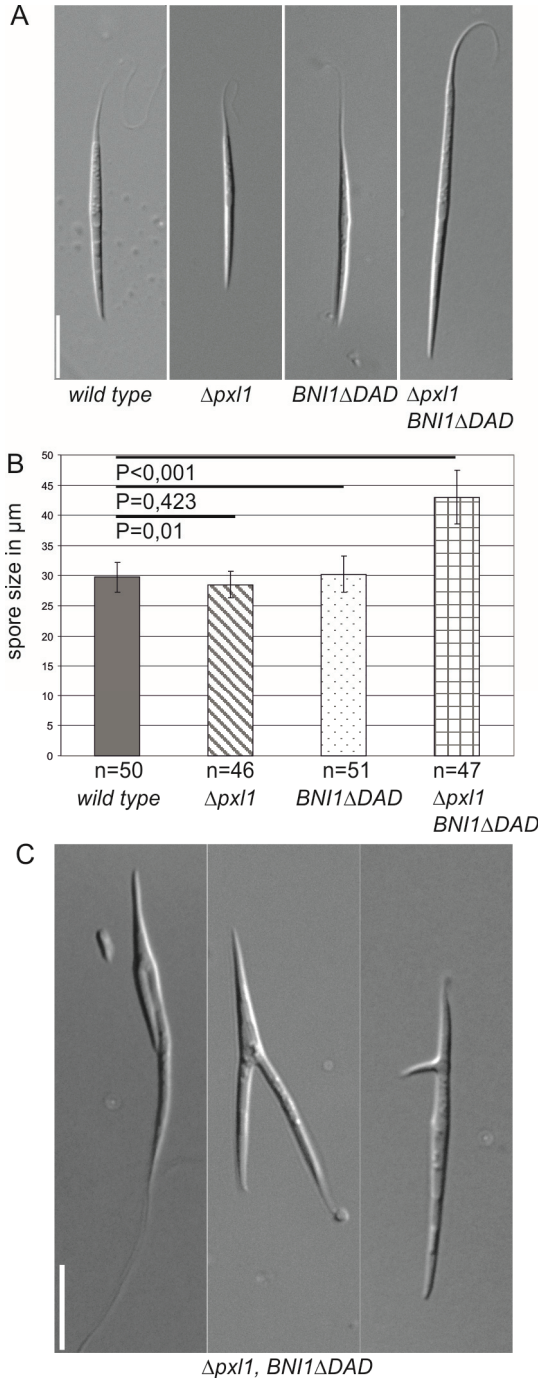

Figure 3: *ΔAgpxl1, AgBNI1ΔDAD* displays synthetic sporulation defects.
A) Representative DIC-images of the wild type, *ΔAgpxl1, AgBNI1ΔDAD* and a mutant combining both deletions. The scale bars represent 10 µm. B) Average spore length for the given number (n) of the strains referred to above. P-values indicating the statistical relevance are stated for the number (n) of spores measured. C) Brightfield images of an additional phenotype that is present in approximately 1% of the spores of the mutant strain *ΔAgpxl1, AgBNI1ΔDAD*. The scale bars represent 10 µm.

The protein family of Rho-type GTPases represents common interaction partners of *Ag*Bni1 and *Ag*Pxl1.

The synthetic sporulation phenotype of the *A. gossypii* mutant strain *ΔAgpxl1, AgBNI1ΔDAD* raised a question about the potential link between these proteins. We were unable to detect any direct interaction between *Ag*Pxl1 and *Ag*Bni1 using the yeast two-hybrid system (data not shown). We considered the

possibility of an indirect interaction including a third protein as a linker. Both types of proteins, formins and paxillins, are described as being involved in the regulation of the actin cytoskeleton, and both proteins are known to interact with small GTPases of the Rho family (Kohno *et al.*, 1996; Watanabe *et al.*, 1997; Gao *et al.*, 2004). Therefore, we speculated that Rho-type GTPases may represent the missing link between *Ag*Bni1 and *Ag*Pxl1. The genome of *A. gossypii* encodes seven Rho-type GTPases: *Ag*Rho1a and *Ag*Rho1b, *Ag*Rho2 to *Ag*Rho5, and *Ag*Cdc42 (Dietrich *et al.*, 2004). As the first step, we decided to determine which of the seven GTPases are capable of activating the formin protein *Ag*Bni1. Because of its characteristic domain structure, *Ag*Bni1 belongs to the group of Diaphanous-related formins. The activation of these proteins involves the disruption of the autoinhibitory interaction of the N-terminal-located Diaphanous inhibitory domain (DID) and the C-terminal-located Diaphanous autoregulatory domain (DAD; Alberts 2001). Active, GTP-bound Rho proteins bind to the Rho binding domain (RBD) of the formin protein, which is likewise located at the N-terminus of the protein. This activation process leads to a disruption of the intramolecular protein interaction of *Ag*Bni1 (Figure 4A). We took advantage of this special regulatory mechanism and performed a modified yeast two-hybrid assay to identify potential activators of *Ag*Bni1. To this end, we fused the N-terminus of *Ag*Bni1, which included the RBD and the DID, to the Gal4 activation domain, and we fused a C-terminal fragment, which included the DAD, to the Gal4 binding domain (Figure 4B). These two-hybrid constructs displayed only weak interactions. To include the Rho-type GTPases in this experiment, we constructed an additional vector. All seven GTPases in their constitutively active forms were fused in frame to the nuclear localization signal of SV40 to ensure that the proteins would be targeted to the nucleus. Then we tested the two-hybrid constructs of the carboxy and amino termini of *Ag*Bni1 combined with all seven GTPases as competitors for the interaction. If a Rho-type GTPase could bind to the Rho-binding domain of *Ag*Bni1 and its affinity was stronger compared to the C-terminal part of *Ag*Bni1, then the interaction of the two-hybrid constructs was blocked, and growth on the corresponding selection medium was inhibited (Figure 4B). Using this inhibition assay, we were able to identify four potential activators of *Ag*Bni1: *Ag*Rho1a, *Ag*Rho1b, *Ag*Rho3 and *Ag*Rho4 (Figure 4C). As a control experiment, we performed a

similar inhibition assay using the wild-type forms of the GTPases. As expected, none of the wild-type GTPases was capable of disrupting the interaction between the N-terminus and the C-terminus of *Ag*Bni1 because they were not in the active state (Figure 4C).

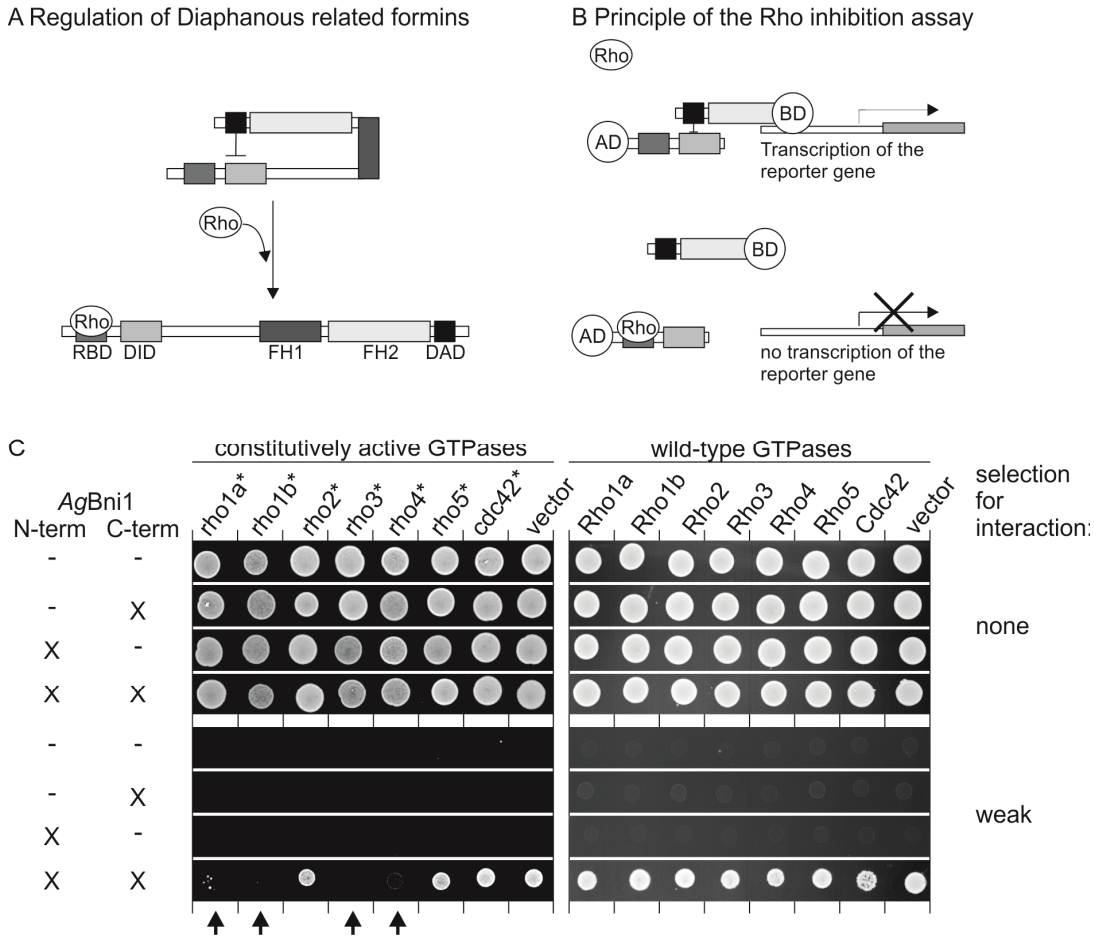

Figure 4: A Rho-inhibition assay identifies four potential activators of *Ag*Bni1.
A) Regulation of the Diaphanous-related formins (DRF). B) Principle of the Rho-inhibition assay. C) The Rho-inhibition assay performed for constitutively active GTPases (left side) and wild-type GTPases as a control (right side). *Ag*rho1a*, *Ag*rho1b*, *Ag*rho3* and *Ag*rho4* are capable of disrupting the interaction in the two-hybrid experiment and are potential activators of *Ag*Bni1. Selection for weak interactions was performed on a medium lacking histidine. For details, see the experimental procedures.

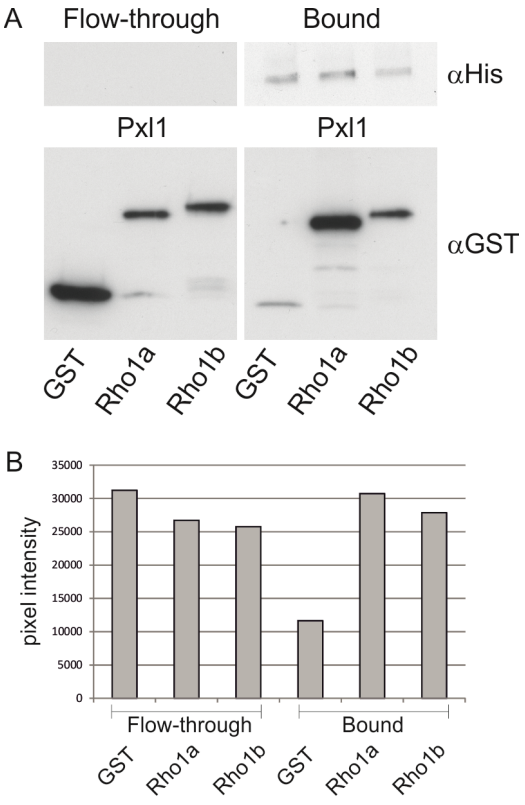

Figure 5: *Ag*Pxl1 interacts directly with *Ag*Rho1a and *Ag*Rho1b.
A) An *in vitro* binding assay was performed using purified proteins. The GTPases were loaded with GDP before the experiment. Pull-down was performed using His_6-*Ag*Pxl1. The bound GST-tagged GTPases were detected using a GST-antibody. B) Determination of the pixel intensities of each probe.

*Ag*Pxl1 interacts directly with *Ag*Rho1a and *Ag*Rho1b.

Paxillins are known to contribute to the regulation of Rho-type GTPases and, consequently, their signaling to downstream effectors. Paxillins fulfill this function by recruiting various GAPs, GEFs and effector proteins to the site of action (Deakin & Turner, 2008). In fungi, it has also been shown that the fungal homologs of paxillins might act as negative regulators of Rho signaling. *Sc*Pxl1 of *S. cerevisiae* interacts preferentially with the inactive, GDP-bound form of *Sc*Rho1, suggesting that this scaffold protein might downregulate its function (Gao *et al.*, 2004). In addition, the physical interaction of *Sc*Pxl1 and *Sc*Rho1 might contribute to the coordination of the GTPases Rho1 and Cdc42 during polarized growth. We considered a similar situation in the close relative, *A. gossypii*. In contrast to *S. cerevisiae*, this fungus possesses two homologs of Rho1 called *Ag*Rho1a and *Ag*Rho1b (Köhli *et al.*, 2008). We wanted to discover if *Ag*Pxl1 interacts with either *Ag*Rho1a or *Ag*Rho1b or even with both GTPases in the GDP-bound state. To this end, we performed pull-down experiments according to the methods of Gao *et al.* (2004). In the first step, His_6-*Ag*Pxl1, GST-*Ag*Rho1a and GST-*Ag*Rho1b were expressed in *E. coli* and purified. The GTPases were loaded with GDP before the experiment, and the pull-down of

protein complexes was performed via His_6-*Ag*Pxl1. We observed the interaction of *Ag*Pxl1 with both GTPases but especially with *Ag*Rho1a, which appeared to be the preferred interaction partner (Figure 5A). We measured the pixel intensities of each probe and could show that the amount of *Ag*Rho1b derived from the pull-down was only approximately 90% compared with the amount of *Ag*Rho1a (Figure 5B).

These results, taken together with our findings on the activation of *Ag*Bni1, led us to focus our investigation on *Ag*Rho1a and *Ag*Rho1b. Both regulators are interaction partners of *Ag*Bni1 and *Ag*Pxl1, so they might represent the missing link between these proteins.

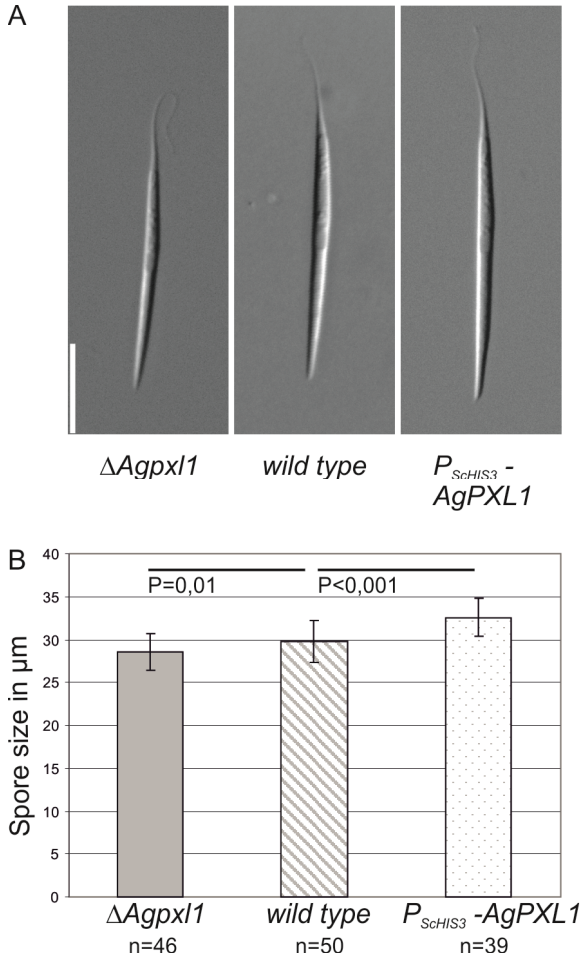

Figure 6: The expression level of *AgPXL1* affects spore length.
A) Representative spores of an *Agpxl1* deletion, a wild type and an *AgPXL1* overexpression strain. The scale bar represents 10 µm. B) Determination of the average size of spores from the above-referenced strains using the given number (n) of spores. The P-values indicate the statistical significance of the differences in size.

Deletion and overexpression of *AgPXL1* affect spore size.

Our previous data suggest a role for the scaffold protein *Ag*Pxl1 in the regulation of spore size. Therefore, we decided to investigate whether only the absence but also the overexpression of *AgPXL1* would influence spore length.

To achieve the overexpression of *AgPXL1,* we replaced its promoter with the *HIS3* promoter of *S. cerevisiae,* which has been previously reported to cause overexpression in *A. gossypii* (Kemper *et al*., 2011). We isolated spores of the *Agpxl1* deletion strain and the *AgPXL1* overexpression strain described above. As mentioned before, the spore size in the deletion strain was slightly decreased to 28 µm compared with the wild type. In contrast, spores produced by the *AgPXL1* overexpression strain displayed an increase in spore length. We detected an average spore size of approximately 32 µm. Determination of the P-values demonstrated that these small deviations were statistically significant. These findings suggest that there is a correlation between the expression level of *PXL1* and spore size (Figure 6A and B), but not with other defects in spore morphology.

Integration of constitutively active forms of *Ag*Rho1a and *Ag*Rho1b leads to an increase in spore size.

Our investigations of the genetic and physical interactions of *Ag*Bni1 and *Ag*Pxl1 suggest a role of the Rho1 signaling pathway in the sporulation of *A. gossypii*. Rho1 signaling in this organism includes two GTPases: *Ag*Rho1a and *Ag*Rho1b. These GTPases can be easily converted into a constitutively active form by a single point mutation (Köhli *et al.*, 2008). However, the substitution of the wild-type gene is lethal in the case of *AgRHO1b* and leads to a general decrease in fitness in the case of *AgRHO1a* (Köhli *et al*., 2008). Therefore, we integrated the alleles for the GTPases in addition to the wild-type copy at the *leu2* locus. The resultant strains thus retained the wild-type genes in their genetic background. We isolated spores of these strains and evaluated their size and morphology. In both cases, we observed an increase in spore length. In the case of *Agrho1a**, we documented an average spore size of approximately 33 µm (Figure 7A and B). Spores that were produced by the mutant strain *Agrho1b** possessed a spore length of 36 µm (Figure 7A and B). We concluded that both GTPases have a direct effect on spore size, on which the influence of *Ag*Rho1b appears to be stronger. This might be because the additional alleles for the GTPases are under the control of their native promoters and that expression of *AgRHO1b* is much stronger compared to *AgRHO1a* (our unpublished results). However, the spore morphology in both

mutant strains was comparable to the wild type. The proportions of the different segments follow the typical pattern without any abnormities (Figure 7A).

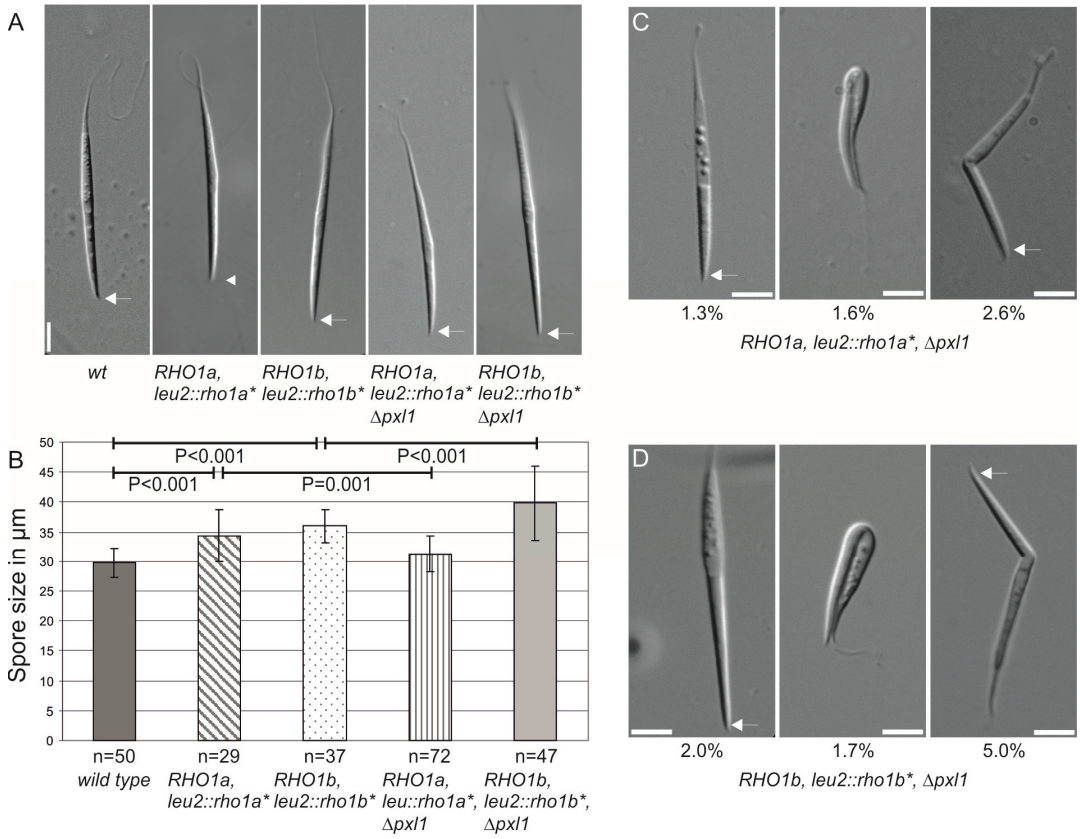

Figure 7: Constitutively active forms of *Ag*Rho1a and *Ag*Rho1b cause an increase in spore length and spore wall defects in an *Agpxl1* deletion background.
A) Brightfield images of representative spores from the wild type, strains carrying additional alleles encoding the constitutively active forms of *Ag*Rho1a and *Ag*Rho1b and the same alleles in an *Agpxl1* deletion background. The scale bars represent 5 µm. B) Average spore sizes for the number (n) of spores from the strains described above. P-values indicate the statistical significance of the differences in size. C) Brightfield images of the spore wall defects associated with the double mutant *Agrho1a*, ΔAgpxl1*. Frequencies of the phenotypes are stated as percentages. D) Brightfield images of spore wall defects associated with the double mutant *Agrho1b*, ΔAgpxl1*. Frequencies of the phenotypes are stated as percentages. The scale bars represent 5 µm. The arrows indicate the anterior side of the spores.

We also wanted to more precisely determine the role of *Ag*Pxl1 in this scenario. Therefore, we combined the deletion of *Agpxl1* with the constitutively active forms of *Ag*Rho1a and *Ag*Rho1b. Unexpectedly, we found an additional increase in the size of the linear spores for the strain carrying an active *Agrho1b** and the *Agpxl1* deletion (Figure 7A and B). The average spore length was approximately 40 µm in this strain. We determined the P-value and found that the difference in spore length was statistically significant (P<0.001). In

contrast, we observed a decrease in spore length in the strain carrying the additional allele for *Agrho1a** and the deletion of *Agpxl1,* compared with the strain *Agrho1a** possessing the *AgPXL1* gene. We measured an average spore size of approximately 31 µm, compared to 33 µm in the double mutant (Figure 7A and B). Again, we determined that this difference in size was statistically significant (P=0.001).

In addition to size, we analyzed approximately 300 spores of each mutant strain for morphological defects. Unlike the wild-type background, the introduction of *Agrho1a** and *Agrho1b** leads to a rising number of abnormal spores in the *Agpxl1* deletion background. As shown in Figures 7C and 7D, we observed several spores that possessed a hyaline membrane compartment (1.3% in *Agrho1a** and 2% in *Agrho1b**), suggesting that the spore wall is thinner compared to the wild type. This might also lead to the formation of the kink that we observed at the connection between the membrane and the tip segment in several spores (4.2% in *Agrho1a**, 6.7% in *Agrho1b**) (Figure 7C and D). We failed to detect comparable morphological defects in spores produced by the wild type. Ultimately, we found that more spores from the *ΔAgpxl1, Agrho1b** mutant displayed morphological defects (8.7%) compared with the *ΔAgpxl1, Agrho1a** strain (5.5%). Remarkably, the phenotypes affecting spore morphology were comparable in both *rho1* mutants, indicating that the observed defects in the spore wall result from a signaling pathway that includes both GTPases.

The deletion of *Ag*Rho1a causes defects in the formation of the membrane compartment of the spore.

The integration of the constitutively active forms of *Ag*Rho1a and *Ag*Rho1b clearly indicates a role for both GTPases in the regulation of spore size. We asked whether the deletion of these regulatory proteins also influences the morphology of the spores. The deletion of *Ag*Rho1b is lethal in *A. gossypii* (Köhli *et al.*, 2008); therefore, experiments on the absence of this protein were not possible. However, we performed additional investigations of the *Agrho1a* deletion strain. Spores prepared from this mutant strain display a size comparable to the wild type, indicating that the deletion of *Ag*Rho1a does not influence spore length.

Nevertheless, we found a phenotype of the *Agrho1a* deletion that affects the spore wall. We observed many spores with defects particularly in the membrane compartment. In this case, the membrane compartment appears to be hyaline, suggesting that the spore wall is particularly thin (Supplemental Figure S2). Moreover, we found that many spores are susceptible to spore lysis. Storage in 0.03% Triton X-100 resulted in swelling of the membrane compartment, which became more severe over time and resulted in destruction of the spores. We documented the spore morphology of 214 spores and observed swelling of the membrane compartment in 20% of the examined spores after three hours of incubation in 0.03% Triton X-100 (Supplemental Figure S2). This indicates a role of *Ag*Rho1a in the formation of the membrane compartment in particular. This function seems to be Rho1a-specific and cannot be fulfilled by the homologous *Ag*Rho1b GTPase.

$Agbni1_{S250P}$ affects spore length and morphology.

Although we observed the sporulation phenotypes of the Rho1 mutants and found that the Rho1 proteins are potential activators of *Ag*Bni1, it still remained unclear whether the effect of Rho1-signaling on sporulation acts via *Ag*Bni1 or a different Rho1 effector. To address this question, we investigated spores from an *Ag*Bni1 mutant that we had isolated in a previous study. In that study, we identified several amino acid substitutions that affect the interaction of *Ag*Bni1 with Rho-type GTPases (Lickfeld & Schmitz, 2011). One mutation that reduces the interaction of *Ag*Bni1 and *Ag*Rho proteins is *Ag*$Bni1_{S250P}$. Figure 8A shows that this mutation does not affect the intramolecular, autoinhibitory binding of the amino- and carboxy-terminal parts of *Ag*Bni1 in the two-hybrid assay. Rather, the mutation affects binding of mainly Rho1b, which became obvious when testing the Rho binding domain of *Ag*Bni1 for interaction with the Rho1 proteins (Figure 8B). Thus, any phenotype observed in this mutant should be caused by the reduction of Rho-binding and not by a potential effect on the autoregulation of *Ag*Bni1. We integrated $Agbni1_{S250P}$ using an integrative plasmid at the *leu2* locus in the *Agbni1* deletion strain. The strain possessing $Agbni1_{S250P}$ was viable, indicating that the mutant allele can complement the lethal deletion of *AgBNI1*. This also indicates that binding of *Ag*Rho1b is not essential for activation of *Ag*Bni1 during vegetative growth. As was done for the

other mutants, we prepared spores from this strain and determined their average length. The spores were approximately 36 µm in size, which was a significant increase in spore length (Figure 8C). Thus, Rho1 signaling to the effector protein *Ag*Bni1 plays an essential role in the determination of spore length.

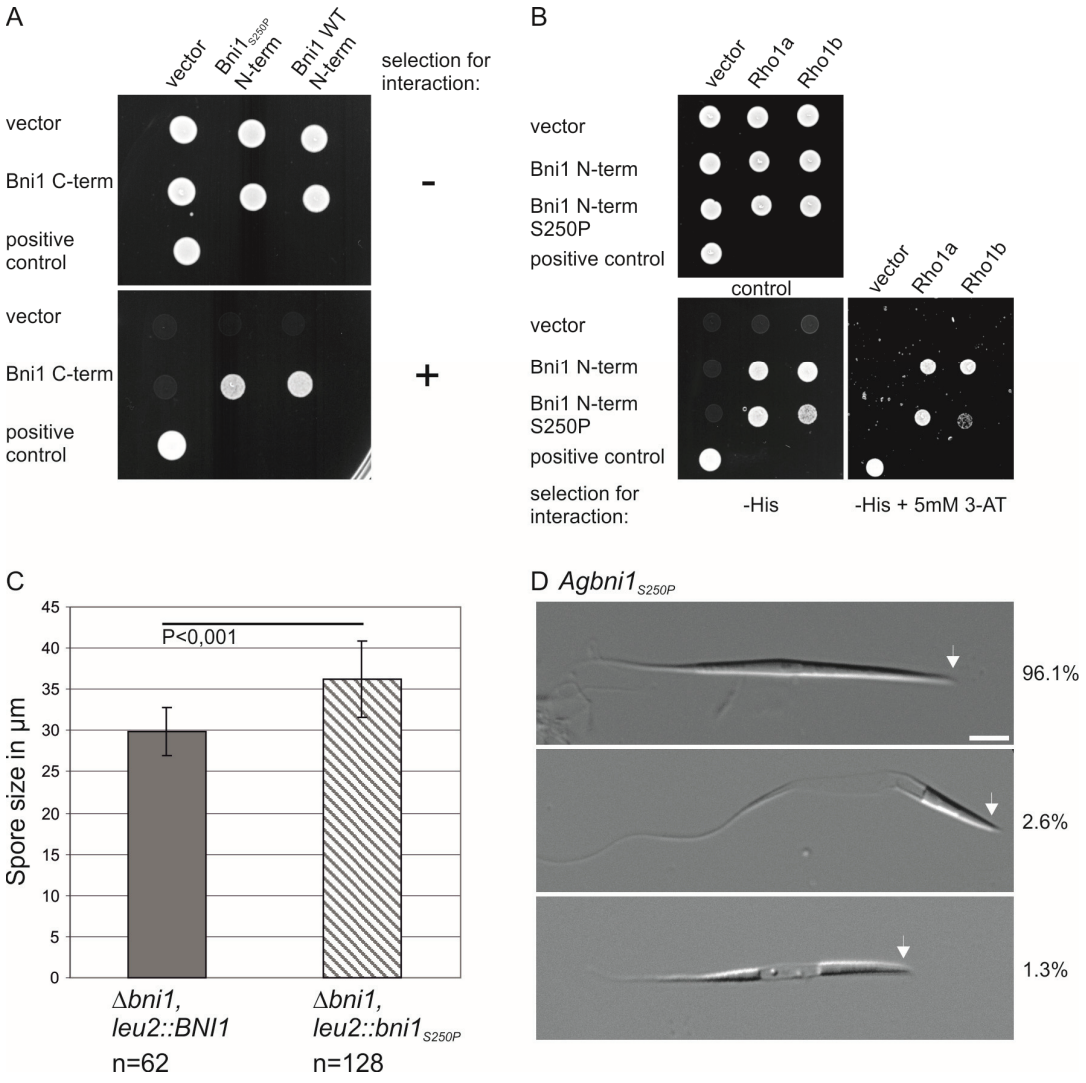

Figure 8: *Agbni1*$_{S250P}$ affects Rho1-binding, spore size and spore integrity.
A) Two-hybrid studies of the interaction of *Ag*Bni1$_{1\text{-}828}$ with and without the S250P-mutation and *Ag*Bni1$_{1522\text{-}1918}$. Selection for the interaction was performed on media lacking histidine. The introduction of the point mutation S250P into *Ag*Bni1 did not disturb the autoinhibitory interaction of the N-terminus and the C-terminus. B) Two-hybrid studies of the effect of the S250P mutation on Rho1-binding. Selection for the interaction was performed either on media lacking histidine or on media lacking histidine but additionally supplemented with 5 mM 3-aminotriazole to increase the stringency of selection. C) Average spore length of a strain carrying a genomic integration of *Agbni1*$_{S250P}$. The spore size was measured for the indicated number of spores (n). The P-value represents the statistical significance. D) Brightfield images of spores from the mutant strain. The frequencies of observation are stated as percentages. The scale bar represents 5 µm. Arrows mark the anterior side of the spore.

Additional microscopic examination revealed an increased number of spores with defects in their membrane compartments. The spore wall appears to be comprised of a hyaline material, especially in the middle of the spore, whereas the posteriorly located tail segment is well established (Figure 8D). Examination of 307 spores isolated from the *Agbni1$_{S250P}$* strain revealed that 3.9% possessed a defect in the membrane compartment, which could not be found in the wild type strain.

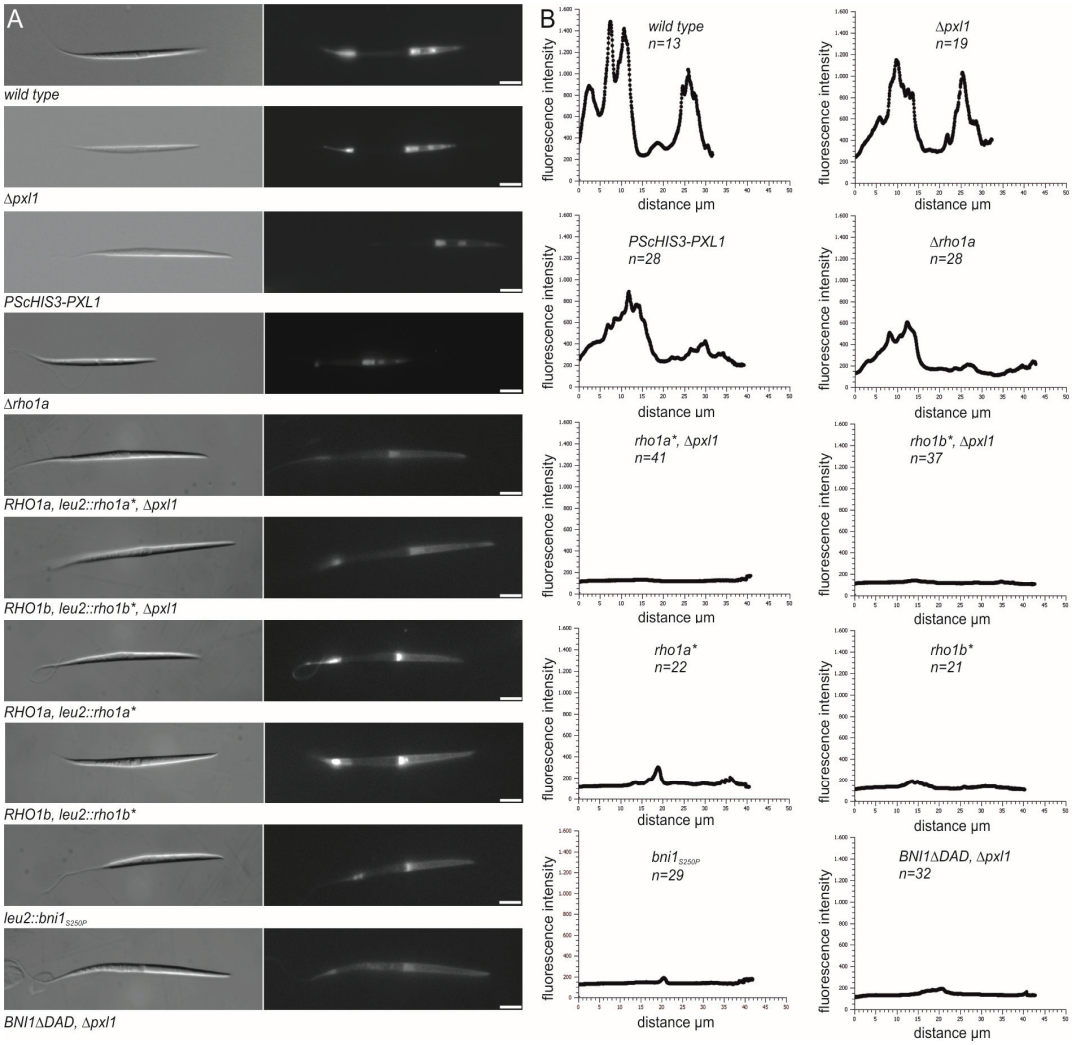

Figure 9: Mutants displaying a sporulation phenotype show variations in their spore-wall chitin content.
A) Calcofluor-white staining of different single and double mutant strains that display sporulation phenotypes. The spores were stained for one hour and analyzed using identical exposure times. Note that fluorescence images of *RHO1a; leu2::rho1a*; Δpxl1, RHO1b; leu2::rho1b*; Δpxl1, RHO1a; leu2::rho1a*, RHO1b; leu2::rho1b*, leu2::bni1S250P*; and *BNI1ΔDAD, Δpxl1* are scaled to a 10-fold intensity to visualize weak signals. The position and intensity of the chitin accumulation varied in different mutant strains. The scale bars represent 5 µm. B) Quantification of the fluorescence intensities using the line-scan function of MetaMorph. The Y-axis indicates the relative fluorescence intensity. The X-axis indicates the distance from the anteriorly located tip of the spore in micrometers. The number (n) of strains measured is stated for each strain.

Mutants displaying defects in spore size and morphology show a significant reduction of chitin content in their mature spores.

During investigation of the different mutant strains that expose sporulation defects, we observed changes in the rigidity of the mature spores compared with the wild type. We asked whether these abnormities correlate with variations in the production of stabilizing materials such as chitin. To answer this question, we stained wild-type and mutant spores with calcofluor white to visualize chitin in the spores. In fact, we found that the spores that were produced by most of the mutants contained less chitin compared with the wild type (Figure 9A). To more precisely determine the extent of these differences in chitin content, we measured the fluorescence intensities along the entire length of the spores from anterior to posterior. Using the line-scan function of the MetaMorph software, we documented the fluorescence intensity relative to the distance from the spore tip.

The experiment revealed that all of the examined mutants presented a reduction in chitin content. The brightness of the images from the mutant spores displayed in Figure 9A had to be increased at least 10-fold to enable visibility. Thus, only the graphs in Figure 9B allow comparison of the signal strength. The mutants could be categorized into two different classes based on the distribution and localization of chitin within the spores. The first class displayed a chitin distribution that is similar to the wild type. We found the characteristic chitin accumulation in the tip segment and one area in the tail cap, but the fluorescence intensity was decreased, indicating that the spores possess less chitin. We observed this phenotype for the *Agpxl1* deletion and overexpression strains, whereas the overexpression strain possessed less chitin compared with the deletion strain. The *Agrho1a* deletion strain displayed a similar phenotype, but the fluorescence intensity was reduced to one-third of the intensity that was measured for wild-type spores (Figure 9B). The second class of mutant strains shows a dramatic decrease in fluorescence intensity, which is only about one-tenth of the intensity we measured for the wild-type spores. Moreover, we were unable to identify the three characteristic chitin-rich rings in the tip segment of the spores. Instead, we found slight chitin enrichment in the middle of the spore at the border between the tip and the membrane segment and an accumulation of chitin in the rigid part of the tail segment. We found this unusual distribution

of chitin in spores of the mutant strains *Agrho1a** and *Agrho1b*.* We observed similar results for both double mutants (*Agrho1a** and *Agrho1b**) that have the additional *Agpxl1* deletion, but their chitin content appears to be even less compared with the single mutants. Staining of spores produced by the strains *Agbni1*$_{S250P}$ and *AgBNI1ΔDAD, ΔAgpxl1* identified the same defect in the spore structure (Figure 9B).

Discussion

In this study, we sought to gain a deeper insight into the molecular mechanisms that control spore morphology in filamentous fungi. For a better understanding of spore morphology defects, we first performed a detailed characterization of wild-type spores. Surprisingly, the needle-shaped spores produced by *Ashbya gossypii*, which appear as simple linear structures, are in fact composite structures formed by three major segments. We identified a tip segment located at the anterior side of the spore, a membrane compartment in the middle section and a tail segment located posteriorly. The formation of the different spore compartments involves an accumulation of distinct materials, which not only yields initial information about the properties of each compartment but also provides the first insights into the mechanism of needle-shaped spore formation.

The tip compartment likely plays an essential role in spore development, and its formation seems to occur in the early stages of spore development. This is supported by several facts. In a previous study, we found that spore formation starts with the appearance of the formin *Ag*Bnr2 at the spindle pole body, where *Ag*Bnr2 polymerizes actin and bundles actin cables (Kemper *et al.*, 2011). These thick actin filaments are identical to the actin structures that localize to the ends of sporangia (Figure 2A) and correlate with the developing tip segment. This is further supported by the position of the nucleus, which is always found directly attached to the tip-directed side of the membrane. The materials found in the tip segment suggest that it is a highly stable structure. Chitin and its deacetylated form chitosan, which is capable of forming additional cross-linking reactions, are found in the anteriorly located tip segment. In addition, we also identified an accumulation of dityrosine in the tip segment (Figure 1C). This overlap was an interesting finding because studies on sporulation in *S. cerevisiae* have revealed that the formation of the dityrosine layer depends on the chitosan layer; mutants that show defects in the production of the chitosan layer also fail to assemble the dityrosine layer (Coluccio *et al.*, 2004), indicating a functional correlation between these substances. In *A. gossypii,* the effect of the deletion of chitin deacetylase, which is responsible for formation of chitosan from chitin, was even stronger

(Supplemental Figure S1), and spores were no longer formed. Furthermore, we identified no morphological phenotypes that lead to defects in the tip compartment. All the morphological alterations that we found were associated with the membrane compartment (Figures 3C, 7C and D). This suggests that the formation of a visible spore relies on the development of the tip compartment.

Although, *A. gossypii* spores are composite structures, the size alterations that we discovered to be associated with several mutants were proportional, suggesting that the proteins that we identified participate in the formation of all three compartments. An initial question that we must discuss is whether the observed changes in size only affect spore length or spore size (length and width). Considering that the maximum increase in length that was observed was 43% of the wild type, a similar increase in width would result in an increase of only 0.5 μm. Combined with the naturally occurring variation of approximately 15%, which we observed in our measurements, this question cannot be adequately answered using light microscopy. Therefore, we will use only the term “spore length” in the following discussion, even though we are aware that it could be size in general that is regulated by the proteins that we identified.

The mutants that we identified in this study suggest that the formation of needle- shaped spores, which are highly polar structures, follows the general mechanisms of cell polarity (Nelson, 2003); All these mutants are defective in genes encoding proteins that are known to be involved in regulation and alignment of the actin cytoskeleton. For *Ag*Bni1, *Ag*Pxl1, *Ag*Rho1a and *Ag*Rho1b, such a function has been shown before only in hyphal tip growth. *Ag*Bni1, as a formin protein, is directly involved in actin polymerization of the actin cables that point toward the growing tip and enable transport of vesicles to the growth site. Loss-of-function mutants of *Ag*Bni1 completely lose cell polarity and do not form hyphae, and gain-of-function mutants display a premature tip-splitting phenotype (Schmitz *et al*., 2006). For *Ag*Pxl1, no direct effect on the actin cytoskeleton has been shown so far, but its homologs from other organisms are known to be involved in actin regulation (Gao *et al.,* 2004), and deletion mutants have a tip-splitting defect. *Ag*Bni1 is also involved in the same process. Therefore, it is very likely that, in addition, *Ag*Pxl1 somehow influences the actin cytoskeleton. We have previously demonstrated actin-related

phenotypes for the two *Ag*Rho1 proteins (Köhli *et al.,* 2008). The results that we obtained in this study present, for the first time, a direct link between the functions of these four proteins in *A. gossypii*; they all participate in regulation of spore length. We obtained a synthetic spore-length phenotype of *AgPXL1* and *AgBNI1* (Figure 3), we demonstrated that *Ag*Bni1 is a potential effector of *Ag*Rho1a and *Ag*Rho1b (Figure 4), and we revealed a direct physical interaction between *Ag*Pxl1 and *Ag*Rho1a and *Ag*Rho1b (Figure 5). The question arising from the fact that all of these actin regulators are involved in the regulation of spore length is how can spore length be determined with the help of actin structures?

A simple mechanism could be based on linear actin cables that are produced by *Ag*Bni1, serving as a template for spore formation and defining the total spore length. However, there are several arguments against such a simple model. First, we found that the spores are not continuous, but rather, they are composite structures. Moreover, we did not observe linear actin structures that span the entire spore length. Only the tip compartment of the spores appears to utilize actin cables as a template during construction. We also did not observe larger spores in the *AgBNI1ΔDAD*, the dominant active variant. Rather, our results support a different model. We found different actin structures in distinct parts of the sporangia (Figure 2), which are probably involved in the formation of the different spore compartments. It seems reasonable that the position of these actin structures, which is determined by the *Ag*Rho1 proteins, *Ag*Pxl1 and *Ag*Bni1, in turn defines the size of the spores. This theory is supported by the fact that the *ΔAgpxl1*, *AgBNI1ΔDAD* mutant, which displayed the largest increase in spore size, had highly disordered actin structures in the sporangia. A possible model for such a scenario is presented in Figure 10. In this model, the action of the *Ag*Rho1 proteins would be balanced by *Ag*Pxl1 between *Ag*Bni1 and other *Ag*Rho1-effector proteins. A similar function has been described for the homologous *Sc*Pxl1 protein, which balances the activities of *Sc*Cdc42 and *Sc*Rho1 during the polarized growth of *S. cerevisiae* (Gao *et al.,* 2004). This balance could be regulated by additional signals, such as phosphorylation of *Ag*Pxl1, which have also been proposed to affect the function of *Ag*Pxl1 in hyphal tip growth (Knechtle *et al.,* 2008). *Ag*Bni1 could then be involved in formation of some of the actin structures in the sporangium

that define spore length, whereas other *Ag*Rho1-effector proteins could be involved in spore wall integrity, which would explain the spore wall defects we observed in some mutant spores. Possible candidates for such effector proteins could be the homologs of *Sc*Fks2 and *Sc*Chs3, the catalytic subunit of the glucan synthase complex and a chitin synthase, which have both been demonstrated to be involved in spore wall biosynthesis in *S. cerevisiae* and which are both regulated by *Sc*Rho1 (Iwamoto *et al.*, 2005; Qadota *et al.*, 1996; Valdivia & Schekman, 2003). Evidence for this theory also stems from the highly reduced chitin content that was observed in the spores of several of our isolated mutants (Figure 9).

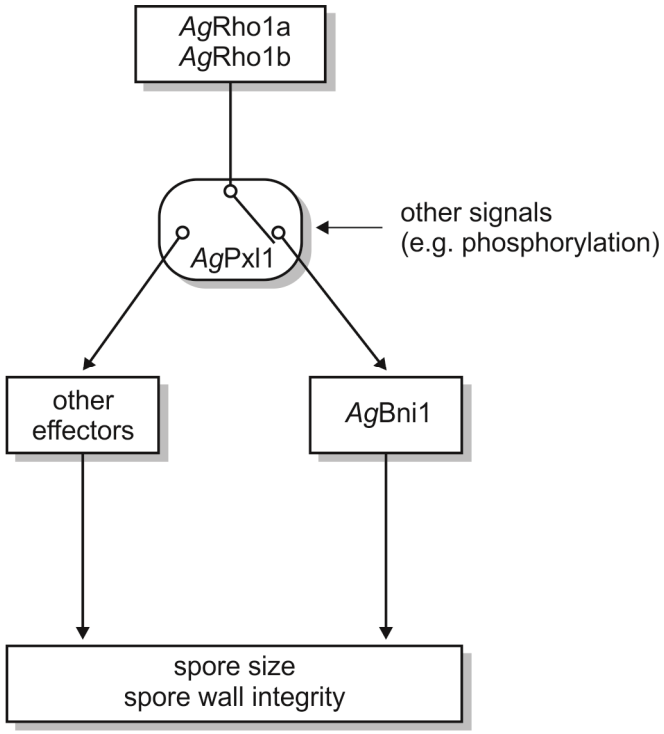

Figure 10: A model for a regulatory network of spore length and spore wall integrity. The action of the *Ag*Rho1 GTPases is balanced by *Ag*Pxl1 between *Ag*Bni1 and the other Rho1 effectors. This balance could be regulated by additional signals such as the phosphorylation of *Ag*Pxl1.

Although the scenario described above appears to be highly probable, at least some of our data also allow an alternative interpretation because dominant active alleles of the two *Ag*Rho1 proteins alone already have a significant effect on spore size. Thus, the phenotype that we observed for the other mutants could also be explained by their influence on the level of active *Ag*Rho1. This is most obvious for the *Ag*Bni1$_{S250P}$ mutant, which at least binds to *Ag*Rho1b with reduced affinity. Consequently, there could be more *Ag*Rho1b-GTP available to activate various, and so far unknown, effector proteins, which in turn would

regulate spore size. The same is also true for the *Ag*Pxl1 protein, which can bind *Ag*Rho1-GDP and could thereby prevent activation. In the *Agpxl1* deletion mutant, this pool of *Ag*Rho1 would then be available for activation. However, changes in spore size are only observed if *AgPXL1* is deleted in an *AgBNI1ΔDAD* background, and the overexpression of *Ag*Pxl1 results in an increase in spore length; these are two arguments against this theory.

In summary, we report that the highly polar, needle-shaped spores of *A. gossypii* are complex, composite structures. The spore length is regulated by a complex regulatory network in which the activity of two homologous *Ag*Rho1 proteins is balanced by a paxillin homolog between different effector proteins, including the formin *Ag*Bni1. Consequently, the balance of these distinct effector proteins appears to be responsible for proper formation of the spore wall, on one hand, and for regulation of spore length, on the other hand.

Experimental procedures

Ashbya gossypii strains and growth conditions

All the *Ashbya gossypii* strains were constructed using PCR-based gene targeting, as described by Wendland *et al.* (2000) and are listed in Table 1. For the generation of the targeting cassettes for deletions or gene fusions, we used template vectors from the pAGT series (Kaufmann, 2009) or pGEN3 (Wendland *et al.*, 2000). The transformation of *Ashbya gossypii* by plasmids was performed according to the methods of Wright & Philippsen (1991). All oligonucleotides, plasmids and templates that were used for this study are listed in Supplemental Tables 1 and 2 .

Ashbya gossypii was cultured either in full medium (AFM) supplemented with or without 200 µg/ml geneticin (Sigma, St. Louis, MO) or in 100 µg/ml ClonNAT (Werner BioAgents, Jena, Germany). For use of the auxotrophic marker, *leu2* cells were cultured in synthetic minimal medium (ASC). To avoid autofluorescence of the medium, we also used a synthetic medium for fluorescence microscopy.

To investigate sporulation, the cells were grown for two days in a synthetic minimal medium. After this incubation period, *A. gossypii* produced sporangia.

Saccharomyces cerevisiae strains and growth conditions

The cultivation of yeast cells and their genetic manipulation were performed according to the methods of Kaiser *et al*. (1994). We used the yeast strain *pJ69-4A* (*MAT*a: *trp1-901 leu2-3,112 ura3-52 his3-200 gal4Δ gal80Δ LYS::GAL1-HIS3 GAL2-ADE2 met2::GAL7-lacZ*) (James *et al.*, 1996) for the two-hybrid experiments.

DNA manipulations, plasmids and constructs

DNA manipulations were conducted according to the methods of Sambrook *et al.* (2001). We used the *Escherichia coli* host strain DH5aF´ (Hanahan, 1983). PCR was performed using either the Dream Taq Polymerase (Fermentas, St. Leon-Roth, Germany) or the Expand High Fidelity PCR System (Roche, Mannheim, Germany). The oligonucleotides were synthesized by Microsynth (Balgach, Switzerland). DNA sequencing was performed by Scientific Research

and Development (Bad Homburg, Germany). For recombination of plasmids and PCR products, the DNA was co-transformed into the *Saccharomyces cerevisiae* strain *DHD5* (*MATa/MATα; ura3-52/ura3-52; leu2-3_112/leu2-3_112; his3Δ1/his3Δ1; MAL2-8C/MAL2-8C; SUC2/SUC2*) (Arvanitidis & Heinisch, 1994). Plasmid DNA was isolated from *E. coli* and *S. cerevisiae* using the High Pure Plasmid Isolation Kit (Roche, Mannheim, Germany). For plasmid isolation from yeast, we used a protocol modified by Schmitz *et al.* (2006).

Fluorescence microscopy

For fluorescence microscopy, we used the same set-up as described in Kemper *et al.* (2011).

Two-hybrid experiments

For all two-hybrid experiments, we used the yeast two-hybrid strain *pJ69-4A* (James *et al.*, 1996) and its *MATα* derivative (Uetz & Hughes, 2000). Two-hybrid constructs that were fused to the Gal4 activation domain were transformed into the *MATa* strain, while the constructs that were fused to the Gal4 binding domain were transformed into the *MATα* derivative. The resultant strains were crossed, and the selection of the target strains was performed using a growth medium that lacked leucine and tryptophan but contained a four-fold concentration of adenine (80 mg/l). Two-hybrid strains carrying both two-hybrid plasmids were cultured to OD_{600}=1 in the selection medium described above. One milliliter of the cell culture was centrifuged and resuspended to OD_{600}=1 in sterile water. Five microliters of each strain was spotted on a two-hybrid reporter medium lacking leucine and tryptophan and without histidine (selection of weak protein-protein interactions) or adenine (selection of strong protein-protein interactions). The growth behavior of the strains was documented two days after incubation at 30°C.

Rho-inhibition assay

For the Rho-inhibition assays, we used the yeast two-hybrid strain *pJ69-4A* (James *et al.*, 1996) and its *MATα* derivative (Uetz & Hughes, 2000). The sequence encoding the N-terminus of *Ag*Bni1 (including amino acids 1-828)

was integrated into the standard two-hybrid vector pGAD424 (James *et al.*, 1996), and the sequence encoding the C-terminus of *Ag*Bni1 (consisting of amino acids 1522-1918) was integrated into pGBT9 (James *et al.*, 1996), resulting in a fusion to either the Gal4 activation or binding domain. For integration of the seven Rho-type GTPases, we constructed the vector pHPS480 that possessed the *ScURA3* selection marker, the *ScADH1* promoter and the nuclear localization signal of SV40. All seven genes encoding Rho-type GTPases of *A. gossypii* in their wild-type and constitutively active forms were integrated into this vector. We co-transformed either the plasmid that encoded the N-terminus of *Ag*Bni1 fused to the Gal4 activation domain or the empty vector pGAD424 as a control with all the plasmids that encoded the Rho-type GTPases in their wild-type or constitutively active forms (including the empty vector pHPS480 as a control) into *pJ69-4A*. Transformants carrying two plasmids were selected on a medium lacking leucine and uracil but containing 80 mg/l adenine. In addition, we transformed either the plasmid encoding the C-terminus of *Ag*Bni1 fused to the Gal4 binding domain or the empty vector pGBT9 into the *MAT*α derivative of *pJ69-4A* and selected transformants on a medium lacking tryptophan and supplemented with 80 mg/l adenine. The strains were crossed in all required combinations, and the target strains were selected via growth on a medium lacking leucine, tryptophan and uracil but containing a four-fold concentration of adenine (80 mg/l). For the Rho-inhibition assays, all the strains were cultured to OD_{600}=1 in the medium described above. Cells from 1 ml of the culture were centrifuged and resuspended in 1 ml sterile water. Five microliters of the cell suspension were spotted on agar plates lacking leucine, tryptophan and uracil and without histidine (selection for weak interactions) or adenine (selection for strong interactions). The growth behavior of the transformants was documented following a 2-day incubation at 30°C.

Expression and purification of recombinant proteins in *Escherichia coli*

Expression of GST-Rho1a, GST-Rho1b and GST (glutathione s-transferase) was performed in *E. coli* BL21(DE3). The transformants were cultured to OD_{600}=1 at 37°C, and protein expression was induced by adding 100 µM IPTG. After induction, the cells were cultured at either 25°C (GST-Rho1a) or 30°C (GST-Rho1b, GST) to avoid the formation of inclusion bodies. The cells were

harvested by centrifugation at OD_{600}=2 and disrupted by sonication. For protein purification, we used glutathione-sepharose-4B (GE) and followed the manufacturer's instructions.

His_6-*Ag*Pxl1 was expressed using the *E. coli* strain BL21(DE3) Codon Plus (Stratagene, La Jolla, CA). Cells were cultured to OD_{600}=0.5 at 37°C, and protein expression was induced by adding IPTG to a final concentration of 200 µM. After induction, the cells were again cultured at 37°C and then harvested at OD_{600}=2. The cells were disrupted by sonication. Purification of His_6-*Ag*Pxl1 was performed using Ni-NTA agarose (Qiagen, Hilden, Germany), according to the instructions of the manufacturer.

Protein concentrations were measured using the Bio-Rad Protein Assay (Bio-Rad, Munich, Germany).

In vitro binding assay

To study the protein interactions of *Ag*Pxl1, *Ag*Rho1a and *Ag*Rho1b, we performed an *in vitro* binding assay modified by Gao *et al.* (2004). For all pull-down experiments, we used 15 µg of His_6-*Ag*Pxl1 and equimolar amounts of GST, GST-*Ag*Rho1a or GST-*Ag*Rho1b. We loaded the purified proteins GST-A*g*Rho1a and GST-*Ag*Rho1b with GDP using a preloading buffer containing 10 mM GDP (20 mM Tris-HCl, pH 7.5; 100 mM NaCl; 5 mM EDTA; 5 mM DTT; 10 mM GDP). GST was treated with the same buffer as a control. The proteins were incubated at 30°C for 30 minutes, $MgCl_2$ was added to a final concentration of 25 mM, and the probes were incubated at 24°C for 15 minutes. His_6-*Ag*Pxl1 was bound to magnetic beads coated with a His_6 antibody (Miltenyi Biotech, Bergisch Gladbach, Germany). The GDP-bound GTPases or GST as a control were added to *Ag*Pxl1 coupled to the magnetic beats, and the probes were incubated for 2 h at 4°C on a shaker in Co-IP buffer (50 mM NaH_2PO_4, 300 mM NaCl, pH 8). Pull-down of the protein complexes was performed using the µMACS Separator System (Miltenyi Biotech). Instead of washing buffer 1, we used a buffer containing 20 mM Tris-HCl (pH 7.5), 100 mM NaCl, 10 mM $MgCl_2$, 5 mM DTT and 0.1% Triton-X-100 and performed 5 washing steps. Elution of the proteins was performed in a volume of 30 µl. For protein analysis, we used 10% SDS-PAGE. For western blot analysis, we used α-His_5 from mouse (Qiagen) and α-mouse-HRP from goat (Santa Cruz Biotechnology,

Santa Cruz, CA) to detect His-tagged proteins. For the detection of GST-tagged proteins, we used α-GST from rabbit (Sigma, St. Louis, MO) and α-rabbit-HRP from goat (Pierce). The proteins were detected via HRP, which was coupled to the second antibodies using the Pierce ECL Western Blotting Substrate (Pierce, Bonn, Germany).

Purification of *Ashbya gossypii* spores

The *A. gossypii* strains were grown on agar plates containing the corresponding selection medium for approximately five days. The spore-containing layer of the mycelium was removed and transferred to a reaction tube. We added 1 ml of sterile water, 200 µl of Glucanex (Sigma, 20 mg/ml) and 50 µl of Zymolyase (MP Biomedicals, Illkirch, France, 10 mg/ml) to the spores. The suspension was incubated for 45 minutes at 37°C on a shaker. The spores were centrifuged (5 minutes, 3000 rpm), and the supernatant containing the residual mycelium was discarded. The spores were washed three times with 0.03% Triton-X-100. The resultant spores were suspended in either 0.03% Triton-X-100 for further investigations or in 33% glycerine for storage at -80°C.

Statistical analysis

The significance levels of the differences in size were determined using Student`s t-test of Excel 2010 (Microsoft, Redmond, WA).

Staining of *Ashbya gossypii* spores

For actin staining, the spores were fixed in 4% formaldehyde for one hour prior to staining. The spores were washed two times with 0.03% Triton-X-100 and resuspended in 50 µl 0.03% Triton-X-100. We added 2.5 µl rhodamine-phalloidin (6.6 µM, Molecular Probes, Invitrogen) and 2.5 µl of 1% Triton-X-100 and incubated the spore suspension for 30 minutes on ice. After being stained, the spores were washed three times with 0.03% Triton-X-100 and analyzed by fluorescence microscopy.

Calcofluor white staining of the spores was performed by adding 5 µl of the dye (2 mg/ml) to 200 µl of the spore suspension (in 0.03% Triton-X-100). The probes were incubated for one hour at room temperature and washed three

times with 0.03% Trition-X-100. These spores were then analyzed using fluorescence microscopy.

To detect membrane structures, we stained the spores with $DiOC_6(3)$. For this purpose, we added 0.5 µl $DiOC_6(3)$ (17.4 µM) to 200 µl of the spore suspension (in 0.03% Triton-X-100) and incubated the samples for 3.5 hours at room temperature. The spores were washed three times with 0.03% Triton-X-100 prior to microscopic analysis.

For eosin Y staining, we added 30 µl of the dye solution (5 mg/ml) to 500 µl of the spore solution in 0.03% Triton-X-100. The probes were incubated at room temperature for 10 minutes and washed three times with 0.03% Triton-X-100. The spores were then analyzed using fluorescence microscopy.

Quantification of the fluorescence intensity of calcofluor-white-stained spores

To determine the fluorescence intensities produced by calcofluor-white staining along the needle-shaped spores produced by *A. gossypii,* we used the line-scan function of the MetaMorph software (Molecular Devices, Sunnyvale, CA). We documented the intensities in correlation to the distance from the spore tip based on 13 to 41 stained spores. We chose an exposure time of 20 ms and scaled all pictures to the same values.

Staining of *Ashbya gossypii* sporangia

A. gossypii strains were cultured in the corresponding selection medium for two days at 30°C to produce sporangia.

For actin staining with rhodamine-phalloidin, 200 µl of the culture was fixed by adding formaldehyde to a final concentration of 4%. The probes were incubated at 30°C for one hour. The cells were washed two times with 0.1 M sodium phosphate buffer at pH 7. The sporangia were collected in 50 µl of sodium phosphate buffer and stained by adding 2.5 µl of rhodamine-phalloidin staining solution (6.6 µM, Molecular Probes, Invitrogen) and 2.5 µl of 1% Triton-X-100. The cells were incubated on ice for 30 minutes and washed three times with 0.1 M sodium phosphate buffer pH 7. Afterwards, the sporangia were analyzed using fluorescence microscopy.

Table 1: *Ashbya gossypii* strains

Strain	Genotype	Construction	Source
ΔlΔt	*Agleu2Δ Agthr4Δ*	-	Altmann-Johl and Philippsen (1996)
*Ag*Hhf1-CFP		-	Kemper *et al.*, 2011
Agpxl1Δ AgBNI1ΔDAD-GFP	*Agpxl1Δ::GEN3 AgBNI1Δ5308-5757-GFP::LEU2 Agleu2Δ Agthr4Δ*	primer: 10.013/10.028, template: pAGT221	this study
Agpxl1Δ	*Agpxl1Δ::GEN3 Agleu2Δ Agthr4Δ*	-	Knechtle *et al.*, 2008
AgBNI1ΔDAD	*AgBNI1Δ5308-5757::GEN3 Agleu2Δ Agthr4Δ*	-	Schmitz *et al.,* 2006
GFP-AgRho1a		-	Köhli *et al.*, 2008
GFP-AgRho1b		-	Köhli *et al.,* 2008
K47	*GEN3-P_{ScHIS3}-GFP-AgBNI1 Agleu2Δ Agthr4Δ*	-	Köhli *et al.*, 2008
AgPXL1-mCherry	*Agleu2Δ Agthr4Δ [AgPXL1-mCherry]*	-	this study
P_{ScHIS3}-AgPxl1	*GEN3-P_{ScHIS3}-AgPXL1 Agleu2Δ Agthr4Δ*	primer: 11.043/11.044, template: pHPS742	this study
*Agrho1a**	*AgRHO1a, leu2::GFP-Agrho1a* Agleu2Δ Agthr4Δ*	pHPS733 DraIII digested	this study
*Agrho1b**	*AgRHO1b, leu2::GFP-Agrho1b* Agleu2Δ Agthr4Δ*	pHPS737 DraIII digested	this study
Agrho1a Agpxl1Δ*	*AgRHO1a, leu2::GFP-Agrho1a* Agpxl1Δ::GEN3 Agleu2Δ Agthr4Δ*	pHPS733 DraIII digested in *Agpxl1Δ*	this study
Agrho1b Agpxl1Δ*	*AgRHO1b, leu2::GFP-Agrho1b* Agpxl1Δ::GEN3 Agleu2Δ Agthr4Δ*	pHPS737 DraIII digested in *Agpxl1Δ*	this study
Agrho1aΔ	*Agrho1aΔ::GEN3*	-	Köhli *et al.*, 2008
Agbni1Δ/AgBNI1	*Agbni1Δ::GEN3/AgBNI1*	-	Schmitz *et al.*, 2006
Agbni1Δ leu2::AgBNI1	*Agbni1Δ::GEN3 leu2::AgBNI1*	pHPS741 DraIII digested in *Agbni1Δ*	this study
Agbni1Δ leu2::Agbni1$_{S250P}$	*Agbni1Δ::GEN3 leu2::Agbni1$_{T748C}$*	pHPS701 DraIII digested in *Agbni1Δ*	this study
Agcda1Δ	*Agcda1Δ::KanR Agleu2Δ Agthr4Δ*	primer: 11.110/11.111, template: pAGT140	this study

Table S1: Plasmids

Name	Backbone	Construction	Insert	Reference
pAGT221	pUC19	-	*GFP-LEU2* cassette	Kaufmann, 2009
pHPS482	pGAD424	-	*AgBNI1*$_{1-2515}$	Schmitz *et al*., 2006
pHPS484	pGBT9	-	*AgRHO3* (RHO3*$_{G219C}$*)*	Schmitz *et al*., 2006
pHPS485	pGBT9	-	*AgRHO4* (RHO4*$_{G333C}$*)*	Schmitz *et al*., 2006
pML30	pGBD-C3	1724bp BamHI-fragment of pAMK1	*AgBNI1*$_{4563-5757}$	this study
pHPS521	pHPS480	623bp EcoRI/BamHI fragment from pHPS264	*AgRHO1a*	this study
pHPS522	pHPS480	617bp EcoRI/BamHI fragment from pHPS266	*AgRHO1b*	this study
pHPS535	pHPS480	553bp EcoRI/BamHI fragment from pHPS194, STOP codon	*AgRHO2*	this study
pHPS536	pHPS480	667bp EcoRI/BamHI fragment from pHPS198, STOP codon	*AgRHO3*	this study
pHPS537	pHPS480	772bp EcoRI/BamHI fragment from pHPS194, STOP codon	*AgRHO4*	this study
pHPS538	pHPS480	887bp EcoRI/BamHI fragment from pHPS199, STOP codon	*AgRHO5*	this study
pHPS539	pHPS480	bp EcoRI/BamHI fragment from pHPS162, STOP codon	*AgCDC42*	this study
pHPS528	pHPS480	623bp EcoRI/BamHI fragment from pHPS265	*AgRHO1a**	this study
pHPS529	pHPS480	617bp EcoRI/BamHI fragment from pHPS267	*AgRHO1b**	this study
pHPS540	pHPS480	553bp EcoRI/BamHI fragment from pHPS489, STOP codon	*AgRHO2**	this study
pHPS541	pHPS480	667bp EcoRI/BamHI fragment from pHPS484, STOP codon	*AgRHO3**	this study
pHPS542	pHPS480	772bp EcoRI/BamHI fragment from pHPS485, STOP codon	*AgRHO4**	this study

Name	Backbone	Construction	Insert	Reference
pHPS543	pHPS480	887bp EcoRI/BamHI fragment from pHPS486, STOP codon	*AgRHO5**	this study
pHPS544	pHPS480	bp EcoRI/BamHI fragment from pHPS227, STOP codon	*AgCDC42**	this study
pHPS480	YEP352	*ScADH1* promoter, NLS (SV40) integrated using HindIII/SbfI restriction sites	-	this study
pGBT9	-	-	-	James *et al*., 1996
pGAD424	-	-	-	James *et al.,* 1996
pTD1	-	-	-	Iwabuchi *et al*., 1993
pVA3	-	-	-	Iwabuchi *et al*., 1993
pHPS717	pTM30	2606bp NsiI/HindIII fragment (Primer: 10.026/10.027, Template: genomic DNA) in PstI/HindIII digested pTM30	*6His-AgPXL1*	this study
pTM30	-	-	-	Morrison and Parkinson, 1994
pHPS270	-	-	*GST-AgRHO1a*	Köhli *et al*., 2008
pHPS272	-	-	*GST-AgRHO1b*	Köhli *et al*., 2008
pHPS711	pUC21	494bp EcoRI/XmaI fragment (Primer: 10.017/10.018, Template: pHPS383) in EcoRI/XmaI digested pUC21	*ScHIS3* promoter	this study
pHPS383	-	-	-	Kemper *et al*., 2011
pHPS742	pHPS711	1830bp EcoRI fragment from pGEN3 ligated into EcoRI digested pHPS711	*GEN3-ScHIS3* promoter cassette	this study
pUC21	-	-	-	Vieira and Messing, 1991
pHPS733	pAGINTlac	2056bp HindIII/SpeI fragment of pHPS249 in HindIII/XbaI digested pAGINTlac	*GFP-AgRHO1a**	this study
pHPS737	pAGINTlac	2488bp HindIII/SpeI fragment of pHPS251 in HindIII/XbaI digested pAGINTlac	*GFP-AgRHO1b**	this study
pAGINTlac	-	-	-	Kemper *et al*., 2011

Name	Backbone	Construction	Insert	Reference
pHPS214	pGAD424	5837bp fragment (Primers: 02.280/02.281, Template:pHPS178) recombined in pGAD424	Gal4AD-*AgBNI1*	this study
pHPS691	pHPS690	construction of *Agbni1*$_{S250P}$ using in vitro mutagenesis (Primer: 10.008/10.009)	*Ag*Bni1$_{S250P}$ (*Agbni1*$_{T748C}$)	this study
pHPS690	pUC21	856bp EcoRI/NcoI fragment of pHPS214 in EcoRI/NcoI digested pUC21	Fragment of *AgBNI1*	this study
pHPS693	pAMK1	606bp MluI/NcoI fragment of pHPS691 in MluI/NcoI digested pAMK1	*Ag*Bni1$_{S250P}$ (*Agbni1*$_{T748C}$)	this study
pHPS701	pAGINTlac	6967bp SmaI/HindIII fragment of pHPS693 in HindIII/HincII digested pAGINTlac	*Ag*Bni1$_{S250P}$ (*Agbni1*$_{T748C}$)	this study
pAMK1	-	-	*AgBNI1*	Schmitz *et al*., 2006
pHPS741	pAGINTlac	6967bp SmaI/HindIII fragment of pAMK1 in HincII/HindIII digested pAGINTlac	*AgBNI1* wt	this study
pHPS710	pHPS482	856bp EcoRI/NcoI fragment of pHPS691 in EcoRI/NcoI digested pHPS482	Gal4AD-*Agbni1*$_{1-2515, S250P}$	this study
pHPS265	pGBT9	-	*RHO1a** (*RHO1a*$_{G204C}$)	Köhli *et al*., 2008
pHPS267	pGBT9	-	*RHO1b** (*RHO1b*$_{G207C}$)	Köhli *et al*., 2008

Table S2: Oligonucleotides

No.	Name	Sequence
10.028	dDAD GFP for	TCTGGAGTACAAGCGCGCGCAGGAGTTTAACCGCAAGATCT CTAAAGGTGAAGAATTATTC
10.013	dDAD GFP rev	GCTGGTCTATCAGTTTCTTGGTGCGGCGCTGGCGAACCTTC ATGATTACGCCAAGCTTGC
10.026	6His Pxl1 for NsiI	AATGATGCATCATCACCATCACCATCACATGTCGCCTTACA ACGTATTG
10.027	Pxl1 rev HindIII	TACCAAGCTTTTAGACGTTGATGAGTCTTG
11.043	PXL1 HIS3Prom for	TTCCGTCAAAAGTTTCACTATGAGAAACAGTCGTAAAGTAT AATATGGTGTATTTACCAATAATG
11.044	PXL1 HIS3Prom rev	CGGACTACCGTTTAGACTTGTGTTCAATACGTTGTAAGGCG ACATCCGGGCTTTGCCTTCGTTTA
11.045	PXL1 HIS3Prom int1	TCCCATCCAGCCGGACATAG
11.046	PXL1 HIS3Prom int2	CGTCCGGTACCTGACATGTG
08.034	AgCDC42 cont rev	GGCTTCTGTCAGCAACTCGT
05.027	G3	TCGCAGACCGATACCAGGATC
10.017	ScHIS3Prom for EcoRI	CTTCGAATTCACACCGATCCGCTGCACGGT
10.018	ScHIS3prom rev XmaI	CCATCCCGGGCTTTGCCTTCGTTTATCTTG
02.280	pGADBNI1-ATG	GAAGATACCCCACCAAACCCAAAAAAAGAGATCGAATTCat gaagaagtccacgcactcg
02.281	pGADBNI1-TAA	CAGTATCTACGATTCATAGATCTCTGCAGGTCGACGGATCC ttacttgtgctcatcgagcattg
10.008	Bni1 S250P ClaI for	GCATGCCACCAAGCCCAACCGTAGAATCGATAGCGAGTTC
10.009	Bni1 S250P ClaI rev	GAACTCGCTATCGATTCTACGGTTGGGCTTGGTGGCATGC
11.110	delta CDA KanR for	TAGCGTATCGAGAAGAACACAGACACAGAGCGACCGTGGAG CAGCGGTGTATTTACCAATAATGT
11.111	delta CDA KanR rev	TATAGAATGTATACTTACTTGGTTCCCTGCAGTAGTAGACT ATGAGATGAGGCCGTCTTTTGTTG
11.112	del CDA cont1	GGCGGACAGAGCACAAAGAC
11.113	del CDA cont2	GCCCGCAGACATGCCATAAG

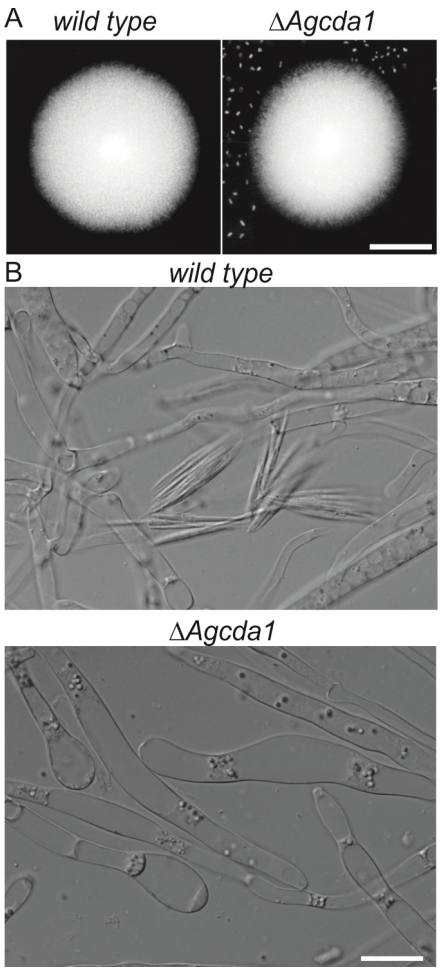

Supplemental Figure S1: Deletion of *Ag*Cda1 causes severe sporulation defects

A) Growth of *ΔAgcda1* and a wild-type mycelium. Both strains were cultured on a full medium for four days at 30°C. The deletion of *Ag*Cda1 did not affect vegetative growth. The scale bar represents 1 cm.

B) Microscopic investigation of spore formation in seven-day-old mycelia derived from a wild type and the *Agcda1* deletion strain. The scale bar represents 10 µm.

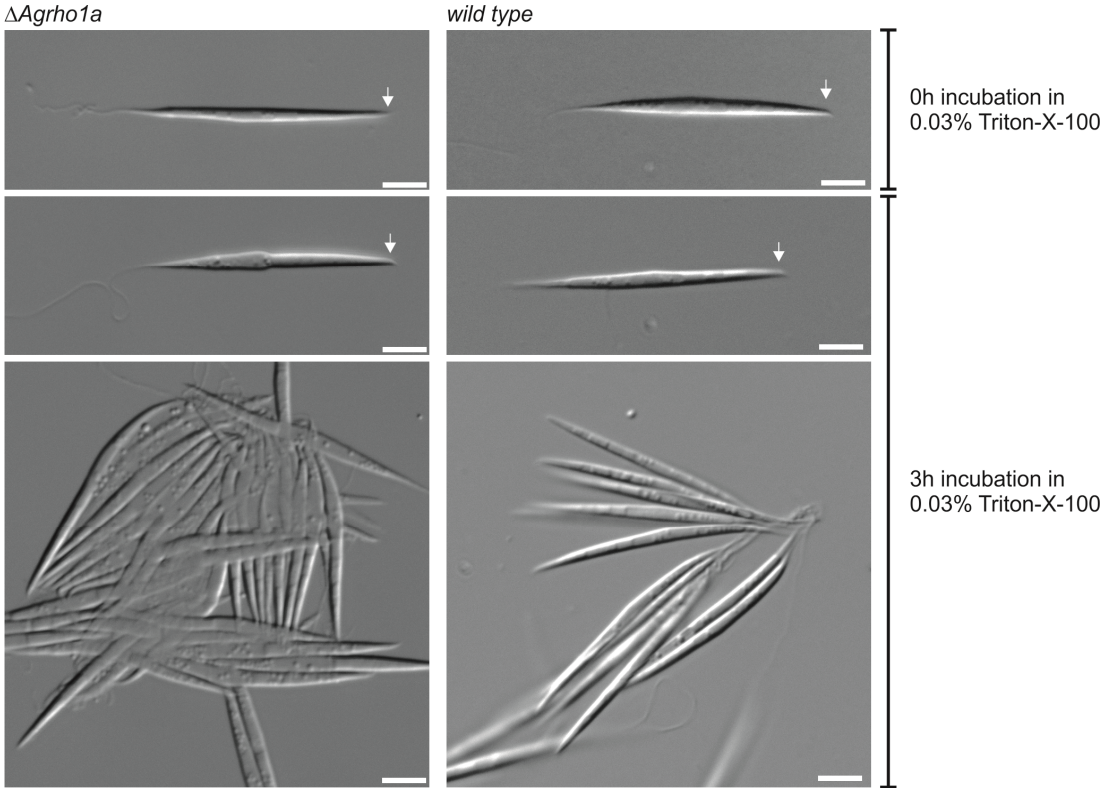

Supplemental Figure S2: The deletion of *AgRHO1a* leads to defects in the spore wall of the membrane compartment.
Spores produced by an *Agrho1a* deletion strain (left side) and an *A. gossypii* wild-type strain (right side). A subset of the *Agrho1a* spores show defects in the membrane compartment of the spores, which leads to swelling. These defects cause spore lysis in approximately 20% of the spores after three hours incubation in 0.03% Triton-X-100. The scale bars represent 5 µm. The arrows indicate the anterior side of the spores.

Acknowledgments

We are grateful to: Jürgen Heinisch and Peter Philippsen for discussions and support, Lucille Schmieding for correction of the manuscript and to Sandra Bartels and Anja Lorberg for providing support for the biochemical experiments. M.L. is a fellow of the graduate college “Cell and Tissue differentiation from an integrative perspective” of the University of Osnabrück.

References

Alberts, A. S., (2001) Identification of a carboxyl-terminal diaphanous-related formin homology protein autoregulatory domain. J Biol Chem 276: 2824-2830.

Altmann-Johl, R. & P. Philippsen, (1996) *AgTHR4*, a new selection marker for transformation of the filamentous fungus *Ashbya gossypii*, maps in a four-gene cluster that is conserved between *A. gossypii* and *Saccharomyces cerevisiae*. Mol Gen Genet 250: 69-80.

Arvanitidis, A. & J. J. Heinisch, (1994) Studies on the function of yeast phosphofructokinase subunits by in vitro mutagenesis. *J Biol Chem* **269**: 8911-8918.

Baker, L. G., C. A. Specht, M. J. Donlin & J. K. Lodge, (2007) Chitosan, the deacetylated form of chitin, is necessary for cell wall integrity in *Cryptococcus neoformans*. *Eukaryot Cell* **6**: 855-867.

Batra, L. R. (1973) Nematosporaceae (Hemiascomycetidae): Taxonomy, Pathogenicity, Distribution and Vector Relations, U.S. Department of Agriculture

Briza, P., A. Ellinger, G. Winkler & M. Breitenbach, (1988) Chemical composition of the yeast ascospore wall. The second outer layer consists of chitosan. *J Biol Chem* **263**: 11569-11574.

Coluccio, A., E. Bogengruber, M. N. Conrad, M. E. Dresser, P. Briza & A. M. Neiman, (2004) Morphogenetic pathway of spore wall assembly in *Saccharomyces cerevisiae*. *Eukaryot Cell* **3**: 1464-1475.

Deacon, J. W. (2006) Fungal Biology. Malden, MA: Blackwell Pub.

Deakin, N. O. & C. E. Turner, (2008) Paxillin comes of age. *J Cell Sci* **121**: 2435-2444.

Dietrich, F. S., S. Voegeli, S. Brachat, A. Lerch, K. Gates, S. Steiner, C. Mohr, R. Pohlmann, P. Luedi, S. Choi, R. A. Wing, A. Flavier, T. D. Gaffney & P. Philippsen, (2004) The *Ashbya gossypii* genome as a tool for mapping the ancient *Saccharomyces cerevisiae* genome. *Science* **304**: 304-307.

Gao, X. D., J. P. Caviston, S. E. Tcheperegine & E. Bi, (2004) Pxl1p, a paxillin-like protein in *Saccharomyces cerevisiae*, may coordinate Cdc42p and Rho1p functions during polarized growth. *Mol Biol Cell* **15**: 3977-3985.

Hanahan, D., (1983) Studies on transformation of *Escherichia coli* with plasmids. *J Mol Biol* **166**: 557-580.

Iwabuchi, K., B. Li, P. Bartel & S. Fields, (1993) Use of the two-hybrid system to identify the domain of p53 involved in oligomerization. *Oncogene* **8**:1693-1696.

Iwamoto, M. A., S. R. Fairclough, S. A. Rudge & J. Engebrecht, (2005) *Saccharomyces cerevisiae* Sps1p regulates trafficking of enzymes required for spore wall synthesis. *Eukaryot Cell* **4**: 536-544.

James, P., J. Halladay & E. A. Craig, (1996) Genomic libraries and a host strain designed for highly efficient two-hybrid selection in yeast. *Genetics* **144**: 1425-1436.

Kaiser C, Michaelis S, Mitchell A. 1994. *Methods in Yeast Genetics. A Cold Spring Harbor Laboratory Course Manual*. Cold Spring Harbor Laboratory Press: Cold Spring Harbor, NY.

Kaufmann, A., (2009) A plasmid collection for PCR-based gene targeting in the filamentous ascomycete *Ashbya gossypii*. *Fungal Genet Biol* **46**: 595-603.

Kemper, M., L. Mohlzahn, M. Lickfeld, C. Lang, S. Wählisch & H. P. Schmitz, (2011) A Bnr-like formin links actin to the spindle pole body during sporulation in the filamentous fungus *Ashbya gossypii*. *Mol Microbiol* **80**: 1276-1295.

Knechtle, P., A. Kaufmann, D. Cavicchioli & P. Philippsen, (2008) The Paxillin-like protein *Ag*Pxl1 is required for apical branching and maximal hyphal growth in *A. gossypii*. *Fungal Genet Biol* **45**: 829-838.

Köhli, M., S. Buck & H. P. Schmitz, (2008) The function of two closely related Rho proteins is determined by an atypical switch I region. *J Cell Sci* **121**: 1065-1075.

Kohno, H., K. Tanaka, A. Mino, M. Umikawa, H. Imamura, T. Fujiwara, Y. Fujita, K. Hotta, H. Qadota, T. Watanabe, Y. Ohya & Y. Takai, (1996) Bni1p implicated in cytoskeletal control is a putative target of Rho1p small GTP binding protein in *Saccharomyces cerevisiae*. *EMBO J* **15**: 6060-6068.

Lickfeld, M. & H. P. Schmitz, (2011) Selection of STOP-free sequences from random mutagenesis for 'loss of interaction' two-hybrid studies. *Yeast* **28**: 535-545.

Morrison, T. B. & J. S. Parkinson, (1994) Liberation of an interaction domain from the phosphotransfer region of CheA, a signaling kinase of *Escherichia coli*. *Proc Natl Acad Sci U S A* **91**: 5485-5489.

Neiman, A. M., (2005) Ascospore formation in the yeast *Saccharomyces cerevisiae*. *Microbiol Mol Biol Rev* **69**: 565-584.

Nelson, W. J., (2003) Adaptation of core mechanisms to generate cell polarity. *Nature* **422**: 766-774.

Pridham, T.G. and Raper, K.B. (1950) *Ashbya gossypii*: Its significance in nature and in the laboratory. Mycologia 42, 603-623.

Prillinger, H., W. Schweigkofler, M. Breitenbach, P. Briza, E. Staudacher, K. Lopandic, O. Molnar, F. Weigang, M. Ibl & A. Ellinger, (1997) Phytopathogenic filamentous (*Ashbya, Eremothecium*) and dimorphic fungi (*Holleya, Nematospora*) with needle-shaped ascospores as new members within the *Saccharomycetaceae*. *Yeast* **13**: 945-960.

Qadota, H., C. P. Python, S. B. Inoue, M. Arisawa, Y. Anraku, Y. Zheng, T. Watanabe, D. E. Levin & Y. Ohya, (1996) Identification of yeast Rho1p GTPase as a regulatory subunit of 1,3-beta-glucan synthase. *Science* **272**: 279-281.

Sambrook J, Russel DW, Sambrook J., (2001). *Molecular Cloning: A Laboratory Manual.* Cold Spring Harbor Laboratory Press: Cold Spring Harbor, NY.

Schmitz, H. P., A. Kaufmann, M. Kohli, P. P. Laissue & P. Philippsen, (2006) From function to shape: a novel role of a formin in morphogenesis of the fungus *Ashbya gossypii*. *Mol Biol Cell* **17**: 130-145.

Simon-Nobbe, B., U. Denk, V. Poll, R. Rid & M. Breitenbach, (2008) The spectrum of fungal allergy. *Int Arch Allergy Immunol* **145**: 58-86.

Suda, Y., R. K. Rodriguez, A. E. Coluccio & A. M. Neiman, (2009) A screen for spore wall permeability mutants identifies a secreted protease required for proper spore wall assembly. *PLoS One* **4**: e7184.

Uetz, P. & R. E. Hughes, (2000) Systematic and large-scale two-hybrid screens. *Curr Opin Microbiol* **3**: 303-308.

Valdivia, R. H. & R. Schekman, (2003) The yeasts Rho1p and Pkc1p regulate the transport of chitin synthase III (Chs3p) from internal stores to the plasma membrane. *Proc Natl Acad Sci U S A* **100**: 10287-10292.

Vieira, J. & J. Messing, (1991) New pUC-derived cloning vectors with different selectable markers and DNA replication origins. *Gene* **100**: 189-194.

Watanabe, N., P. Madaule, T. Reid, T. Ishizaki, G. Watanabe, A. Kakizuka, Y. Saito, K. Nakao, B. M. Jockusch & S. Narumiya, (1997) p140mDia, a mammalian homolog of *Drosophila* diaphanous, is a target protein for Rho small GTPase and is a ligand for profilin. *EMBO J* **16**: 3044-3056.

Wendland, J., Y. Ayad-Durieux, P. Knechtle, C. Rebischung & P. Philippsen, (2000) PCR-based gene targeting in the filamentous fungus *Ashbya gossypii*. *Gene* **242**: 381-391.

Wright, M. C. & P. Philippsen, (1991) Replicative transformation of the filamentous fungus *Ashbya gossypii* with plasmids containing *Saccharomyces cerevisiae* ARS elements. *Gene* **109**: 99-105.

3.4 Dissection of Rho-GTPase function in polar growth and sporulation of *Ashbya gossypii*

M. Lickfeld & H.P. Schmitz

Department of Genetics, University of Osnabrück, Barbarastr. 11,
49076 Osnabrück, Germany

manuscript in preparation

Summary

All morphological changes within the fungal life cycle require reorganization of the actin cytoskeleton. Remodeling of the cytoskeleton in response to internal and environmental signals is often realized by small GTPases of the Rho family. In this study, we characterize the Rho-type GTPases *Ag*Rho1a, *Ag*Rho1b, *Ag*Rho3 and *Ag*Rho4 of the filamentous fungus *Ashbya gossypii*, which are all potential activators of the formin *Ag*Bni1, with special respect to their role in regulation of hyphal tip growth and spore formation. Using an *Ag*Rho1-GTP specific binding domain we show that the majority of *Ag*Rho1-GTP is found at the hyphal tip, while at the membrane-pool in the older parts of the hyphae only sporadically some spots of active protein appear. Using a constitutively active allele, we could identify a function for the *Ag*Rho4 protein: Such mutants display defects in the maintenance of cell polarity and the control of the growth direction of hyphae. Furthermore, we found that *Ag*Rho4 is directly involved in spore formation: The protein localizes to the membrane of sporangia and to the outer border of forming spores. In addition, the strain possessing a constitutively active allele of *AgRHO4* produces spores that are susceptible to lysis.

Introduction

In the filamentous growing fungus *Ashbya gossypii*, morphological changes are directly correlated with changes in the organization of the actin cytoskeleton. Such changes include, for example, the establishment of cell polarity or the rearrangements at the hyphal tip during tip splitting of fast growing, mature hyphae. Recent work also identified drastic changes in actin cytoskeleton organization during sporulation, a process that requires massive reorganization of cellular morphology (Chapter 3.3). In the past, several factors have been identified that play an important role for the regulation of the actin cytoskeleton (Wendland & Philippsen, 2001, Köhli *et al.*, 2008a, Knechtle *et al.*, 2006). Among these the formin *Ag*Bni1 as an actin-polymerizing protein is essential for polarized growth. The deletion of *Ag*Bni1 leads to a complete loss of cell polarity and to the production of large, potato-shaped cells (Schmitz *et al.*, 2006), indicating an essential function for the formation of hyphae. But in addition, a recent work also revealed a role for *Ag*Bni1 in the regulation of spore size and integrity (Chapter 3.3). In this study, we also identified four Rho-type GTPases of *A. gossypii* that are capable of activating *Ag*Bni1: *Ag*Rho1a, *Ag*Rho1b, *Ag*Rho3 and *Ag*Rho4 (Chapter 3.3). While much information is available about the function of the *Ag*Rho1 proteins, the role of the others is less well understood: Rho1 signaling in *A. gossypii* includes two homologous GTPases that result from a gene duplication (Dietrich *et al.*, 2004). An *Agrho1b* deletion strain is unable to produce a mycelium (Köhli *et al.*, 2008a). Thus, *Ag*Rho1b is the essential Rho1 homolog, while the deletion of the homologous protein *Ag*Rho1a is viable. Although *Agrho1a* deletion cells produce a mature mycelium, the growth speed is slightly decreased and hyphae are susceptible for lysis at the tips of fast growing hyphae (Köhli *et al*., 2008a, Wendland & Philippsen, 2001), suggesting a central function for the stabilization of growing tips. Both Rho1 proteins are located to the cell cortex of growing hyphal tips, which is compatible with an involvement in glucan biosynthesis. Strikingly, *Ag*Rho1a can be also found in the cytoplasm at lower temperatures (25°C). The meaning of this cytoplasmic localization remained unknown so far. However, both Rho1 GTPases fulfill distinct functions, which were originally described for the Rho1 signal transduction pathway: While *Ag*Rho1a plays an important role

in actin organization, *Ag*Rho1b is mainly involved in cell wall biosynthesis (Köhli *et al.*, 2008a).

Like *Ag*Rho1a and *Ag*Rho1b, *Ag*Rho3 has an important function for the growing tip of hyphae. *Agrho3* deletion cells produce a mature mycelium but the growth speed is significantly decreased compared to the wild type (Wendland & Philippsen, 2001). The germination of *Agrho3* spores fails at higher temperatures like 37°C, which results in lysis of the young germ tubes. Interestingly, mature mycelia of the *Agrho3* deletion strain show characteristic swellings at their hyphal tips, which expose a short period of isotropic growth (Wendland & Philippsen, 2001). This swelling is similar to what is observed if a hypha is treated with the actin destabilizing drug Latrunculin A, which suggests that *Ag*Rho3 might play a role in actin regulation at the hyphal tip.

In contrast to *Ag*Rho1a, *Ag*Rho1b and *Ag*Rho3, little is currently known about the function of *Ag*Rho4 in *A. gossypii.* The deletion of *Ag*Rho4 is viable and does not show any defects during vegetative growth (Wendland *et al.*, 2000). Concluding, *Ag*Rho4 is not essential and its role in *A. gossypii* remains in the dark. However, the fact that *Ag*Rho4 has the potential to activate *Ag*Bni1 suggests that it might also play a role in actin regulation.

This study aimed towards a better understanding of the role of the four Rho-type GTPases *Ag*Rho1a, *Ag*Rho1b, *Ag*Rho3 and *Ag*Rho4 in actin regulation during hyphal growth and sporulation.

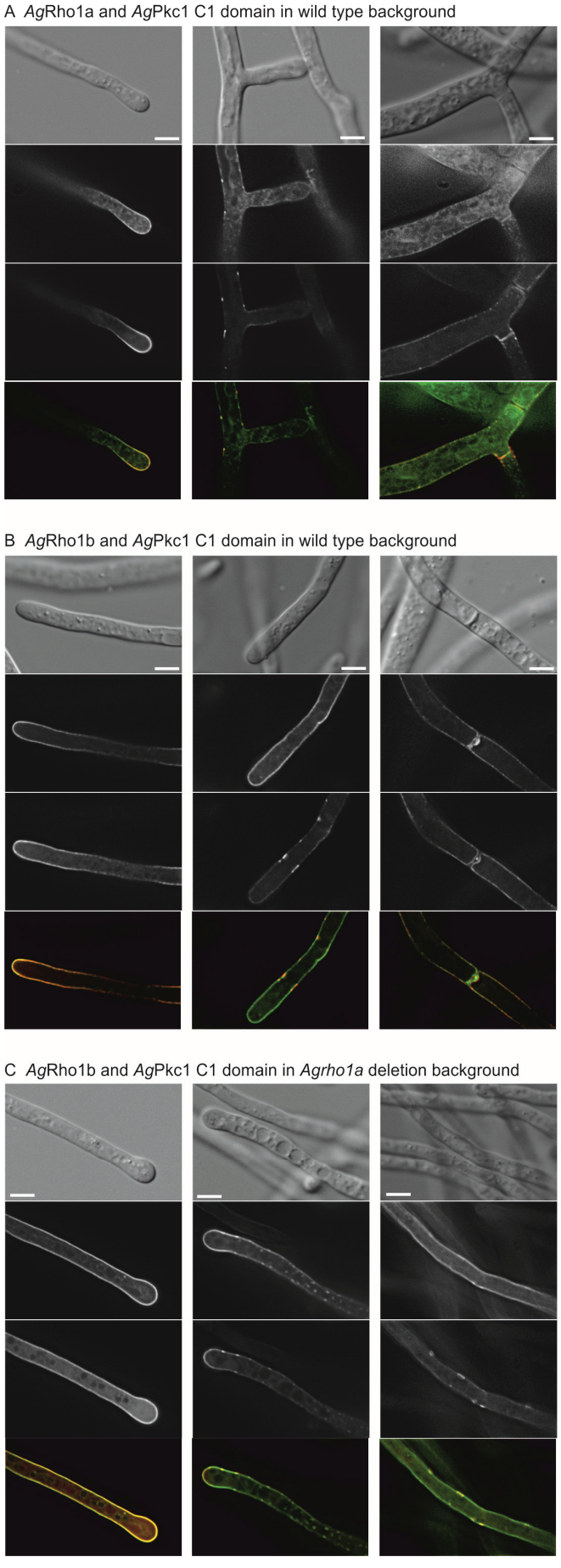

Figure 1: Investigations on active *Ag*Rho1 GTPases *in vivo.* The localization of tdTomato-*Ag*Pkc1$_{374-637}$ indicates GTP-Rho1 proteins. A) Co-localization studies of GFP-*Ag*Rho1a and tdTomato-*Ag*Pkc1$_{374-637}$ in a wild type *A. gossypii* strain. B) Co-localization studies of GFP-*Ag*Rho1b and tdTomato-*Ag*Pkc1$_{374-637}$ in a wild type *A. gossypii* strain. C) Co-localization studies of GFP-*Ag*Rho1b and tdTomato-*Ag*Pkc1$_{374-637}$ in an *Agrho1a* deletion strain. All scale bars represent 5 µm.

Results

*Ag*Rho1a and *Ag*Rho1b are active at the tip of growing hyphae.

The Rho1 signaling pathway plays a major role for polarity establishment, cell wall remodeling and the regulation of the actin cytoskeleton (Qadota *et al.*, 1996, Kamada *et al.*, 1996, Nonaka *et al.*, 1995, Levin, 2011). Rho1 signaling in *A. gossypii* includes two homologous proteins that result from a gene duplication: *Ag*Rho1a and *Ag*Rho1b (Köhli *et al.*, 2008a). Localization of both Rho1 homologs, which can be found in *A. gossypii,* was investigated in detail by Köhli *et al.* (2008a). Both GTPases can be observed at the cortex of growing hyphae. We asked whether *Ag*Rho1a and *Ag*Rho1b are active at the entire cell cortex and searched for a possibility to distinguish the GTP- and GDP-bound forms of the Rho1 proteins *in vivo*. The approach performed in this study takes advantage of the interaction between the Rho1 homologs and the C1 domain of *Ag*Pkc1, which is restricted to the GTP-bound forms of the Rho1 proteins (Köhli *et al*., 2008a). Therefore, the C1 domain of the protein kinase C was used as an indicator for the active state of *Ag*Rho1a and *Ag*Rho1b. Sequence alignment with the well-characterized homolog *Sc*Pkc1 from *S. cerevisiae* (Nonaka *et al.*, 1995) and *Ag*Pkc1 identified the amino acids 374-637 of *Ag*Pkc1 as the C1 domain. *Ag*Pkc1$_{374\text{-}637}$ was tagged with the fluorescent protein tdTomato (Shaner *et al.*, 2004) and co-localization studies of the Pkc1 C1 domain and both Rho1 GTPases were performed. Because the protein kinase interacts with both GTPases it was impossible to perform a specific characterization of either *Ag*Rho1a or *Ag*Rho1b in a wild type background. Our studies in an *A. gossypii* wild type strain can only shed light on the general localization of active Rho1 signaling. The studies performed in the wild type showed that the Rho1 proteins at the cell cortex of the growing tip of hyphae co-localized with the C1 domain of *Ag*Pkc1, which we used as an indicator for the active state of the GTPases (Figure 1A, left side; Figure 1B, left side). This finding suggests that most of the Rho1 GTPases that are located at the growing tip are active, which is also compatible with their involvement in glucan synthesis and cell wall integrity. We also had a closer look to hyphae that were located at the older, mature parts of the mycelium, which no longer showed tip growth. Here, both Rho1 proteins were located to the cortex of these hyphae and to septa (Figure 1A, middle and

right side; Figure 1B, middle and right side). Co-localization with the C1 domain of *Ag*Pkc1 revealed that the Rho1 proteins were not active at the entire cell cortex. Instead, we found that GTP-bound Rho1 proteins were concentrated at some specific spots (Figure 1A, middle; Figure 1B, middle). Such a concentration is sometimes visible, when looking at the total protein pool (Figure 1A, middle), but sometimes these spots only represent a fraction of the total GTPase-pool (Figure 1B, middle). These hot spots of *Ag*Rho1 activity are probably sites that require high rates of cell wall biosynthesis and thus also high Rho1-activity. They might therefore be sites were cell wall damage needs to be repaired or sites of future branch formation. Additionally, Rho1 was found in its active state at septa (Figure 1A, right side; Figure 1B, right side), which is also a place where high cell wall biosynthesis occurs.

Due to the overlap of effector proteins of both Rho1 GTPases a differentiation between *Ag*Rho1a and *Ag*Rho1b activity can be only made for regions, where localization of both proteins does not overlap. This is the case for the hypha-internal localization of *Ag*Rho1a. While GFP-*Ag*Rho1a is clearly visible inside the hyphae, the reporter for active Rho1 only stains the hyphal cortex (Figure 1A). Thus, the internal *Ag*Rho1a pool is not active. A way to further distinguish between activity of *Ag*Rho1a and *Ag*Rho1b would be using deletion strains of one of the two Rho1 homologs. However, the deletion of *AgRHO1b* is lethal in *A. gossypii* (Köhli *et al.*, 2008a), therefore we were unable to perform further investigations on the localization of active *Ag*Rho1a in an *Agrho1b* deletion background. However, we monitored the localization of active *Ag*Rho1b in an *Agrho1a* deletion strain. On the basis of these examinations, *Ag*Rho1b is active at the cortex of the growing hyphal tip and at some hot spots in the back of hyphae that might correspond to sites of damage repair or potential sites of future branch formation (Figure 1C).

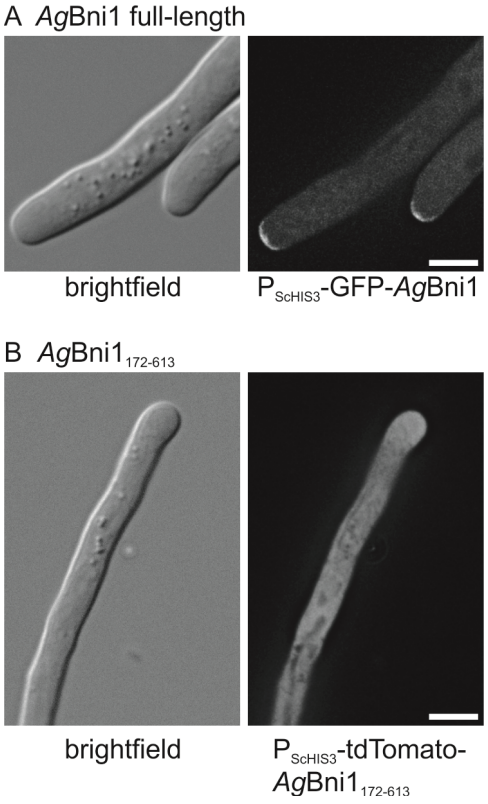

Figure 2: Localization of the Rho binding domain of *Ag*Bni1 in hyphal tips
A) Localization of full-length GFP-*Ag*Bni1 using the overexpression strain constructed by Köhli *et al.*, 2008b. *Ag*Bni1 shows a crescent-shaped accumulation at the hyphal tip. The scale bar represents 5 µm.
B) Localization of tdTomato-*Ag*Bni1$_{172-613}$. The Rho binding domain of *Ag*Bni1 shows a cytoplasmic localization. The scale bar represents 5 µm.

The interaction of Rho-type GTPases with the Rho binding domain of the effector *Ag*Bni1 is not sufficient to target the formin to the hyphal tip.

The C1-domain of *Ag*Pkc1 is not the only effector of GTP-Rho1 proteins in *A. gossypii*. As mentioned above, we identified a region within *Ag*Bni1 (amino acids 172-613) that is capable of binding to both, *Ag*Rho1a and *Ag*Rho1b in their GTP-bound form in a two-hybrid assay (Lickfeld & Schmitz, 2011, Chapter 3.2). Using a similar approach as for *Ag*Pkc1, we wanted to address if this region is sufficient to target this Rho binding domain to identical sites as the full length *Ag*Bni1 protein. That means we wanted to determine if this domain, apart from activation of *Ag*Bni1, also contributes to the localization of *Ag*Bni1. To answer this question, we tagged the smallest fragment of *Ag*Bni1, which we identified to interact with the four potential activators *Ag*Rho1a, *Ag*Rho1b, *Ag*Rho3 and *Ag*Rho4 (Lickfeld & Schmitz, 2011) with the fluorescent protein tdTomato (Shaner *et al.*, 2004). If the interaction of the formin and the Rho-type GTPases would be a key factor for *Ag*Bni1 recruitment, the typical crescent-shaped localization of the Rho binding domain that can be observed for the full-length protein, would be expected. Microscopical investigations revealed that tdTomato-*Ag*Bni1$_{172-613}$ was distributed to the entire cytoplasm of the mycelium

(Figure 2B). We did not observe the cortical accumulation at the growing tip that we revealed for the *Ag*Bni1 full-length protein (Figure 2A). These results allow two conclusions: Either the partial domain fused to tdTomato does not fold correctly and thus is not accessible for the Rho GTPases, or the fragment of *Ag*Bni1, which was identified to interact with *Ag*Rho1a, *Ag*Rho1b, *Ag*Rho3 or *Ag*Rho4 is not sufficient to target the protein to the hyphal tip. In the latter case additional components must be responsible for the characteristic recruitment of *Ag*Bni1 to the growing tip.

_Ag_Rho3 localizes to internal structures.

While there exist detailed information about the localization of the homologous GTPases *Ag*Rho1a and *Ag*Rho1b little is known about the localization of the other potential *Ag*Bni1 activators *Ag*Rho3 and *Ag*Rho4. To get a more precise idea about the subcellular localization of *Ag*Rho3, an N-terminal fusion of this GTPase with mCherry was performed in this study. Therefore, we constructed a plasmid carrying the native *AgRHO3* promoter, mCherry as fluorescent marker (Shaner *et al.*, 2004) and the full-length *AgRHO3* gene including a CAAX-box. Fluorescent proteins must be fused to the N-terminus of Rho-type GTPases because this type of proteins is posttranslational modified at the C-terminal CAAX-box (Adamson *et al.*, 1992). An *A. gossypii* wild type strain was transformed with the plasmid encoding the fusion protein. The localization of *Ag*Rho3 in different developmental stages of the mycelium was examined. In a one day old mycelium *Ag*Rho3 was distributed over the entire length of vegetative growing hyphae (Figure 3A, first row). On a closer look, a pattern that resembles the organization of internal membranes instead of an even cytosolic localization can be observed. Rho-type GTPases are modified by isoprenylation, which contributes to membrane association. Thus, a co-localization of *Ag*Rho3 with internal membrane structures seems reasonable. We also investigated the localization of this GTPase in a two day old mycelium that shows different stages of sporulation. Again, *Ag*Rho3 was distributed in the entire developing sporangium without any specific localization pattern (Figure 3A, second and third row). We made a similar observation in mature sporangia which already contain spores. *Ag*Rho3 can be found in the entire cell compartment (Figure 3A, fourth row).

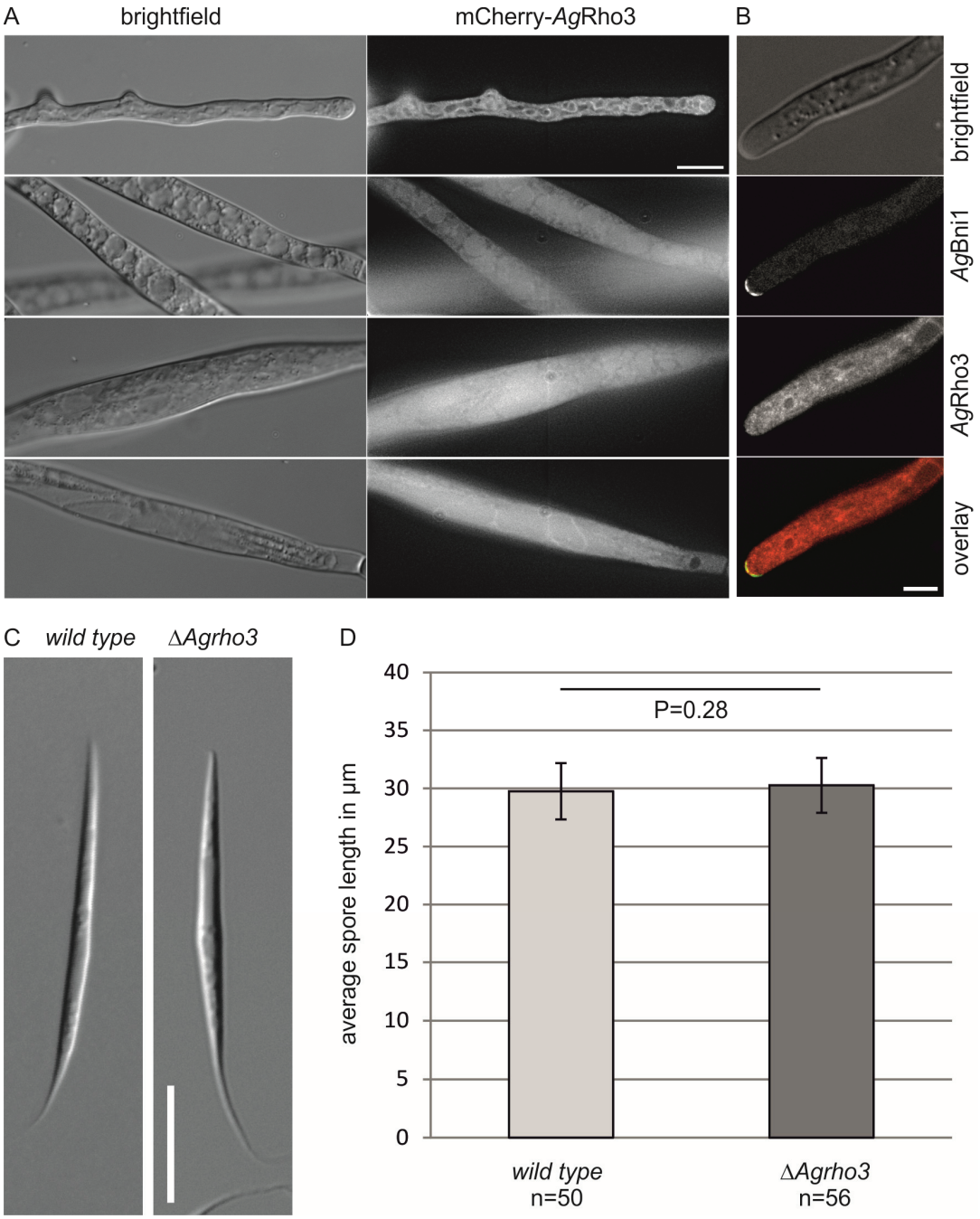

Figure 3: Analysis of *Ag*Rho3-localization and effects on spore formation.
A) Localization of mCherry-*Ag*Rho3 in different developmental stages. The scale bar represents 5 µm.
B) Co-localization studies of GFP-*Ag*Bni1 and mCherry-*Ag*Rho3. The scale bar represents 5 µm.
C) Spores isolated from an *A. gossypii* wild type and an *Agrho3* deletion strain. The deletion of *AgRHO3* does not affect spore morphology. The scale bar represents 10 µm.
D) Average spore length of wild type and *Agrho3* deletion spores. The number n represents the number of spores measured.

As stated above, we identified *Ag*Rho3 as a potential activator of the formin *Ag*Bni1 using a modified two-hybrid system (Lickfeld & Schmitz, 2011). Such a function would require co-localization of *Ag*Rho3 and *Ag*Bni1 *in vivo*. Therefore, we decided to perform co-localization studies of *Ag*Rho3 and its potential formin effector. An *A. gossypii* strain that possesses a GFP-tagged allele of *AgBNI1* was transformed with the plasmid encoding mCherry-*Ag*Rho3. In vegetative growing hyphae *Ag*Bni1 was located to the hyphal tip in a crescent-shaped accumulation (Figure 3B). Simultaneously, *Ag*Rho3 was located to the entire cytoplasm (Figure 3B). Even though there is no exclusive co-localization of both fluorescence signals, the *Ag*Rho3 signal overlaps with the *Ag*Bni1 signal. Thus, these findings do not provide evidence against the theory that *Ag*Rho3 is an activator of *Ag*Bni1.

The deletion of *AgRHO3* does not affect spore length.

During our localization studies we found that *Ag*Rho3 can be found in developing and mature sporangia (Figure 3A). Previous investigations revealed that the GTPases *Ag*Rho1a and *Ag*Rho1b are directly involved in the production of the linear spores of *A. gossypii* (Chapter 3.3). Therefore, we asked whether *Ag*Rho3 also plays a role for spore development. To answer this question, spores of an *Agrho3* deletion strain (Wendland & Philippsen, 2001) were isolated and further analyzed for sporulation phenotypes. The spores produced by the mutant strain showed a spore morphology comparable to the wild type without any deviations (Figure 3C). We also tested if the deletion of *Ag*Rho3 affects the length of the needle-shaped spores. Investigation of 56 spores isolated from the deletion strain revealed an average spore length of about 30 µm (Figure 3D). The average spore size of a wild type strain was about 30 µm (n=50), indicating that the deletion of *Ag*Rho3 does not influence spore length and morphology in *A. gossypii*.

The main *Ag*Rho4 pool is visible in sporangia.

Similar to our experiments on *Ag*Rho3, we performed investigations on the localization of *Ag*Rho4. The fluorescent protein mCherry was fused to the N-terminus of *Ag*Rho4 under the control of its native promoter. An *A. gossypii* wild type strain was transformed with the plasmid encoding the fusion construct and

analyzed by fluorescence microscopy. Only a very weak fluorescence signal in young, one day old hyphae can be detected at some parts of the cell cortex (Figure 4A, first row). Contrasting, investigations performed at the second day after cultivation in minimal medium revealed a clear and intense fluorescence signal for mCherry-*Ag*Rho4 at the entire cortex of the developing sporangia and, to lesser extent, in the cytoplasm. *Ag*Rho4 can be detected in hyphal segments that just started with sporulation (Figure 4A, second and third row) as well as in sporangia that already contain mature spores (Figure 4A, fourth row). Strikingly, *Ag*Rho4 was also located to the mature, needle-shaped spores (Figure 4A, fourth row). These results indicate a role of *Ag*Rho4 for spore formation in *A. gossypii.*

_Ag_Rho4 localization can be observed simultaneously with the sporulation-specific spindle pole component _Ag_Spo21.

In a next step, we tried to get a more precise idea about the developmental stage in which *Ag*Rho4 can be observed using fluorescence microscopy. On the basis of the first microscopical examinations it seems reasonable that *Ag*Rho4 plays a role for sporulation. To get deeper insight into the time-point where *Ag*Rho4 localization can be observed, we took advantage of a sporulation-specific component of the spindle pole body. *Ag*Spo21 co-localizes with the spindle pole body specifically during spore development and is involved in remodeling of this structure (Kemper *et al.*, 2011). This time-specific localization pattern can be used to determine the time-point when sporulation starts. For this experiment, a strain carrying a double-GFP tagged allele of *AgSPO21* was transformed with the plasmid encoding mCherry-*Ag*Rho4 . Using fluorescence microscopy, *Ag*Spo21 was found at the spindle pole body while *Ag*Rho4 was restricted to the cortex of the sporangia simultaneously two days after cultivation in minimal medium (Figure 4B). Following localization of both proteins over time revealed that the localization of *Ag*Rho4 at the entire membrane of sporangia occurs specifically during sporulation.

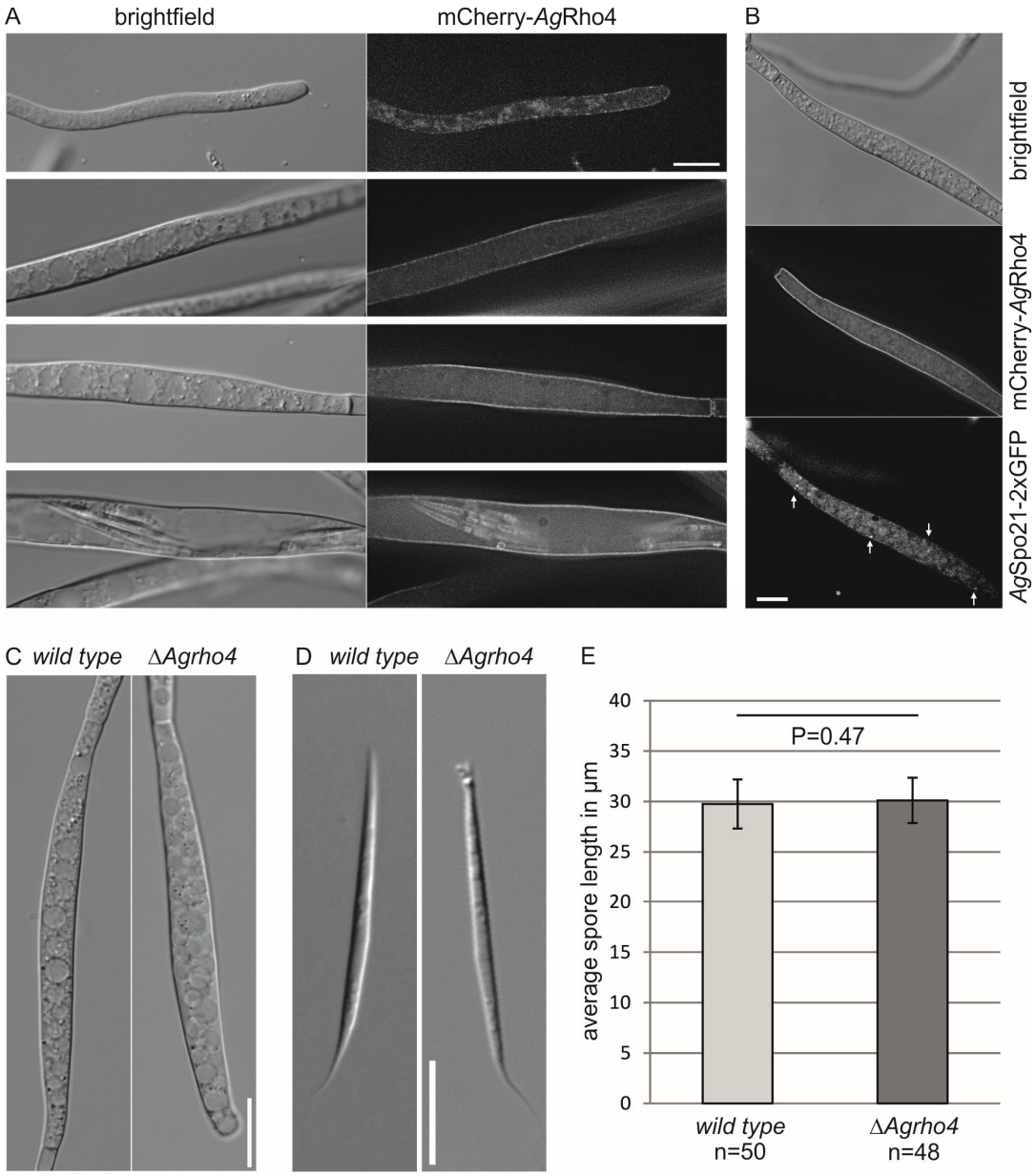

Figure 4: Analysis of *Ag*Rho4-localization and effects on spore formation.
A) mCherry-*Ag*Rho4 is located to the cell cortex. Young vegetative growing hypha (first row), two day old hyphae and sporangia that contain mature spores (second, third and fourth row). The scale bar represents 5 µm.
B) mCherry-*Ag*Rho4 and *Ag*Spo21-2xGFP can be observed simultaneously in sporangia. The arrows indicate the dot-like accumulation of *Ag*Spo21 at the spindle pole body. The scale bar represents 5 µm.
C) Comparison of sporangia from an *A. gossypii* wild type and the *Agrho4* deletion strain. Deletion of *AgRHO4* does not affect the development of sporangia. The scale bar represents 5 µm.
D) Spores derived from an *A. gossypii* wild type and the *Agrho4* deletion strain. The deletion of *AgRHO4* does not affect spore morphology. The scale bar represents 10 µm.
E) Average spore length of *A. gossypii* wild type and *Agrho4* deletion spores. The deletion of *AgRHO4* does not affect spore length. The number n represents spores measured from each strain. A student`s t-test shows that there is no statistically significant change in size ($P<0.47$).

The deletion of *AgRHO4* does not affect sporulation.

To get a more precise idea about the function of *Ag*Rho4 an *Agrho4* deletion strain (Wendland *et al.*, 2000) was analyzed at different time points during spore development. First, we had a look on early sporangia formation and compared the morphology with sporangia of a wild type strain. Both strains showed no differences regarding shape or size of sporangia (Figure 4C). We also considered the possibility of a direct effect of *Ag*Rho4 on the formation of the needle-shaped spores. This idea was also supported by our observation that *Ag*Rho4 directly localized to the needle-shaped spores (Figure 4A, fourth row). Furthermore, previous studies revealed that the two homologous Rho-type GTPases *Ag*Rho1a and *Ag*Rho1b have a direct effect on spore size and the spore wall (Chapter 3.3). We wanted to find out whether *Ag*Rho4 also affects spore development and prepared spores of the *Agrho4* deletion strain. The determination of spore length on the basis of 48 spores revealed an average size of 30 µm, which is similar to the spore length of the wild type (n=50, Figure 4E). Furthermore, spores of *Agrho4* were examined for spore wall phenotypes. Investigation of 48 spores revealed that the morphology of spores produced by the *Agrho4* deletion was normal without any deviations (Figure 4D).

The *Agrho4* deletion strain did not show any growth defects, which might be due to the fact that another GTPase (e.g. *Ag*Rho3) can fulfill the function of *Ag*Rho4. To further characterize the function of *Ag*Rho4, we decided to construct a strain that possesses a constitutively active form of this GTPase.

The constitutively active form of *Ag*Rho4 causes defects in vegetative growth and an increase in spore size.

We investigated if the genomic integration of the constitutively active form of *Ag*Rho4 has an effect on the growth behaviour of *A. gossypii.* Rho-type GTPases can be easily converted to the constitutively active form by a single point mutation. Thus, *Agrho4** combined with a *NAT1* marker gene was integrated by homologous recombination into the *Agrho4* deletion strain described above.

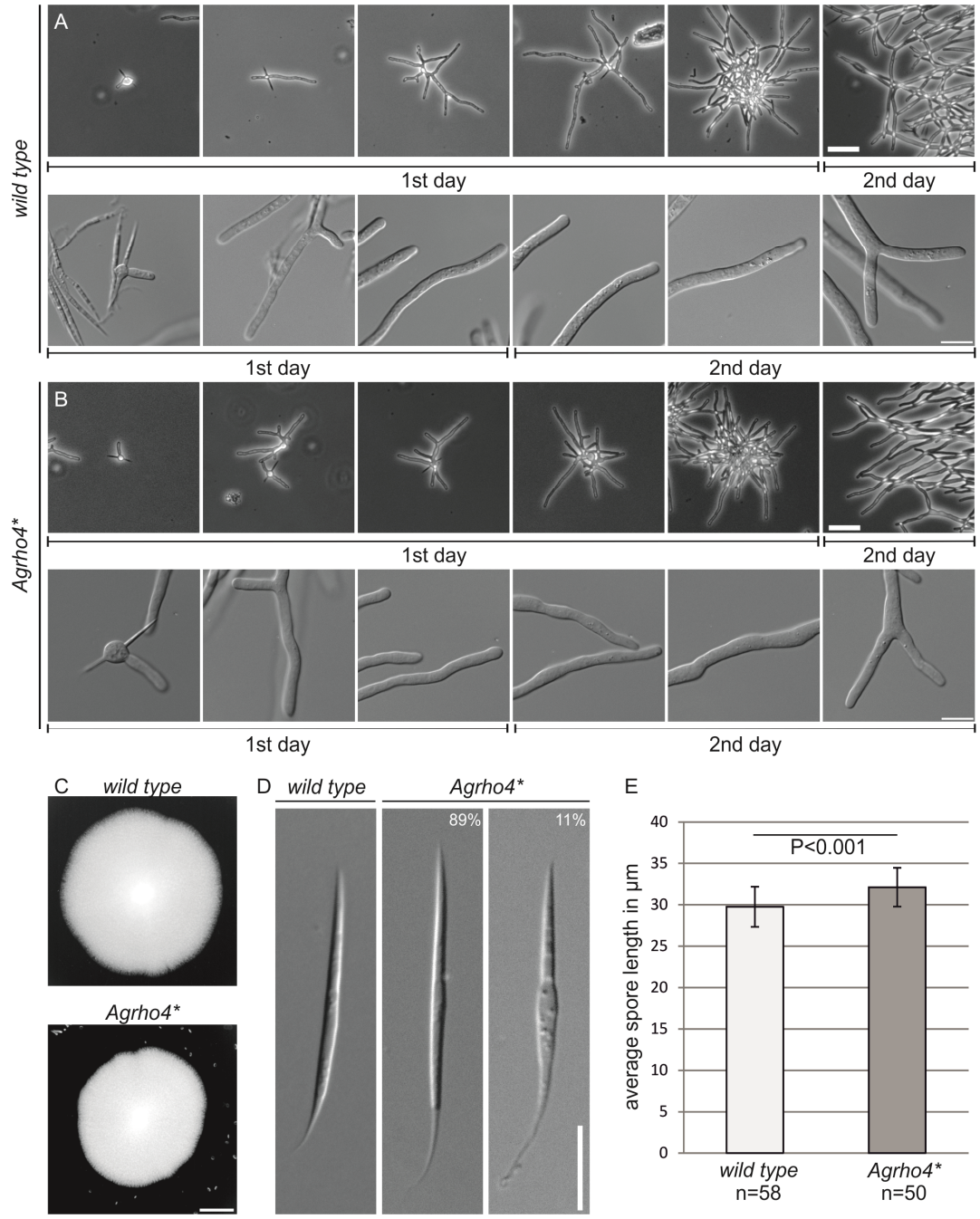

Figure 5: Growth phenotypes of an active *AgRHO4* allele.
A) Microscopical observation of one and two day old mycelia of an *A. gossypii* wild type strain using a 10x (first row, the scale bar represents 40 µm) and a 100x (second row, the scale bar represents 10 µm) magnification.
B) Microscopical observation of one and two day old mycelia of *Agrho4** using a 10x (first row, the scale bar represents 40 µm) and a 100x (second row, the scale bar represents 10 µm) magnification.
C) Macroscopical comparison of the growth behaviour of an *A. gossypii* wild type and the *Agrho4** strain. Mycelia were documented five days after cultivation on full medium. The scale bar represents 1 cm.
D) Spores isolated from an *A. gossypii* wild type and the *Agrho4** strain documented after 1 hour incubation in 0.03% Triton-X-100. 11% of the *Agrho4** spores showed defects in the membrane compartment. The scale bar represents 10 µm.
E) Determination of the average spore length of wild type and *Agrho4** spores. Spore length of *Agrho4** is slightly increased. A student`s t-test shows that this increase is statistical significant (P<0.001).

Macroscopic comparison of the growth behaviour of an *A. gossypii* wild type and the *Agrho4** strain showed that the mutant possessing the constitutively active form of *Ag*Rho4 grows more slowly compared to the wild type (Figure 5C). The resulting strain was analyzed by light microscopy. *Agrho4** showed normal germination and produced young mycelia without any abnormities (Figure 5B). However, the morphological growth defects of *Agrho4** became visible at the second day after cultivation. Hyphae appeared with an irregular shape with a variation in hyphal diameter of 2.13 µm compared to 0.79 µm of the wild type (n= 10, measured in the first 50 µm of the hyphae from the tip). In addition, hyphae showed defects in polarity, which go hand in hand with changes in the growth direction (Figure 5B). The timing of this observation is compatible with our finding that *Ag*Rho4 can be found in higher amounts by fluorescence microscopy at this time point, too. All in all, our findings suggest a function of *Ag*Rho4, which is important for a late developmental stage. In addition to hyphal growth tests, we checked the mutant strain for alterations in spore length. The size of 58 spores produced by *Agrho4** was measured and the average spore length was determined. In fact, we found a slight increase in spore length. The average size of the mutant strain was about 32 µm compared to 30 µm in the wild type (Figure 5E). Performance of a student`s t-test shows that this slight increase is statistical relevant ($P<0.001$). Additionally, we found that many spores produced by *Agrho4** were susceptible for lysis. Examination of 89 randomly chosen spores after one hour incubation in 0.03% Triton-X-100 revealed that 11% of the spores show defects in the membrane compartment. These defects result in swelling of this part of the spore and lysis (Figure 5D). Together with the localization of *Ag*Rho4 at the spore cortex, this points towards a role of Rho4 in spore wall formation.

Discussion

In this study, we performed detailed investigations on four Rho-type GTPases that were originally identified as potential *Ag*Bni1 activators in *A. gossypii*. While there is some information about the function of the two Rho1 homologs and *Ag*Rho3, the role of *Ag*Rho4 remained completely unclear, so far. Here, we examined the localization of the four GTPases, their role during vegetative growth and for spore development in *A. gossypii* with an emphasis on identifying in which processes the different Rho proteins signal via *Ag*Bni1.

We have shown before that the two *Ag*Rho1 proteins regulate spore length via *Ag*Bni1 (Chapter 3.3). If *Ag*Bni1 activation also occurs during hyphal tip growth remains unclear. As described by Köhli *et al.*, (2008a), we found that the two Rho1 homologs of *A. gossypii* mainly localized to the cell cortex of growing hyphae. This localization pattern is distinct from the small crescent localization of *Ag*Bni1 at the hyphal tip (Köhli *et al.*, 2008b, compare also Figure 2A). Therefore, we used the C1 domain of *Ag*Pkc1 to visualize only the active (GTP-bound) Rho1-proteins. These investigations revealed that the Rho1 GTPases are also active at the entire cortex (Figure 1A, B and C, left side) and not only at a small crescent-shaped area of growing tips. Therefore, it seems unlikely that the Rho1 proteins signal via *Ag*Bni1 during hyphal tip growth. This is further supported by our finding that the localization of the Rho binding domain of *Ag*Bni1 fused to tdTomato does not resemble the localization of the Rho1 proteins (Figure 2B). This suggests that interaction of Rho proteins with the effector *Ag*Bni1 is not sufficient for the localization of *Ag*Bni1 to the growing tip. This would be in good agreement with previous findings: Localization of *Ag*Bni1 strongly depends on the polarisome components *Ag*Spa2 and *Ag*Pea2. Deletion of either *Ag*Spa2 or *Ag*Pea2 results in a strong reduction or even in loss of the tip localization of the formin *Ag*Bni1 (Köhli *et al.*, 2008b). In contrast, deletion of the fourth component *Ag*Bud6 has no effect on the localization of *Ag*Bni1. However, we cannot exclude that this construct is mistargeted due to misfolding caused by the fusion to the fluorescent protein.

For the action of the *Ag*Rho1 proteins at the hyphal tip it seems more likely that the proteins regulate cell wall biosynthesis, a function that has been shown for the *Ag*Rho1 protein before (Köhli *et al.*, 2008a). Because the hyphal tip is the

growing part of the mycelium, there is a high demand for new cell wall material produced by the glucan synthase complex, which is regulated by Rho1 (Qadota *et al.*, 1996). In older parts of the mycelium we found that only a fraction of the Rho1 proteins is active. Interestingly, we also observed special sites within the cell wall of mature hyphae where Rho1 activity was concentrated (Figure 1A, B and C, middle). Due to the role of Rho1 signaling in the production of β-glucan, such an accumulation of active Rho1 proteins might correlate with cell wall repair.

In contrast to the cortical localization of *Ag*Rho1a and *Ag*Rho1b, *Ag*Rho3 localized to both, cortical and internal structures of hyhpae (Figure 3A). *Ag*Rho3 was shown to play a key role for maintenance of cell polarity in *A. gossypii.* The deletion of this GTPase leads to short periods of isotropic growth at hyphal tips (Wendland & Philippsen, 2001). This phenotype suggests an essential function of *Ag*Rho3 specifically at the growing tip. Such a function would be compatible with the activation of the formin *Ag*Bni1, which was also identified as a key factor for cell polarity (Schmitz *et al.*, 2006). In fact, the abundant appearance of *Ag*Rho3 does not exclude co-localization of the protein with *Ag*Bni1. Thus, *Ag*Bni1 might be also *in vivo* an effector of *Ag*Rho3 (Figure 3B). However, the fluorescence signal of mCherry-*Ag*Rho3, which we found to be distributed over the entire hypha, did not show any enrichment at the cortex of the hyphal tip. A small amount of Rho proteins might be sufficient to activate *Ag*Bni1 at this position. In contrast to hyphal growth, *Ag*Rho3 seems to be not involved in sporulation. Although *Ag*Rho3 localizes to developing and mature sporangia of *A. gossypii*, the deletion of this Rho protein did not affect spore development. Spores produced by the *Agrho3* deletion strain show a morphology that is comparable to the wild type without any deviations (Figure 3 C and D).

Only little information was available about the function of *Ag*Rho4. The deletion of the protein has no obvious phenotype on hyphal growth (Wendland *et al.*, 2000) and sporulation (Figure 4C,D and E). Analysis of a strain possessing a constitutively active form of *Ag*Rho4 gave a first impression of an *Ag*Rho4-specific function. We found that the *Agrho4** strain produces hyphae that are variable in the diameter and show deviations in the growth direction (Figure 5B). This finding shows that *Ag*Rho4 is involved in maintenance of cell polarity and control of the growth direction. The phenotype resembles a combination of the

phenotypes observed for *Agrsr1* and *Agrho3* deletions (Bauer *et al.*, 2004, Wendland & Philippsen, 2001). The *Agrho4** mutant frequently loses polarity, which is similar to the deletion of *Agrho3*, but in contrast to this mutant it does not maintain the polarity axis, when re-establishing polarized growth. The growth axis alternates with each event of polarity loss, leading to a zigzag curve, which is less pronounced, but reminds on the growth pattern of the *Agrsr1* deletion.

This also suggests that *Ag*Rho3 and *Ag*Rho4 have slightly overlapping functions in *A. gossypii*. A similar mechanism is described for Rho3 and Rho4 in the closely related organism *S. cerevisiae* (Matsui & Toh-e, 1992). However, it seems as if *Ag*Rho3 functions more during vegetative growth, whereas *Ag*Rho4 functions mainly in sporulation. This is supported by our finding that the growth defects of *Agrho4** can be observed as late as on second day after cultivation and that mCherry-*Ag*Rho4 shows an increasing fluorescence intensity over time and can be observed in high amounts at the second day after cultivation (Figure 4A). All in all, our results suggest a function for *Ag*Rho4 that is important in mature but not young mycelia. Furthermore, we revealed a role of *Ag*Rho4 in spore formation in *A. gossypii.* First, we found that *Ag*Rho4 directly localizes to the developing spores and to the cortex of sporangia (Figure 4A). Second, we could show that the genomic integration of *Agrho4** leads to an increase in the length of the needle-shaped spores and to lysis defects in a fraction of *Agrho4** spores (Figure 5D and E). These results indicate a direct involvement of *Ag*Rho4 in spore formation in *A. gossypii.* If these *Ag*Rho4 functions are achieved via *Ag*Bni1 remains unclear. In young, vegetatively growing hyphae a slight signal of mCherry-*Ag*Rho4 is visible at the membrane, again not excluding a co-localization with *Ag*Bni1. In sporangia and at spores *Ag*Bni1-GFP is not visible (our own unpublished observation), therefore it is unlikely that during sporulation *Ag*Rho4 signals to *Ag*Bni1.

In summary, our work presented here will further help in understanding how specificity is achieved for different Rho-type GTPases that share common effector proteins. In the case of *Ag*Bni1 our work indicates that different Rho-type GTPases act on the protein in different cellular processes. These might be maintenance of growth polarity at the hyphal tip for *Ag*Rho3 and sporulation for

the *Ag*Rho1 proteins. In addition we identified *Ag*Rho4 as a factor that is involved in spore formation.

Experimental procedures

Ashbya gossypii strains and growth conditions

All the *Ashbya gossypii* strains were constructed using PCR-based gene targeting, as described by Wendland *et al.*, 2000 and are listed in table 1. For the generation of the targeting cassettes for deletions or gene fusions, we used template vectors from the pAGT series (Kaufmann, 2009). The transformation of *A. gossypii* by plasmids was performed according to the methods of Wright & Philippsen (1991). All oligonucleotides, plasmids and templates that were used for this study are listed in tables 2 and 3.

Ashbya gossypii was cultured either in full medium (AFM) supplemented with or without 200 µg/ml geneticin (Sigma, St. Louis, MO) or in 100 µg/ml ClonNAT (Werner BioAgents, Jena, Germany). For use of the auxotrophic marker, *leu2* cells were cultured in synthetic minimal medium (ASC). To avoid auto-fluorescence of the medium, we also used a synthetic medium for fluorescence microscopy.

To investigate sporulation, the cells were grown for two days in a synthetic minimal medium. After this incubation period, *A. gossypii* produced sporangia.

DNA manipulations, plasmids and constructs

DNA manipulations were conducted according to the methods of Sambrook *et al.* (2001). We used the *Escherichia coli* host strain DH5aF´ (Hanahan, 1983). PCR was performed using either the Dream Taq Polymerase (Fermentas, St. Leon-Roth, Germany) or the Expand High Fidelity PCR System (Roche, Mannheim, Germany). The oligonucleotides were synthesized by Microsynth (Balgach, Switzerland). DNA sequencing was performed by Scientific Research and Development (Bad Homburg, Germany). For recombination of plasmids and PCR products, the DNA was co-transformed into the *Saccharomyces cerevisiae* strain *DHD5* (*MATa/MATα; ura3-52/ura3-52; leu2-3_112/leu2-3_112; his3Δ1/his3Δ1; MAL2-8C/MAL2-8C; SUC2/SUC2*) (Arvanitidis & Heinisch, 1994). Plasmid DNA was isolated from *E. coli* and *S. cerevisiae* using the High Pure Plasmid Isolation Kit (Roche, Mannheim, Germany). For plasmid isolation from yeast, we used a protocol modified by Schmitz *et al.*, 2006.

Fluorescence microscopy

For fluorescence microscopy, we used the same set-up as described in Kemper *et al.*, 2011.

Purification of *Ashbya gossypii* spores

The *A. gossypii* strains were grown on agar plates containing the corresponding selection medium for approximately five days. The spore-containing layer of the mycelium was removed and transferred to a reaction tube. We added 1 ml of sterile water, 200 µl of Glucanex (Sigma, 20 mg/ml) and 50 µl of Zymolyase (MP Biomedicals, Illkirch, France, 10 mg/ml) to the spores. The suspension was incubated for 45 minutes at 37°C on a shaker. The spores were centrifuged (5 minutes, 3000 rpm), and the supernatant containing the residual mycelium was discarded. The spores were washed three times with 0.03% Triton-X-100. The resultant spores were suspended in either 0.03% Triton-X-100 for further investigations or in 33% glycerine for storage at -80°C.

Statistical analysis

The significance levels of the differences in size were determined using Student`s t-test of Excel 2010 (Microsoft, Redmond, WA).

Table 1: *Ashbya gossypii* strains

Strains	Genotype	Construction	Source
ΔlΔt	*Agleu2Δ Agthr4Δ*	-	Altmann-Johl and Philippsen (1996)
K47	*GEN3-P$_{ScHIS3}$-GFP-AgBNI1 Agleu2Δ Agthr4Δ*	-	Köhli *et al.*, 2008
Agrho1aΔ	*Agrho1aΔ::GEN3*	-	Köhli *et al.,* 2008
AgBNI1-GFP	*AgBNI1-GFP-GEN3 Agleu2Δ Agthr4Δ*	-	Schmitz *et al.*, 2006
Agrho3Δ	*Agrho3Δ::GEN3 Agleu2Δ Agthr4Δ*	-	Wendland & Philippsen, 2001
Agrho4Δ	*Agrho4Δ::GEN3 Agleu2Δ Agthr4Δ*	-	Wendland *et al.,* 2000
AgSpo21-2xGFP	*AgSPO21-2xGFP-KanMX Agleu2Δ Agthr4Δ*	-	Kemper *et al.,* 2011
*Agrho4**	*Agrho4*-NAT1 Agleu2Δ Agthr4Δ*	introduction of *Agrho4** *NAT1* from pML166 by homologous recombination into *Agrho4Δ*	this study
Agprk1Δ	*Agprk1Δ::KanR Agleu2Δ Agthr4Δ*	*KanR* amplified with 10.044/10.045 from pAGT140, integration by homologous recombination	this study

Table 2: Oligonucleotides

No.	Name	Sequence
09.009	Rho3Prom HindIII	TCGTAAGCTTAGCGCCACCAGCAATGCCAC
09.010	Rho3Prom BamHI	GACTGGATCCCTTGTGTTTGTAGAGCTTGG
09.044	RHO3 CAAX EcoRI for	GCTCGAATTCTCCTCTGTGTGGGTCGAGCT
09.045	RHO3 CAAX SpeI rev	ACCAACTAGTGCATCTACAAGACCACACATCGGA
09.011	Rho4Prom HindIII	TCGTAAGCTTTTCAGCTCCCGTGTTTGCCC
09.012	Rho4Prom BamHI	GACTGGATCCTTCGTTCTGTCTGCCTCTTG
09.042	RHO4 CAAX EcoRI for	GCTCGAATTCTAGCGCAGGGCCGTTGCAAG
09.043	RHO4 CAAX SpeI rev	CACCAACTAGTGCATCTACAAGACCACACATCGG
10.017	ScHIS3Prom for EcoRI	CTTCGAATTCACACCGATCCGCTGCACGGT
10.018	ScHIS3prom rev XmaI	CCATCCCGGGCTTTGCCTTCGTTTATCTTG
10.019	tdtomato for XmaI	AAAGCCCGGGATGGTGAGCAAGGGCGAGGA
10.020	tdtomato rev BglII	GAATAGATCTCTTGTACAGCTCGTCCATGC
10.024	PKC C1 for BglII	GAAGAGATCTGTAGGGTTCAGCAAATCCAAC
10.025	PKC C1 rev SacII	GCTTCCGCGGAAGCTTTTAATATATTAGGCGCGTTTGTC
10.035	Rho4 nat1 for	GAAGGGCATGTTCAAGAAGAAGCAGCAGCGGGACCCGCAGGCGCAGGA ACCGTTACGGTATTTTAC
10.036	Rho4 nat1 rev	GACTAGATGCCTAACTACACGGTCACGCAGGCCTCGACAGCGGACACA GTGTTCCTTAATCAAGG
10.021	Bni1frag for BglII	CAAGAGATCTATTCTGCTACATAAAGCCAC
10.022	Bni1frag rev SacII	GCTTCCGCGGAAGCTTTTATGCTTCAGTTCCTCTGTGTT
10.044	del PRK1 for	TTCGTACTGAGGTCGTATTTTATACGGTTCCATACAGCGGACAGGGGT GTATTTACCAATAATGT
10.045	del PRK1 rev	TAATAGAAATGAACTGGCATTTTCTATTAGACAATGATCAACATGGAT GAGGCCGTCTTTTGTTG
10.046	PRK1del cont1	AGCTGTTCGTGCTTGTAGTG
10.047	PRK1del cont2	ACGAATCTCTAGGCGATTGG

Table 3: Plasmids

Name	Backbone	Construction	Insert	Source
pHPS572	YCPlac111	P_{AgRHO3} amplified with 09.009/09.010 from pAG11320, HindIII/BamHI digested; mCherry from BamHI/EcoRI digested pHPS495, *AgRHO3* amplified with 09.044/09.045 from pHPS555, EcoRI/SpeI digested	P_{AgRHO3}-mCherry-*AgRHO3*	this study
pHPS495	YCPlac111	-	P_{AgATG8}-mCherry-*AgATG8*	this study
pHPS555	YCPlac111	-	$P_{AgRHO1b}$-$YFP_{155-239}$-*AgRHO3*	this study
pHPS573	YCPlac111	P_{AgRHO4} amplified with 09.011/09.012 from pAG6786 HindIII/BamHI digested; mCherry from BamHI/EcoRI digested pHPS495; *AgRHO4* amplified with 09.042/09.043 from pHPS556, EcoRI/SpeI digested	P_{AgRHO4}-mCherry-*AgRHO4*	this study
pHPS556	YCPlac111	-	$P_{AgRHO1b}$-$YFP_{155-239}$-*AgRHO4*	this study
pHPS715	pHPS250	Integration of tdTomato-*AgPKC1* $_{1122-1911}$, digested with HindIII	$P_{AgRHO1b}$-GFP-*AgRHO1b*, P_{ScHIS3}-tdTomato-*AgPKC1* $_{1122-1911}$	this study
pHPS250	-	-	GFP-*AgRHO1b*	Köhli *et al.,* 2008
pHPS731	pHPS715	Integration of GFP-*Ag*Rho1a from pHPS248, digested with BamHI/SpeI	$P_{AgRHO1b}$-GFP-*AgRHO1a*, P_{ScHIS3}-tdTomato-*AgPKC1* $_{1122-1911}$	this study
pHPS714	pUC21	P_{ScHIS3} amplified with 10.017/10.018 from pHPS383, EcoRI/XmaI digested; tdTomato amplified with 10.019/10.020 from pAGT353, XmaI/BglII digested; *AgPKC1* $_{1122-1911}$ amplified with 10.024/10.025 from genomic DNA, digested with BglII/SacII	P_{ScHIS3}-tdTomato-*AgPKC1* $_{1122-1911}$	this study
pHPS383	-	-	P_{ScHIS3}-*AgBNR2-GFP*	Kemper *et al.,* 2011
pHPS248	-	-	GFP-*AgRHO1a*	Köhli *et al.,* 2008
pML161	pUC21	integration of *AgRHO4* including flanking regions of the genome from pAG6786, digested with HindII/SacI;	*AgRHO4*	this study

Name	Backbone	Construction	Insert	Source
pML164	YCPlac111	integration of *AgRHO4** from pML162 into yeast vector, digested with HindII/SacI	*AgRHO4**	this study
pML166	pML164	amplification of *NAT1* with 10.035/10.036 from pAGT207, integration by homologous recombination	*AgRHO4* NAT1,* integration cassette	this study
pHPS713	pUC21	P_{ScHIS3} amplified with 10.017/10.018 from pHPS383, EcoRI/XmaI digested; tdTomato amplified with 10.019/10.020 from pAGT353, XmaI/BglII digested; *AgBNI1* $_{615\text{-}1839}$ amplified with 10.021/10.022 from pHPS482	P_{ScHIS3}-tdTomato-*AgBNI1* $_{615\text{-}1839}$	this study
pHPS719	YCPlac111	P_{ScHIS3}-tdTomato-*AgBNI1* $_{615\text{-}1839}$ from pHPS713, digested with HindIII	P_{ScHIS3}-tdTomato-*AgBNI1* $_{615\text{-}1839}$	this study
pAGT353	-	-	tdTomato	Kaufmann, 2009
pAGT207	-	-	*NAT1*	Kaufmann, 2009
pHPS485	-	-	Gal4BD-*Ag*Rho4*	Schmitz *et al.,* 2006
pHPS482	-	-	Gal4AD-*Ag*Bni1-N	Schmitz *et al*., 2006
pUC21	-	-	-	Vieira and Messing, 1991
YCPlac111	-	-	-	Gietz and Sugino, 1988
pAGT140	-	-	*KanR*	Kaufmann, 2009

References

Adamson, P., C. J. Marshall, A. Hall & P. A. Tilbrook, (1992) Post-translational modifications of p21rho proteins. *J Biol Chem* **267**: 20033-20038.

Arvanitidis, A. & J. J. Heinisch, (1994) Studies on the function of yeast phosphofructokinase subunits by in vitro mutagenesis. *J Biol Chem* **269**: 8911-8918.

Bauer, Y., P. Knechtle, J. Wendland, H. Helfer & P. Philippsen, (2004) A Ras-like GTPase is involved in hyphal growth guidance in the filamentous fungus *Ashbya gossypii*. *Mol Biol Cell* **15**: 4622-4632.

Deacon, J. W., (2006) Fungal Biology. Malden, MA: Blackwell Pub.

Dietrich, F. S., S. Voegeli, S. Brachat, A. Lerch, K. Gates, S. Steiner, C. Mohr, R. Pohlmann, P. Luedi, S. Choi, R. A. Wing, A. Flavier, T. D. Gaffney & P. Philippsen, (2004) The *Ashbya gossypii* genome as a tool for mapping the ancient *Saccharomyces cerevisiae* genome. *Science* **304**: 304-307.

Gietz, R.D. and Sugino, A., (1988) New yeast–*Escherichia coli* shuttle vectors constructed with *in vitro* mutagenized yeast genes lacking six-base pair restriction sites. *Gene*, **74**, 527–534.

Hanahan, D., (1983) Studies on transformation of *Escherichia coli* with plasmids. *J Mol Biol* **166**: 557-580.

Kamada, Y., H. Qadota, C. P. Python, Y. Anraku, Y. Ohya & D. E. Levin, (1996) Activation of yeast protein kinase C by Rho1 GTPase. *J Biol Chem* **271**: 9193-9196.

Kaufmann, A., (2009) A plasmid collection for PCR-based gene targeting in the filamentous ascomycete *Ashbya gossypii*. *Fungal Genet Biol* **46**: 595-603.

Kemper, M., L. Mohlzahn, M. Lickfeld, C. Lang, S. Wählisch & H. P. Schmitz, (2011) A Bnr-like formin links actin to the spindle pole body during sporulation in the filamentous fungus *Ashbya gossypii*. *Mol Microbiol* **80**: 1276-1295.

Knechtle, P., J. Wendland & P. Philippsen, (2006) The SH3/PH domain protein *Ag*Boi1/2 collaborates with the Rho-type GTPase *Ag*Rho3 to prevent nonpolar growth at hyphal tips of *Ashbya gossypii*. *Eukaryot Cell* **5**: 1635-1647.

Köhli, M., S. Buck & H. P. Schmitz, (2008a) The function of two closely related Rho proteins is determined by an atypical switch I region. *J Cell Sci* **121**: 1065-1075.

Köhli, M., V. Galati, K. Boudier, R. W. Roberson & P. Philippsen, (2008b) Growth-speed-correlated localization of exocyst and polarisome components in growth zones of *Ashbya gossypii* hyphal tips. *J Cell Sci* **121**: 3878-3889.

Levin, D. E., (2011) Regulation of cell wall biogenesis in *Saccharomyces cerevisiae*: the cell wall integrity signaling pathway. *Genetics* **189**: 1145-1175.

Lickfeld, M. & H. P. Schmitz, (2011) Selection of STOP-free sequences from random mutagenesis for 'loss of interaction' two-hybrid studies. *Yeast* **28**: 535-545.

Matsui, Y. & A. Toh-e, (1992) Isolation and characterization of two novel ras superfamily genes in *Saccharomyces cerevisiae*. *Gene* **114**: 43-49.

Nonaka, H., K. Tanaka, H. Hirano, T. Fujiwara, H. Kohno, M. Umikawa, A. Mino & Y. Takai, (1995) A downstream target of *RHO1* small GTP-binding

protein is *PKC1*, a homolog of protein kinase C, which leads to activation of the MAP kinase cascade in *Saccharomyces cerevisiae*. *EMBO J* **14**: 5931-5938.

Qadota, H., C. P. Python, S. B. Inoue, M. Arisawa, Y. Anraku, Y. Zheng, T. Watanabe, D. E. Levin & Y. Ohya, (1996) Identification of yeast Rho1p GTPase as a regulatory subunit of 1,3-beta-glucan synthase. *Science* **272**: 279-281.

Sambrook J, Russel DW, Sambrook J., (2001). *Molecular Cloning: A Laboratory Manual.* Cold Spring Harbor Laboratory Press: Cold Spring Harbor, NY.

Schmitz, H. P., A. Kaufmann, M. Köhli, P. P. Laissue & P. Philippsen, (2006) From function to shape: a novel role of a formin in morphogenesis of the fungus *Ashbya gossypii*. *Mol Biol Cell* **17**: 130-145.

Shaner, N. C., R. E. Campbell, P. A. Steinbach, B. N. Giepmans, A. E. Palmer & R. Y. Tsien, (2004) Improved monomeric red, orange and yellow fluorescent proteins derived from *Discosoma* sp. red fluorescent protein. *Nat Biotechnol* **22**: 1567-1572.

Vieira, J. & J. Messing, (1991) New pUC-derived cloning vectors with different selectable markers and DNA replication origins. *Gene* **100**: 189-194.

Wendland, J., Y. Ayad-Durieux, P. Knechtle, C. Rebischung & P. Philippsen, (2000) PCR-based gene targeting in the filamentous fungus *Ashbya gossypii. Gene* **242**: 381-391.

Wendland, J. & P. Philippsen, (2001) Cell polarity and hyphal morphogenesis are controlled by multiple rho-protein modules in the filamentous ascomycete *Ashbya gossypii*. *Genetics* **157**: 601-610.

Wright, M. C. & P. Philippsen, (1991) Replicative transformation of the filamentous fungus *Ashbya gossypii* with plasmids containing *Saccharomyces cerevisiae* ARS elements. *Gene* **109**: 99-105.

4 Concluding remarks

The findings presented in this study contribute to a better understanding of the composition and the assembly of the needle-shaped spores produced by the filamentous ascomycete *A. gossypii.* The needle-shaped spores possess a composite structure that consists of three major segments: a rigid tip segment, a fragile membrane compartment and a stable tail cap. A protein network consisting of the Rho-type GTPases *Ag*Rho1a and *Ag*Rho1b, the paxillin-like protein *Ag*Pxl1 and the formin *Ag*Bni1, four proteins that have been previously described to play a role for cell polarity, was identified to regulate the length of the linear spores of *A. gossypii.* Strikingly, the function of this network affects the entire spore and is not restricted to a specific spore compartment. This finding hints that the determination of spore length in *A. gossypii* is realized by a higher-level process that affects the entire spore. The remodeling of the actin cytoskeleton during spore formation might play a key role for the determination of the spore size. Such a regulation mechanism might be responsible for the arrangement of the different regions of actin accumulation within developing sporangia.

Two formins have been identified to have an important function during sporulation in *A. gossypii.* Each of these proteins plays a role in different processes during spore formation (Figure 1). *Ag*Bnr2 links actin to the spindle pole body during sporulation and plays a key role for the arrangement of nuclei within the developing sporangium. These investigations identified heavily-bundled actin structures that correlate with the developing tip segments of the spores. The *Ag*Bnr2 homolog *Sc*Bnr1 of *S. cerevisiae* bundles actin filaments to actin cables (Moseley & Goode, 2005). Therefore, *Ag*Bnr2 as a Bnr-like formin might also be involved in a bundling of actin filaments during spore formation (Figure 1). This idea is supported by the observation that *Ag*Bnr2 co-localizes to these actin structures about the entire length. Such a role in actin bundling would be compatible with a function in the positioning of the nucleus within the spore: The nucleus has a fixed position within the spore, which is directly adjacent to the tip segment (Figure 1). It seems reasonable that *Ag*Bnr2 and its

function in the connection of nuclei to actin structures are directly involved in the positioning of the nucleus.

In contrast to *Ag*Bnr2, which is involved in the assembly of actin structures that act as a template for the development of specifically the tip segment, *Ag*Bni1 is involved in a regulation mechanism that affects all three spore compartments. Thereby, *Ag*Bni1 might play a role for the assembly and rearrangement of actin structures in developing sporangia (Figure 1).

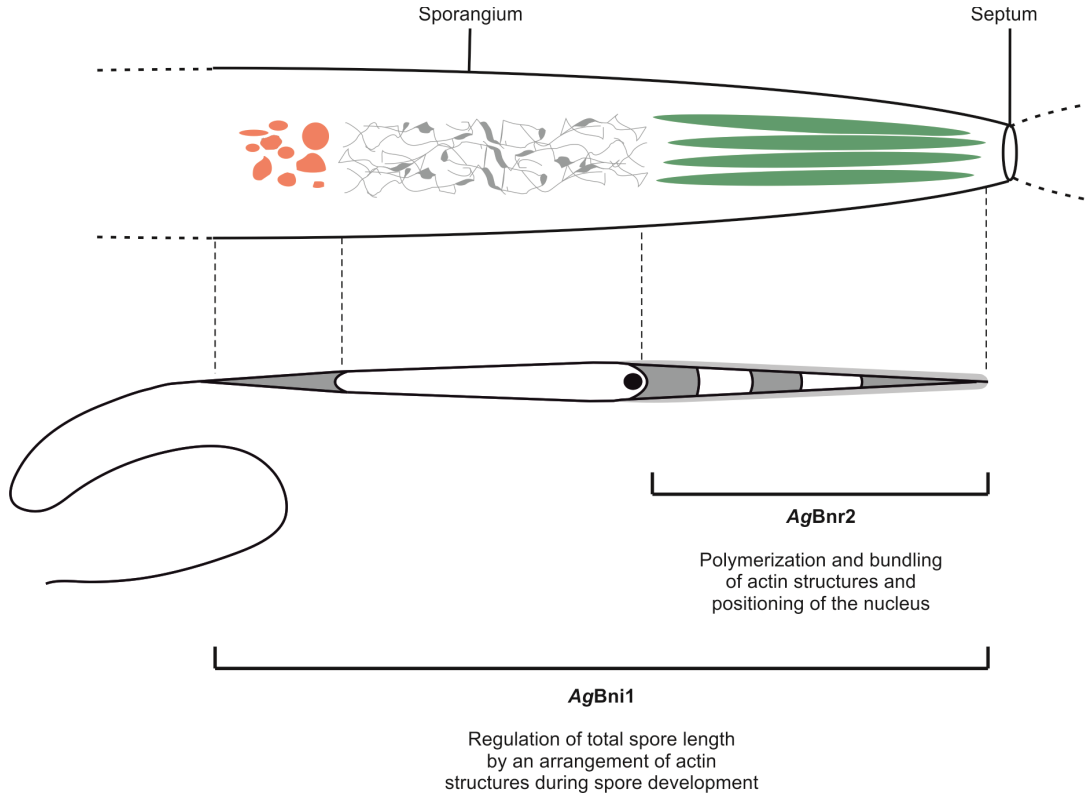

Figure 1: The formins *Ag*Bnr2 and *Ag*Bni1 fulfill different functions during spore formation in *A. gossypii.*
The figure shows one half of a developing sporangium including the three different zones of actin accumulation (shown in orange, grey and green, see also Chapter 3.3) that correlate with the different segments of developing spores.

Furthermore, the investigations presented in this study revealed an involvement of the Rho-type GTPase *Ag*Rho4 in polarity establishment and maintenance. Investigations of a strain that possess a constitutively active allele of this GTPase identified defects in the diameter of hyphae and irregular changes in their growth direction. Interestingly, *Ag*Rho4, which seems to be a factor for polarity in *A. gossypii,* also plays a role during spore formation. The introduction

of the constitutively active form of *Ag*Rho4 causes a slight increase in spore length and causes lysis defects of mature spores. Thus, a key conclusion of the work presented here is, that proteins that are known to play a role for cell polarity in *A. gossypii* can have a simultaneous function in the production of the highly polar spores of this fungus.

Reference

Moseley, J. B. & B. L. Goode, (2005) Differential activities and regulation of *Saccharomyces cerevisiae* formin proteins Bni1 and Bnr1 by Bud6. *J Biol Chem* **280**: 28023-28033.

5 Appendix

5.1 The *AgPXL1* deletion and overexpression strains show septation defects.

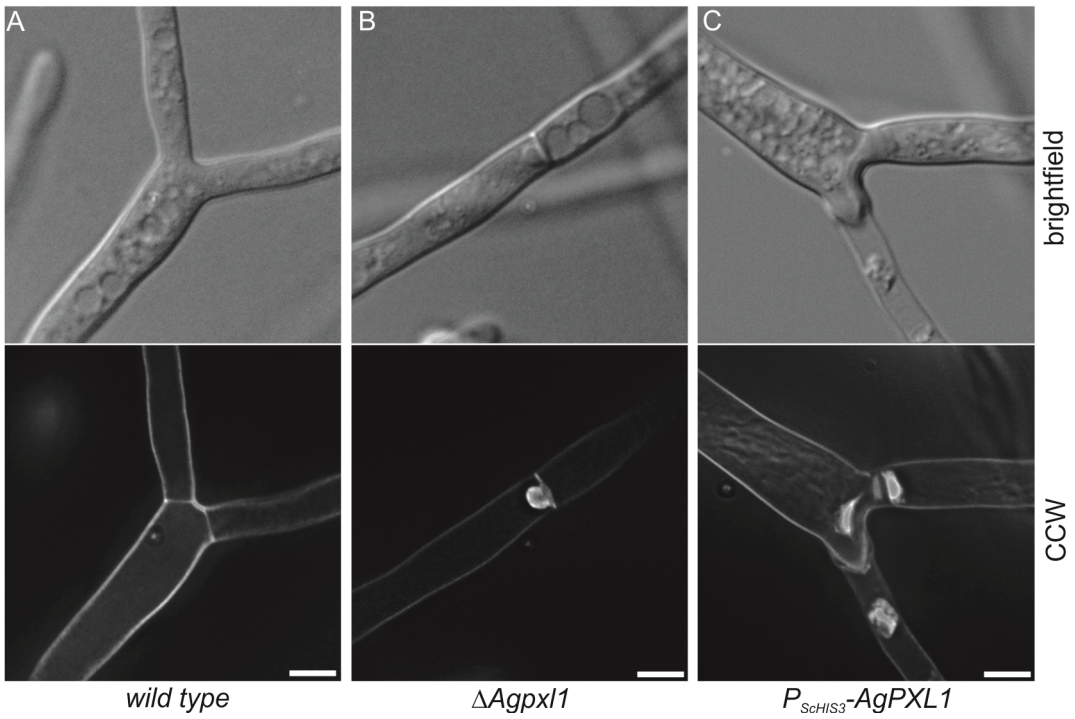

Figure 1: *AgPXL1* mutants show septation defects in a mature mycelium. A) Normal septation in a wild type *A. gossypii* strain. Staining with calcofluor white (CCW) indicates chitin accumulation in the cell wall and at septa. Septation is abnormal in *ΔAgpxl1* (B) showing invaginations and in P_{ScHIS3} *–AgPXL1* (C) that produces irregularly shaped and thick septa. The scale bars represent 5 µm.

In addition to the sporulation phenotypes described in chapter 3.3, we also observed septation phenotypes in both, the *Agpxl1* deletion and overexpression strain. Defects in the formation of septa are so strong that they can be even observed on the basis of brightfield images. Septa of very old hyphae appear irregularly shaped compared to the wild type. This phenotype becomes more obvious after staining with calcofluor white, a fluorescent dye that specifically stains chitin, which is concentrated at these structures. Fluorescence microscopy supports our observation that the position and structure of septa is abnormal (Figure 1A,B and C). However, the septation defects we observed in our studies were slightly different in the deletion and overexpression strain. In the *Agpxl1* deletion strain, we observed septa showing an invagination. In the

AgPXL1 overexpression strain, we observed very thick septa and abnormalities of their position. Under consideration of the septum localization, we described for *Ag*Pxl1 before, these results indicate an important role of *Ag*Pxl1 in septum formation.

Our investigations of the chitin accumulation in spores produced by the *Agpxl1* deletion and the overexpression strain (Chapter 3.3, Figure 9) revealed a direct effect of *Ag*Pxl1 on the amount of chitin in mature spores. The septation defects in mature mycelia presented here supports our theory that *Ag*Pxl1 is involved in the regulation of chitin accumulation in mycelia and spores. It remains unclear so far, whether *Ag*Pxl1 affects the production or the delivery of this substance to specific sites like e.g. septa in *A. gossypii.*

5.2 *Ag*Prk1 is essential *A. gossypii.*

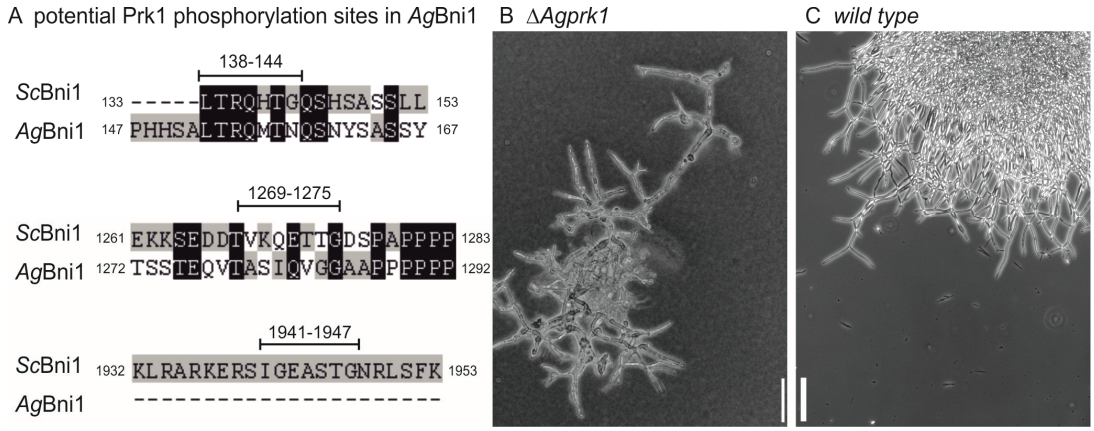

Figure 2: *Ag*Prk1 as a potential activator of the formin *Ag*Bni1.
A) Alignment of the Prk1 phosphorylation motifs identified for *Sc*Bni1 with the sequence of *Ag*Bni1. The three sites identified for Bni1 in *S. cerevisiae* are not fully conserved in Bni1 of *A. gossypii.* B) Deletion of *AgPRK1* leads to severe growth defects. The growth behaviour of the homokaryotic *Agprk1* deletion strain was documented on agar with a 10x magnification. The scale bar represents 100 µm. C) Wild type control strain documented with a 10x magnification. The scale bar represents 100 µm.

Previous examinations on the activation of formins in diverse organisms revealed that this class of proteins is not only regulated by Rho-type GTPases, but also by other signals (Wang *et al.*, 2009). Therefore, phosphorylation was shown to be an essential step to achieve full activation of formin proteins. Investigations in the close relative *S. cerevisiae* identified the actin regulating

kinase *Sc*Prk1 (p53 Regulatory Kinase) and its homolog *Sc*Ark1 as key factors for the activation of *Sc*Bni1 (Wang *et al.*, 2009). On the basis of sequence analysis, the authors identified three potential phosphorylation sites in *Sc*Bni1 provided by the motif [L/V/I]xxxxTG in the Rho binding domain, the FH1 domain and near the Diaphanous autoregulatory domain (Figure 2A). The determination of threonin phosphorylation of *Sc*Bni1 revealed that the deletion of *ScPRK1* results in a reduced *Sc*Bni1 phosphorylation level to about 55%. *Sc*Bni1 isolated from the double deletion *ΔScprk1, ΔScark1* showed a phosphorylation level reduced to even 15%. Furthermore, the authors found that phosphorylation of either one of the Prk1 motifs is sufficient to disrupt the intramolecular interaction of *Sc*Bni1. Unphosphorylated *Sc*Bni1 inhibited actin polymerization in an *in vitro* actin polymerization assay, which was not observed for the phosphorylated form of the formin. All in all, the authors propose a model in which the autoregulatory interaction of *Sc*Bni1 is released by *Sc*Prk1 phosphorylation. Thereby, the authors put the function of the Rho-type GTPases in *Sc*Bni1 activation into question (Wang *et al.*, 2009).

We were interested in the activation of the formin *Ag*Bni1 and thought about a similar situation in the closely related organism *A. gossypii.* The genome of *A. gossypii* encodes only one protein that is homologous to *Sc*Prk1 and *Sc*Ark1. In a next step, we analyzed the amino acid sequence of *Ag*Bni1 for potential Prk1 phosphorylation motifs. The three [L/V/I]xxxxTG motifs, which can be found in Bni1 of *S. cerevisiae* cannot be identified in the homologous protein of *A. gossypii* (Figure 2A). The phosphorylation site, which was identified in the Rho binding domain of *Sc*Bni1, is incomplete, but the best conserved of the three sites from *Sc*Bni1 in *Ag*Bni1. The other potential phosphorylation motifs cannot be found in the sequence of *Ag*Bni1 (Figure 2A). This finding suggests that the phosphorylation motifs that were identified for *Sc*Bni1 are not fully conserved in *Ag*Bni1. Nevertheless, the homologous gene *AgPRK1* in *A. gossypii* was deleted to get deeper insight into a possible function in *Ag*Bni1 activation. The deletion of *AgPRK1* should cause severe growth defects in a very early step of germination if *Ag*Prk1 represents the main activator of *Ag*Bni1. If *Ag*Prk1 is really the key factor for the activation of *Ag*Bni1, the phenotype of the deletion of *Ag*Prk1 would resemble the *Agbni1* deletion strain. Spores of an *Agbni1* deletion strain start with germination but are unable to reach the hyphal growth

phase. Instead of polar growth they show isotropic growth, which leads to the production of giant, potato-shaped cells containing up to 100 nuclei (Schmitz *et al.*, 2006). Integration of the *Agprk1*-deletion cassette leads to the production of a heterokaryotic mycelium. To get a homokaryotic deletion strain, spores derived from the heterokaryotic strain must be dissected on selective medium containing geneticin. We were unable to observe a mature mycelium produced by a homokaryotic *Agprk1* deletion strain macroscopically. More detailed investigations using light microscopy visualized a very small mycelium that shows severe growth defects (Figure 2B). Homokaryotic *Agprk1* deletion strains produce hyphae but filamentous growth is very slow and stops in a very early stage. In addition, the deletion strain is very susceptible for cell lysis even on solid medium (Figure 2B).

All in all, we found that the actin regulating kinase *Ag*Prk1 is essential in *A. gossypii*. However, it remains unclear whether this essential function is restricted to the activation of *Ag*Bni1, even though the phenotype we observed for the *Agprk1* deletion strain might correlate with defects in the organization of the actin cytoskeleton. For example, we observed characteristic swellings, which resemble the phenotype of cells that were treated with the actin-depolymerizing drug Latrunculin A (Köhli *et al.*, 2008). Our findings do not allow answering the question, whether *Ag*Prk1 contributes to the activation of *Ag*Bni1. However, the phenotype of *Agprk1* supports the theory that this kinase has a function in actin regulation, which will be investigated in future studies.

References

Köhli, M., S. Buck & H. P. Schmitz, (2008) The function of two closely related Rho proteins is determined by an atypical switch I region. *J Cell Sci* **121**: 1065-1075.

Schmitz, H. P., A. Kaufmann, M. Köhli, P. P. Laissue & P. Philippsen, (2006) From function to shape: a novel role of a formin in morphogenesis of the fungus *Ashbya gossypii*. *Mol Biol Cell* **17**: 130-145.

Wang, J., S. P. Neo & M. Cai, (2009) Regulation of the yeast formin Bni1p by the actin-regulating kinase Prk1p. *Traffic* **10**: 528-535.

6 Abbreviations

°C	Degree Celsius
3-AT	3-Aminotriazole
A. gossypii	*Ashbya gossypii*
AD	Activation domain
Ag	*Ashbya gossypii*
ATP	Adenosine triphosphate
BD	Binding domain
bp	Base pairs
cAMP	Cyclic adenosine monophosphate
CCW	Calcofluor White
CFP	Cyan fluorescent protein
cm	Centimeter
CP	Central plaque
DAD	Diaphanous autoregulatory domain
DAPI	4´,6-diamidino-2-phenylindole
DIC	Differential interference contrast
DID	Diaphanous inhibitory domain
$DiOC_6(3)$	3,3`-Dihexyloxacarbocyanine Iodide
DNA	Deoxyribonucleic acid
dNTP	Deoxynucleoside triphosphate
DRF	Diaphanous related formin
dsRed	*Discosoma* red fluorescent protein
DTT	Dithiothreitol
E. coli	*Escherichia coli*
e.g.	For example (latin: exempli gratia)
EDTA	Ethylenediaminetetraacetic acid
FH	Formin homology
FRET	Förster resonance energy transfer
GAP	GTPase activating protein
GDI	Guanosine nucleotide dissociation inhibitor
GDP	Guanosine diphosphate
GEF	Guanine nucleotide exchange factor
GFP	Green fluorescent protein
GOI	Gene of interest
GST	Glutathione S-transferase
GTP	Guanosine triphosphate
h	Hours
His_5	Pentahistidine
His_6	Hexahistidine
HPLC	High-performance liquid chromatography
HRP	Horseradish peroxidase
IL	Inner layer
IPTG	Isopropyl-β-D-thiogalactopyranoside

l	Liter
Lat A	Latrunculin A
leu	Leucine
M	Molar
MAP	Mitogen-activated protein
Met	Methionine
mg	Milligram
min	Minute
ml	Milliliter
mM	Millimolar
MP	Meiotic outer plaque
MTOC	Microtubule organization centre
NLS	Nuclear localization sequence
nM	Nanomolar
No.	Number
NTA	Nitrilotriacetic acid
OD	Optical density
OP	Outer plaque
PAGE	Polyacrylamide gel electrophoresis
PCR	Polymerase chain reaction
Ras	Rat sarcoma
RBD	Rho binding domain
Rho	Ras homology
RNA	Ribonucleic acid
s	Second
S. cerevisiae	*Saccharomyces cerevisiae*
S. pombe	*Schizosaccharomyces pombe*
Sc	*Saccharomyces cerevisiae*
SDS	Sodium dodecyl sulfate
SNAP	Synaptosomal-associated protein
SNARE	Soluble NSF attachment protein receptor
SPB	Spindle pole body
SV40	Simian virus 40
tryp	Tryptophan
U	Units
UV	Ultraviolet
wt	Wild type
YFP	Yellow fluorescent protein
µl	Microliter
µm	Micrometer
µM	Micromolar

7 Anlage 1

Erklärung über die Eigenständigkeit der erbrachten wissenschaftlichen Leistung

Ich erkläre hiermit, dass ich die vorliegende Arbeit ohne unzulässige Hilfe Dritter und ohne Benutzung anderer als der angegebenen Hilfsmittel angefertigt habe. Die aus anderen Quellen direkt oder indirekt übernommenen Daten und Konzepte sind unter Angabe der Quellen gekennzeichnet.

Eigenleistung an der Studie: "A Bnr-like formin links actin to the spindle pole body during sporulation in the filamentous fungus *Ashbya gossypii*" (Kapitel 3.1):

- Konstruktion des Stammes DisMet (*ΔAgbnr1* P_{ScMET3} *AgBNR2*) als Basis für die Versuche zur Herunterregulierung der Expression von *AgBNR2* im *Agbnr1* Deletionshintergrund; Vorversuche zum Wachstumsverhalten des Stammes unter verschiedenen Methionin-Konzentrationen.

- Konstruktion des Stammes *ΔAgspo21*; Wachstumstest; mikroskopische Analyse des Sporulationsverhaltens im Vergleich zum Wildtyp.

- Konstruktion des Plasmids für die Expression von *AgBNR2*-2xGFP.

- Konstruktion des Plasmids zur Überexpression von *AgBNR2-GFP* unter der Kontrolle des *ScHIS3*-Promotors (P_{ScHIS3} *AgBNR2-GFP*).

Bei der Auswahl und Auswertung folgenden Materials haben mir die nachstehend aufgeführten Personen in der jeweils beschriebenen Weise entgeltlich/unentgeltlich geholfen:

Mithilfe an der Studie: "Selection of STOP-free sequences from random mutagenesis for 'loss of interaction' two-hybrid studies" (Kapitel 3.2):

- Herr Marc Zuckermann half im Rahmen seiner Bachelorarbeit bei der Konstruktion des Plasmids pHPS592 (pGAD424-*ScURA3*).

- Herr Severin Schweisthal half im Rahmen seiner Bachelorarbeit bei den Zwei-Hybrid-Versuchen der Bni1-Mutanten Nr. 3, 4, 5 und 6.

Weitere Personen waren an der inhaltlichen materiellen Erstellung der vorliegenden Arbeit nicht beteiligt. Insbesondere habe ich hierfür nicht die entgeltliche Hilfe von Vermittlungs- bzw. Beratungsdiensten (Promotionsberater oder andere Personen) in Anspruch genommen. Niemand hat von mir unmittelbar oder mittelbar geldwerte Leistungen für Arbeiten erhalten, die im Zusammenhang mit dem Inhalt der vorgelegten Dissertation stehen.

Die Arbeit wurde bisher weder im In- noch im Ausland in gleicher oder ähnlicher Form einer anderen Prüfungsbehörde vorgelegt.

(Ort, Datum) (Unterschrift)

8 Danksagung

Ich möchte mich an dieser Stelle bei den Leuten bedanken, die meine Doktorarbeit auf verschiedene Weise unterstützt haben.

Zunächst möchte ich mich bei Dr. Hans-Peter Schmitz für die Möglichkeit bedanken, meine Promotion in seinem Projekt durchführen zu können. Danke für die unermüdliche Diskussionsbereitschaft und die Hilfe und Unterstützung bei diversen Labor- und Computerfragen.

Des Weiteren danke ich Prof. Dr. Jürgen Heinisch für seine Unterstützung während meiner Doktorarbeit sowie die Übernahme des Erstgutachtens.

Für das Erstellen des Zweitgutachtens und die Teilnahme in der Prüfungskommission bedanke ich mich bei Prof. Dr. Achim Paululat. Des Weiteren danke ich apl. Prof. Dr. Hans Merzendorfer für die Teilnahme in meiner Prüfungskommission.

Ich bedanke mich außerdem für die finanzielle und fachliche Unterstützung der Doktorarbeit durch das Stipendium im Rahmen des Graduiertenkollegs "Cell and Tissue differentiation from an integrative perspective" der Universität Osnabrück.

Ich danke der gesamten Arbeitsgruppe Genetik für die gute Zusammenarbeit sowie die Diskussions- und Hilfsbereitschaft. Es war eine schöne Zeit mit euch, an die ich mich immer gerne erinnern werde.
Ganz besonders danke ich den jetzigen und ehemaligen Kollegen aus Labor 330, Sabrina, Michael, Nele, Marc, Severin, Niko, Doris, Sandra, Verena, Yvonne und Kristina, für die gute Stimmung im Labor.
Doris danke ich außerdem für das Korrekturlesen meiner Arbeit und eine unterhaltsame Tagung in Marburg. Für die Wochenend-Mitfahrgelegenheit und die damit verbundenen guten Gespräche geht ein besonderer Dank an Katja. Bei unseren TAs Sabrina und Sandra bedanke ich mich für zahlreiche wertvolle Tipps im Laboralltag.

Außerdem danke ich der Arbeitsgruppe von Prof. Dr. Peter Philippsen in Basel für die gute Zusammenarbeit und zwei schöne *Ashbya*-Workshops in Basel und Osnabrück.

Ein ganz besonderer Dank gilt meiner Familie, speziell meinen Eltern, die mir diesen Weg ermöglicht haben und mich unentwegt in jeglicher Hinsicht unterstützt haben. Ihr wart mir während der gesamten Zeit eine große Stütze.

Ich danke Frank dafür, dass er für mich da ist. Danke, dass Du Dich immer mit mir gefreut hast, aber auch ein geduldiger Zuhörer in schwierigen Situationen warst. Danke auch für Deine Unterstützung bei computertechnischen Fragen.